A stretch of 17 amino acids in the prosaposin C-terminus is critical for its binding to sortilin and targeting to lysosomes

Libin Yuan

Department of Anatomy and Cell Biology
McGill University, Montreal

August 2009

A thesis submitted to the Faculty Graduate Studies and Research in partial fulfillment of the requirements of the degree of Doctor of Philosophy

This thesis is dedicated to my family:

My father, my mother, my sisters, my wife and my son,

who are the sources of my inspiration.

I thank you all for your support

Abstract

Newly synthesized soluble lysosomal proteins are transported from the Golgi apparatus to the lysosomes by two mannose 6-phosphate receptors. However, the sphingolipid activator protein prosaposin is targeted by the alternative trafficking receptor, sortilin. Prosaposin is the precursor of four lysosomal saposins required for the hydrolysis of sphingolipids. A previous study demonstrated that the removal of its C-terminus abolished the trafficking of prosaposin to the lysosomes.

To identify the sequences and amino acids involved in the interaction of prosaposin to sortilin and its transport to the lysosomes, we generated six prosaposin deletion constructs and examined the effect of truncation by co-immunoprecipitation and confocal microscopy. The experiments revealed that a 17 amino acid stretch in the first half of the C-terminus (aa524-540) was necessary for the binding of prosaposin to sortilin and essential for its transport to the lysosomes.

Since the pH is able to induce conformational changes in the four saposin domains, we performed a pH-dependent binding assay to test whether or not the binding of prosaposin to sortilin was affected by different pHs. The experiments demonstrated that binding of prosaposin to sortilin occurred at 6.0 or higher. A substantial decrease in binding was detected at pH 5.5, and at pH 5.0 both proteins did not form complexes. This result indicated that the binding of prosaposin to sortilin is pH-dependent.

Since hydrophilic residues usually modulate pH-dependent protein interactions we introduced six site-directed point mutations in hydrophilic residues within the first half of the C-

terminus. The results showed that the mutation of single hydrophilic amino acids did not affect the binding of prosaposin to sortilin.

Considering that tryptophan, cysteine and proline residues are important in protein structure and function, we also introduced eight site-directed point mutations to these residues within the 17 amino acid stretch in the C-terminus. The experiments revealed that two tryptophans (W530 and W535), and two cysteines (C528 and C536) were essential for the transport of prosaposin to the lysosomes. In addition, one proline residue (P532) was critical for the proper folding of prosaposin during its synthesis, which was demonstrated by the MG132 Proteasome Inhibition Assay.

In conclusion, we have narrowed down the sortilin recognition site on the prosaposin molecule to a specific 17-residue stretch in the first half of the C-terminus and discovered the essential residues in this region for the lysosomal trafficking of prosaposin.

Résumé

Les protéines lysosomiales solubles récemment identifiées et synthétisées sont transférées de l'appareil de Golgi des cellules vers les lysosomes par deux récepteurs, des mannoses 6-phosphates. Cependant l'activateur sphingolipidique de la prosaposine est ciblé sur la lysosomes par un récepteur alternatif, la sortiline. La prosaposine est le précurseur de quatre saposines lysosomiales requises pour l'hydrolyse des sphingolipides. Une étude récente a déjà démontré que l'élimination de la terminaison-C de la sphingolipide empêche le transport de la prosaposine vers les lysosomes.

Pour identifier les séquences d'acides aminés impliqués dans l'interaction de la prosaposine avec la sortiline et ainsi clarifier le mode de transport de ces séquences vers les lysosomes, nous avons procédé, par co-immunoprécipitation et immunomicroscopie confocale et à l'élimination de six séquences distinctes de la saposine. Ces expériences ont montré que la première moitié de la terminaison-C (aa524-540) la séquence des 17 résidus peptidiques est nécessaire pour permettre la liaison de la sortiline à la prosaposine et le transport de la prosaposine vers les lysosomes.

Le pH du milieu agit sur l'interaction d'un ligand à son récepteur. Nous avons donc analysé la liaison de la prosaposine à la sortiline à différents pH. Les résultats on montré que la liaison de la prosaposine à la sortiline se fait à un pH de 6.0 ou plus. Par contre la prosaposine ne forme pas de complexes avec la sortiline à des pH de 5.0 et 5.5.

Puisque les résidus hydrophiles modulent normalement l'interaction des protéines nous avons introduit des mutations focales (point mutations) sur six sites de tels résidus hydrophiles

de la terminaison-C de la prosaposine. Les résultats ont montré que de telles mutations n'ont aucun effet sur la liaison de la sortiline à la prosaposine.

Considérant que le tryptophane, la cystéine et la proline forment des séquences importantes de la structure et de la fonction des protéines, nous avons inséré huit mutations focales additionnelles sur la séquence de 17 résidus de la terminaison-C de la prosaposine. Les résultats ont révélé que deux molécules de tryptophane (W530 etW535) et deux molécules de cystéine (C528 et C536) sont essentielles au transport de la prosaposine vers les lysosomes. Par ailleurs, une molécule de proline (P532) provoque la dégradation de la prosaposine par des protéosomes.

En conclusion nous avons circonscrit certains aspects moléculaires de la relation de la sortiline à la prosaposine. Nous avons montré en particulier que la liaison de la sortiline à la prosaposine se situe au niveau d'un site précis du segment de la terminaison-C de la prosaposine dont certains éléments jouent un rôle essentiel dans le transport de la prosaposine vers les lysosomes.

ACKNOWLEDGMENTS

First of all, I would like to thank my supervisor, Dr. Carlos Morales for his generous support, excellent instruction and constant encouragement. He has been a great source of wisdom throughout my studies. Thank you!

I am most grateful to Dr. Hermo, Dr. Presley and Dr. Pshezhesky for all the generous support and extremely helpful advice that they gave me throughout the past years. I would also like to thank Dr. Clermont for kindly translating the abstract of this thesis into French.

Thank you all to my colleagues, Maryssa Canuel, Jibin Zeng and Xianyan Ni, who have contributed with technical supports and helpful discussions.

I would like to extend my gratitude to all the students who have worked in our lab for their support and friendship: Ji-hae Kim, Myriam Block, Jacob Hassan and Ann Kokidakis.

I am truly grateful to my parents and my wife for their optimism and support. I also thank my son, who is one of the sources of happiness in my life.

This work was supported by the grant from the Canadian Institute for Health Research (CIHR).

Table of Contents

List of Tables and Figures

Abbreviations

2-ME: 2-Mercaptoethanol

AI: Androgen-independent

AOAH: Acyloxyacyl-hydrolase

apoA-V: Apolipoprotein A-V

AR: Androgen receptor

ARF: ADP ribosylation factor

ARG: Androgen-regulated gene

ASM: Acid sphingomyelinase

ATF-3: Activating transcription factor 3

BDNF: Brain-derived neurotrophic factor

BMP: Bis(monoacylglycero)phosphate

CCV: Clathrin-coated vesicle

CD: Circular dichroism

CGN: cis-Golgi network

ChAT: Choline acetyltransferase

CNS: Central nervous system

CO-IP: Co-immunoprecipitation

CoQ10: Coenzyme Q10

CPY: Carboxypeptidase Y

DHT: Dihydrotestosterone

DMEM: Dulbecco's modified Eagle's medium

DRM: Detergent-resistant membrane

ER: Endoplasmic reticulum

ERAD: Endoplasmic reticulum-associated protein degradation

ERKs: Extracellular signal-regulated kinases

FBS: Fetal bovine serum

GalNAc: N-Acetylgalactosamine

GD: Gaucher disease

GGA: Golgi-associated, γ-adaptin homologous, ARF binding protein

GLUT4: Glucose transporter isoform 4

GM2-AP: GM2 activator protein

GPCR: G-protein-coupled receptor

GSL: Glycosphingolipid

GSV: GLUT4 storage vesicle

GULP: Engulfment adapter protein 1

HRE: Hormone-responsive element

ICD: Inclusion-cell disease

iGb3: Isoglobotrihexosylceramide

IGF: Insulin-like growth factor

IHC: Inner hair cell

JNK: c-Jun N-terminal kinase

LAM: Lipoarabinomannan

LAMP: Lysosome-associated membrane protein

LBPA: Lysobisphosphatidic acid

LDLR: low density lipoprotein receptor

LIMP：Lysosomal integral membrane protein

LPL: Lipoprotein lipase

LRP: Low-density lipoprotein receptor-related protein-1

LSD: Lysosomal storage disorder

M6PR: Mannose 6-phosphate receptor

MAPK: Mitogen-activated protein kinase

MLD: Metachromatic leukodystrophy

MSAP: MIR-interacting saposin-like protein

MVB: Multivesicular body

NeuAc: N-acetyl-D-neuraminic acid

NGF: Nerve growth factor

NKT: Natural killer T cell

NMD: Nonsense mediated decay

NPD: Niemann-Pick disease

NT: Neurotensin

NT3: Neurotrophin 3

NTR: Neurotensin receptor

OHC: Outer hair cell

PBS: Phosphate buffered saline

PI: Phosphatidylinositol

PI3K: Phosphoinositide 3-kinase

PNS: Peripheral nervous system

proBDNF: Precursor of brain-derived neurotrophic factor

proCD: procathepsin D

proNGF: Nerve growth factor precursor

PrSt: Prostate stromal cell

PS: Phosphatidylserine

PSAP: Prosaposin

RAP: Receptor-associated protein

RORE: Retinoic acid-receptor-related orphan receptor α subunit-binding element

RORα: Retinoic acid-receptor-related orphan receptor α subunit

RPE: Retinal pigment epithelium

SAP: Sphingolipid activator protein

SAPK: Stress-activated protein kinase

SAPLIP: Saposin-like protein

SK: Sphingosine kinase

SP-B: Pulmonary surfactant protein B

Tg: Thyroglobulin

TGN: Trans-Golgi network

TNFα: Tumor necrosis factor α

uPA: Urokinase plasminogen activator

uPAR: Urokinase plasminogen activator receptor

VDCC: Voltage-dependent calcium channels

VPS10p: Vacuolar protein-sorting 10 protein

Chapter 1

1.1 Introduction

Most newly synthesized soluble hydrolases are transported from the Golgi apparatus to the lysosomes by two mannose 6-phosphate receptors (MPRs) [1, 2]. However, the nonenzymic sphingolipid activator proteins (SAPs) are targeted by the alternative trafficking receptor, sortilin [3]. Sortilin is a 95-100kD membrane protein expressed in several tissues, such as brain, testis, and spinal cord [4]. Sortilin consists of a short cytoplasmic domain containing a lysosomal sorting signal, a single transmembrane domain, and a luminal segment composed of a single VPS10 domain [4, 5]. The VPS10 motif is also found in the VPS10p receptor, the sorting receptor implicated in the transport of carboxypeptidase Y (CPY) to the yeast lysosomal vacuole [6]. More recently, sortilin has been implicated as an alternative receptor to the MPR for some soluble hydrolases [7, 8].

Prosaposin (PSAP) is the precursor of four heat-stable SAPs termed saposins A, B, C D [9-12]. Prosaposin contains four central and two peripheral domains. The four central domains, also referred to as B-type domains, are delimited by three linker regions and correspond to the functional saposins [13, 14]. Subsequent to the lysosomal transport of prosaposin, the linker regions of the central domains are proteolytically cleaved to liberate the four saposins into the lumen of the lysosomes [15]. The lysosomal hydrolysis of sphingolipids with short oligosaccharide side chains requires the presence of these SAPs [16].

The peripheral domains, also referred to as A-type domains, are situated at the N-terminus and C-terminus of prosaposin [14]. While the B-type domains are composed by 80 amino acid

residues, the A-type domains are comprised by 34 amino acid residues corresponding to a saposin-like structure [13, 14]. Deletion analysis revealed that unlike the N- terminus, removal of the C-terminus abolished the trafficking of prosaposin to the lysosomes [17, 18]. Furthermore, chimeric albumin proteins linked to saposin D and the C-terminus of prosaposin reached the lysosomes [17, 18].

In this study, we have identified the critical domain within the first half of the C-terminus of prosaposin (aa524-540) that is responsible for the binding to sortilin and required for the targeting of prosaposin to the lysosomes.

1.2 Review of the Literature

1.2.1 Degradation of Sphingolipids

1.2.1.1 Role of membrane sphingolipids

Sphingolipids are a class of lipids derived from long-chain bases, aliphatic amino alcohol sphingosine, and involved in eukaryotic membrane composition [19]. They form the stable outer leaflet of the plasma membrane lipid bilayer and protect cell against harmful extracellular factors [20]. Glycosphingolipids (GSLs), which belong to a subclass of sphingolipids, were also found involved in cell-cell recognition, cell growth and differentiation [21]. As an essential component of cell membrane, glycosphingolipids play very important roles in regulating cell development through the specific interactions of the glycan structures with neighbouring cell membrane or cell factors from extracellular matrix [22]. They also function as antigens and type-specific markers, mediate cell adhesion, and modulate signal transduction as receptors [22].

1.2.1.2 Structure of sphingolipids

A sphingosine bonded with a fatty acid forms a ceramide. Addition of a polar head group to the ceramide forms a sphingolipid molecule. According to Stoffel et al., there are three main types of sphingolipids dependent on their different types of polar head groups: sphingomyelins, gangliosides and glycosphingolipids. Sphingomyelins contain a phosphocholine or a phosphoethanolamine head group. Gangliosides have a head group with at least three sugar residues, and one of them is sialic acid. Therefore, gangliosides are negatively charged lipids at neutral pH. A glycosphingolipid head group is a simple sugar or an oligosaccharide side chain [23].

Since gangliosides also contain sugar residues, they are often considered as a distinct

subgroup of glycosphingolipids. Based on the types of the sugar groups joined in a β-glycosidic linkage to ceramide, glycosphingolipids are classified into four subgroups: neutral glycosphingolipids, sulfatoglycosphingolipids, fucoglycosphingolipids and gangliosides. Neutral glycosphingolipid molecules contain one or more sugars connected directly to the ceramide moiety [24, 25]. Sulfatoglycosphingolipids contain sulfate ester groups and fucoglycosphingolipids are fucosylated compounds while gangliosides are characterized by the presence of sialic acids [26].

1.2.1.3 Degradation of plasma membrane

It is well known that the cell plasma membrane continuously flows and recycles between cell surface and organelles through the vacuolar system [27]. During the endocytic flow, plasma membrane buds into coated pits, which are internalized to form endocytic vesicles and transported from the cell surface to the lysosomes [28]. Lysosomes are major degradative compartments of eukaryotic cells, containing a large variety of acid hydrolases to degrade proteins, lipids, nucleic acids, and carbohydrate molecules [29]. In the lysosomes, part of the plasma membrane is incorporated in the lysosomal membrane, free from digestion of lysosomal hydrolases due to the protection of a thick glycocalyx coat on the luminal surface of the membrane [30, 31]. The glycocalyx is the carbohydrate portion of highly N-glycosylated lysosomal integral membrane proteins (LIMPs) and lysosomal associated membrane proteins (LAMPs) [30, 31]. Meanwhile, a part of the internalized membrane recycles back to the cell surface carrying cell surface receptors that escape from degradation [27]. This recycling process enhances the ability of the cell surface to internalize ligands and other materials [27]. In addition to the incorporation of plasma membrane to the lysosomal membrane and partial membrane recycling, a subset of plasma membrane is degraded by acid lysosomal hydrolases. This process

has been implicated in the down regulation of surface receptors and in membrane turnover [32]. During this process, part of the membrane invaginates into the lumen of the endosomes and multivesicular bodies to form intra-endosomal vesicles [28]. The convex curvature of those small vesicles (40-100 nm in diameter) favours spreading the head groups of the glycosphingolipids on the outer leaflet of intra-endosomal/lysosomal vesicles membrane and makes them more easily accessible for the lysosomal hydrolases [33]. In addition, while the endosomal pH value decreases, the composition of the internal membrane changes and most of membrane-stabilizing cholesterol is removed [34, 35]. Bis(monoacylglycero)phosphate (BMP), a negatively charged phosphate lipid which favours a strong curvature, is also increased to facilitate the membrane degradation [34, 35]. Through the lysosomal digestion process, glycosphingolipids are cleaved into small molecules by glycosidases, with the stepwise release of sphingosine, fatty acid, monosaccharides, glycerol, sulfate and sialic acids [36].

Lysosomal glycosidases are water-soluble enzymes at low pH with the ability of binding to negatively charged membrane or water soluble substrates [36]. They are also able to digest membrane-bound substrates with long sugar chains that reach to the aqueous space [37]. However, the glycosphingolipids with short saccharide chain (of one to four sugar residues) cannot access the active sites of the glycosidases [28]. Therefore the glycosphingolipid degradation requires activator proteins and negatively charged lysosomal lipids to disturb the membrane structure and to expose the glycosphingolipids to glycosidases [38, 39].

1.2.1.4 Activator proteins

Until now, five activator proteins have been described. One of them is the GM2 activator protein (GM2-AP). The other four are sphingolipid activator proteins (SAPs) termed saposins [40, 41].

GM2 -AP is a 17.6kD glycoprotein in its deglycosylated form and is encoded by a gene on chromosome 5 [42, 43]. It acts as an essential activator for the degradation of ganglioside GM2 by N-acetyl-β-hexosaminidase A [44]. During the process of hydrolysis, GM2-AP helps the enzyme to cleave off a GalNAc and a NeuAc residue from GM2 and converts it to GM3 [45]. In addition, it also stimulates the conversion of GM2 to GA2 by a clostridial sialidase [46].

According to Fürst et al., N-acetyl-β-hexosaminidase A and sialidase cannot cleave ganglioside GM2 on membrane surfaces because they are not able to extend far enough into the aqueous phase. GM2-AP contains a hydrophobic cavity that harbours the ceramide moiety of ganglioside GM2 [39]. It inserts into the bilayer of intra-lysosomal vesicles, lifts ganglioside GM2 out of the membrane, and presents it to the active site of β-hexosaminidase A [39]. GM2-AP showed strong binding ability to acidic glycosphingolipids, including gangliosides and sulphated glycosphingolipids [45]. The negatively charged sugar residue or sulfate group in gangliosides are important for the binding of GM2 activator to sphingolipid molecules [45]. GM2-AP probably interacts with the trisaccharide structure of the GM2 and presents the GalNAc and NeuAc residues to β-hexosaminidase A or sialidase [47].

According to Wilkening et al., GM2-AP and Saposin B are probably required for the degradation of membrane-bound ganglioside GM1 catalyzed by galactosylceramidase. Both Saposin B and the GM2-AP significantly enhance the degradation of the ganglioside GM1 with the help of anionic phospholipids such as BMP and phosphatidylinositol (PI). Specifically occurring in inner membranes of endosomes and lysosomes, anionic phospholipids dramatically increases the binding of both galactosylceramidase and activator proteins to the membranes [48].

The deficiency of the GM2-AP blocks the degradation of the ganglioside GM2 and leads to the AB variant of GM2-gangliosidoses, in which the accumulation of ganglioside GM2 and glycolipid GA2 in neuronal cells leads to the early death of the patients [49].

The other four activator proteins are saposins, which are individually termed Saposin A, Saposin B, Saposin C and Saposin D. Saposins are acidic, heat-stable glycoproteins with the size of 13-15kD [50]. They are derived from a common precursor, prosaposin. In the central segment of prosaposin backbone, saposins are arranged in tandem as four saposin B-type domains [13, 51].

All of four saposins show homology to each other [52]. However, they have different substrate specificities [13]. For example, Saposin A is required for the degradation of galactosylceramide by galactosylceramidase [53]. Saposin B shows a broader specificity but mainly for sulfatide by arylsulfatase A *in vivo* [36]. While Saposin C is required for the lysosomal degradation of glucosylceramide by glucosylceramidase, Saposin D stimulates lysosomal ceramide degradation by acid ceramidase [54, 55].

Inherited deficiency of any saposin leads to the accumulation of nondegradable membranes within the lysosomal compartment and to the development of lysosomal storage diseases (LSD) [56-59].

In summary, a complicated mechanism regulates the selective degradation of sphingolipids in membrane catabolism. Thus, activator proteins are essential factors in down-regulation and membrane turnover by facilitating the catalysis of specific sphingolipids. In addition, changes in the lipid composition of intra-lysosomal vesicle membrane, including decreased cholesterol and increased BMP, facilitates the interaction between the hydrolase and the activator protein and ensures the degradation of the targeted membrane.

1.2.2 The Saposins

All of the four saposins share a common structure characterized by six conserved cysteines, a conserved N-linked glycosylation site, a conserved proline residue, and 15 positions that are characterized by large hydrophobic amino acids [52]. Each saposin contains one domain of ~80 amino acids and its six conserved cysteines forms three disulfide bridges [60-63]. Saposins contain four (Saposin B) or five α-helices (saposin A, C, D), which form a "saposin fold" [51, 62, 64]. This characteristic structure of saposins is shared by several other proteins, including prosaposin (PSAP), acid sphingomyelinase (ASM), acyloxyacyl-hydrolase (AOAH), pulmonary surfactant protein B (SP-B), NK-lysin, granulysin, *Entamoeba histolytica* amoebapores, plant aspartic protease, *Dictyostelium discoideum* countin, and MIR-interacting saposin-like protein (MSAP) [65-71]. All of these proteins, with varying functions, compose the saposin-like protein (SAPLIP) family. All SAPLIPs share membrane perturbing properties [36, 65].

Saposins, in particular, are SAPLIPs involved in the lysosomal degradation of sphingolipids, although they possess different substrate specificities and structural properties [72].

1.2.2.1 Saposin A

1.2.2.1.1 Structure

Saposin A is a 16kD glycoprotein, consisting of about 84 amino acids [13]. In addition to the presence of three conserved disulfide bonds, a glycosylation site and the amphipathic helical fold motif common to the other three saposins, saposin A also contains an additional glycosylation site and a single tryptophan [73]. Circular dichroism (CD) analysis indicated that saposin A is enriched in an α-helical structure. To be precise saposin A possess 41%-53% of helical content at pH4.5 with the rest of the molecule forming random coils [13, 15]. The crystal structure of saposin A reveals five α-helices, which form a compact monomeric saposin fold with a

hydrophobic pocket inside the molecule [74]. Under different conditions, saposin A adopts variable conformations. For example, saposin A is found in a monomeric state at pH7.0 and assembles into dimmers at pH4.8 in the presence of detergent C(8)E(5) [74].

According to Leita et al., saposin A has a specific oligosaccharide moiety, which is dominated by acetyllactosamine-type oligosaccharides and about 83% of sugars are fucosylated at the reducing end of N-acetylglucosamine residues [75].

1.2.2.1.2 Function

Saposin A is required for the degradation of galactosylceramide by galactosylceramidase as well as the hydrolysis of 4-methylumbelliferyl-β-glucoside and glucosylceramide by glucosylceramidase [10, 76]. Stimulation of glucosylceramidase by saposin A is similar to that by saposin C [13]. Kinetic studies indicate that saposins A and C bind to glucosylceramidase at the same site [13, 41]. During hydrolysis, both saposin A and saposin C probably bind directly to the enzymes causing a conformational change in their structure [77].

Full activity of the enzymes also requires the presence of a negatively charged acidic lipid such as phosphatidylserine (PS) [77]. Acidic lipids form a water-soluble complexes with glucosylceramidase and both saposins [41]. Morimoto et al. proposed a binding model for glucosylceramidase to the activators and/or substrates. According to the model the binding sites of the enzyme include: one for the carbohydrate of the substrate, one for an aglycone, one for the acidic lipid, and one for a saposin [41]. The binding of saposin A to galactosyl- and glucosylceramide is highly dependent on the pH since an acidic environment increases the hydrophobic property of saposin A [78].

Interestingly, saposin A was found to bind to lipid bilayer. The amphipathic helices at the amino and carboxyl termini, as well as the middle region of the molecule, are inserted into the

lipid bilayer to about five carbon bond lengths [73]. However, the binding of saposin A to membrane appears to be restricted [78]. Recent observations suggest that the interaction of saposin to membrane bilayer may induce membrane changes [79].

In addition to these observations, saposin A is believed to affect the composition of the intraendosomal and intralysosomal membranes. Along the endocytic pathway the cholesterol concentration in these membranes decreases whereas the anionic phospholipid BMP increases [80]. In fact saposin A has been implicated in the removal of lipids and preliminary evidence suggests that the glycosylation of saposin A is important for this function. [80]

Saposin A is also required for the loading of lipid antigens onto antigen-presenting molecules CD1d [81]. CD1 molecules are glycoproteins that bind lipid antigens in the endocytic pathway and present the antigens at the cell surface to natural killer T (NKT) cells [82]. Saposin A transfers phosphatidylserine and sulfatide to CD1d for the recognition of these lipid antigens by NKT cells [81].

1.2.2.2 Saposin B

1.2.2.2.1 Structure

Saposin B was the first activator protein identified in 1964 by Mehl [16], with a mass of 8.8kD after deglycosylation and a broader specificity in the degradation of glycosphingolipids [83, 84]. Saposin B has lower sequence identity to the other three saposins. While the sequence identity between saposin B and the other saposins ranges from 15% to 22%, the sequence identities among saposins A, C, D range from 34% to 39% [85]. Circular dichroism (CD) studies indicate that saposin B contains 45-50% helical conformation and that the helical axes were almost parallel [86]. Compared with saposin A, saposin B contains only one glycosylation site and lacks tryptophan, while sharing the common structure of three conserved disulfide bonds

and a multi-amphipathic helical bundle motif [73]. Saposin B has three major glycosylated isoforms, according to the sugar glycosyl substituent on the glycosylation site [86]. The isoform with the sugar substituent $Man_2GluNac_2Fuc$ is the most abundant accounting for 35-40% of all the isoforms of saposin B [87]. Glycosylation of Saposin B is essential for its full lipid-extraction activity since removal of its carbohydrate side chains reduces its membrane-destabilizing activity [88].

The protein backbone of saposin B is composed of four amphipathic α-helices arranged in a long hairpin that is bent into a simple V-shape. A study on a synthesized peptide (sapB-18), which is corresponding to the region spanning between residues 52-69, suggested that this region is consistent with a 44% α-helix content and involved in the recognition and binding of GM1 ganglioside [89]. This region also contains a variant insertion Gln-Asp-Gln, that is coded by the alternative splicing exon 8 on prosaposin gene and appears to affect the binding of prosaposin B to lipids [90]. In fact, the insertion was found to abolish the binding capacity of saposin B to GM1-ganglioside but increase its affinity for sulfatide and sphingomyelin. [90].

To exert the functions in degradation of sphingolipids, two monomers of saposin B form a shell-like homodimer that encloses a large hydrophobic cavity [51]. According to Stokeley et al., the saposin B dimer presents two conformations respectively termed AB dimer and CD dimer. The AB dimer contains a closed central cavity while the cavity of CD dimer is more open [91]. These authors found that the CD dimer showed greater conformational drift than the AB dimer. The conformational change was characterized by a so-called “scissor” motion of the two monomers. The “scissor” motion could compress the central hydrophobic cavity to form a more closed cavity than that of the AB dimer. An H-bond between the Q53 and Y54 side chains of the two opposing monomers probably hold the dimer. Arguably, these investigators suggest that this

motion may play a key role in lipid extraction from membrane bilayer [91]. Similarly, Ahn et al. proposed that the open conformation (the CD dimer) may interact directly with the membrane, promote a reorganization of the lipid alkyl chains, and extract the lipid substrate through the change to the closed conformation by "scissor" motion [51].

1.2.2.2.2 Function

Saposin B has multiple functions and broad specificity in sphingolipid degradation. It is required for the degradation of sulfatide by arylsulfatase A and globotriaosylceramide and digalactosylceramide by α-galactosidase A *in vivo* [36]. It also mediates the degradation of ganglioside GM1 by galactosylceramidase by cooperating with GM2 activator protein [48]. This broad specificity might explain the extensive lipid binding property of saposin B [92].

The degradation of sphingolipids by enzymes and saposin B is pH-dependent [93, 94]. For example, the optimal pH value for degradation of globotriaosylceramide is pH 4.6 [93] and the pH optimum for the degradation of sulfatide is around pH 4.3[94]. The acidic pH also induces the change in hydrophobicity of saposin B, triggers its binding to lipid's membranes [72], and destabilizes the membrane by forming deep gaps [79]. Ciaffoni et al. found that saposin B simultaneously extracts from membrane neutral (phosphatidylcholine) and anionic (phosphatidylinositol) phospholipids and that it transfers phospholipids between lipid surfaces. The optimal pH for both the phospholipid binding and transfer activities were at acidic pH values [95]. The binding was inhibited by mono- and divalent cations, phosphate and sulphite while BMP and phosphatidic acid were essential for the binding and degradation of sphingolipid [94].

In addition to being involved in the degradation of sphingolipids, saposin B also functions in other transport activities [96]. Saposin B has been demonstrated to bind and transport coenzyme Q10 (CoQ10) and γ-Tocopherol inside the cell [97]. CoQ10 is an essential component of the

mitochondrial respiratory chain [98]. Saposin B binds to CoQ10 and transfers it to erythrocyte ghost membrane [98]. Thus, it is suggested that saposin B is a CoQ10 binding/transport protein [99]. γ-Tocopherol is the major form of dietary vitamin E [100]. It is absorbed by intestine, then secreted in chylomicrons, transferred to peripheral tissues and finally taken by liver for lysosomal degradation [101]. Jin et al. found that saposin B is capable of binding γ-Tocopherol. Thus, these authors suggest that saposin B transfers γ-Tocopherol from liver lysosomes to microsomes for degradation and/or excretion to bile duct [97, 101].

Like saposin A, saposin B also plays a role in antigen presenting [83]. It transports and presents lipid antigens in endosomal compartments, for example, α-galactosylceramide and isoglobotrihexosylceramide (iGb3), to NKT cell, which might promote the positive selection of NKT cells [81, 83]. Among the four saposins, the role of saposin B in lipid antigen presenting probably is the most prominent [83]. This presenting process is accomplished through the binding of CD1d molecules to lipid antigens in the endocytic pathway with help of saposin B as a lipid transfer protein [83].

1.2.2.3 Saposin C

1.2.2.3.1 Structure

Saposin C was initially isolated as a glycoprotein of 8.5kD from spleen of patients with Gaucher disease [54]. It contains 80 amino acids, with a single asparagine residue as glycosylation site and lacks tryptophan residues [73]. The N-linked oligosaccharides are mainly of the monoantennary oligomannose-type [75]. The six cysteine residues form three disulfide bonds, which are essential for maintaining the functional properties of saposin C [60, 102]. The break-down of those disulfide bridges significantly reduces the activity of glucosylceramidase, which requires saposin C for the degradation of glucosylceramide [102]. These disulfide bonds

also contribute to the formation of a “saposin fold”, which is composed of five α-helices [64]. While all charged amino acids are exposed outside, the hydrophobic residues are hidden in the protein core forming a hydrophobic pocket [103]. The enzymatic activation domain is located at carboxyl-terminal half of saposin C, spanning between residues 47 and 62 [104, 105]. However, the segment spanning between residues 22 and 31 contributes to the neurotrophic activity of prosaposin [106]. The fusogenic domain of saposin C localizes at the amino-terminal half of this molecule spanning between residues 4 and 20, which also forms the first and second helices. Lys13 and Lys17 are critical for the fusogenic induction of negatively charged phospholipid membranes by saposin C [107, 108].

Saposins C is a compact molecule in its monomeric state [74]. However, acidic conditions and membrane binding induce conformational changes in the molecule and self-association of saposin C monomers into dimer or trimer [64, 74]. Generally, saposin C is in a monomeric state at pH 7.0, is in a dimeric state at pH 4.0 [64], and forms trimer in presence of detergent C(8)E(5) at pH4.8 [58]. Hawkins et al. found that saposin C has a compact closed conformation in the absence of SDS whereby the hydrophobic cavity is not exposed [109]. However, in the presence of SDS, saposin C has an open conformation with an exposed hydrophobic core [109].

1.2.2.3.2 Function

Saposin C is required for the lysosomal degradation of glucosylceramide to ceramide and glucose by glucosylceramidase [54]. Glucosylceramidase is a lysosomal membrane protein that cleaves the O-β-D-glucosidic linkage of glucosylceramide and aryl-β-glucosides [110]. The enzyme requires saposin C to gain access to the membrane-embedded glucosylceramide [111]. In addition, saposin C also renders glucosylceramidase protease-resistance and protects it from degradation [112]. Saposin C also exhibits the stimulatory effect on sphingomyelinase activity

for the degradation of sphingomyelin and functions as an activator protein for the hydrolysis of galactosylceramide [76, 113].

Unlike the action mode of saposin B and GM2-activator protein, which only bind to lipids and membrane, saposin C directly binds and activates Glucosylceramidase [54, 77]. Furthermore, saposin C is the only saposin that promotes the binding of glucosylceramidase to phosphatidylserine-containing membranes [114], and enhances the enzyme activity [110].

It is accepted that the interaction between saposin C and intracellular membranes is a pH-dependent process affected by the content of negatively charged unsaturated phospholipids, such as phosphatidylserine or phosphatidylinositol [78, 108, 115]. Acidic pH causes a conformational change of saposin C, increases its hydrophobic properties and promotes the binding of saposin C to sphingolipids [114, 115]. Therefore, saposin C is capable of destabilizing acidic phospholipid-containing membranes in a pH-dependent fashion [116].

Once an acidic pH triggers the conformational change of saposin C, the amphipathic helices at the amino- and carboxyl-termini of saposins C penetrate into the lipid bilayer to about five carbon bond length， binding to the head group of acidic phospholipids [73, 117]. Meanwhile, the middle helical region of saposins C is reoriented and exposed outside of membrane surface [73]. This reorientation of the middle region probably exposes a binding site, which is critical for the interaction of the intracellular membrane with glucosylceramidase [73, 118].

Subsequently, it is believed that saposin C induces a membrane restructuring in two steps that begins with the formation of a patch-like structural domain, and then followed by the occurrence of membrane destabilization and the increase of membrane thickness [119, 120]. The formation of a patch-like domain is independent of acidic phospholipids [119, 120]. This step is followed by a membrane destabilization process dependent on acidic phospholipids causing

membrane thickness reduction. The reduction in membrane thickness is attributed to lipid loss or to some sort of interdigitating process occurring between the membrane and saposin C [79, 119]. Finally, glucosylceramide in the destabilized membrane is accessed and degraded by the enzyme. [111].

In addition to the functions in sphingolipids degradation, saposin C has neuritogenic effects [121, 122] and functions as a multipotential modulator of diverse biological activities in prostate cancer and stromal cells [123]. According to Koochekpour et al., saposin C can up-regulate urokinase plasminogen activator (uPA) and its receptor (uPAR) as well as c-Jun expression. It also stimulates proliferation, migration and invasion of prostate stromal or cancer cells. It activates p42/44, stress-activated protein kinase/c-Jun NH_2-terminal kinase (SAPK/JNK) and the mitogen-activated protein kinase (MAPK) pathways in prostate stromal and cancer cells [123]. Saposin C also activates the Akt signalling pathway, down-regulates caspase-3, -7, and -9 expression in prostate cancer cells under serum-starvation stress [124]. In addition, saposin C decreased cell apoptosis via the PI3K/Akt pathway [124].

Like saposin A and B, saposin C also functions in antigen presentation [81, 125]. Saposin C disturbs the intra-lysosomal membrane, extracts diverse lipids, like mycolic acid, phosphatidylserine and LAM, and loads onto CD1d molecules [81, 126]. Since CD1d binds to both self and bacterial lipid antigens and presents them to NKT cells, saposin C probably plays important roles in host defense [125, 127].

1.2.2.4 Saposin D

1.2.2.4.1 Structure

Saposin D was isolated from Gaucher spleen and purified to homogeneity as a 10kD, 83 amino acids activator protein [9]. Saposin D lacks tryptophan and contains a single N-

glycosylation site [73]. In fact, 90% of its total oligosaccharides linked to this N-glycosylation site are oligomannose-type oligosaccharides, varying from two to six hexose residues [61, 75]. The “saposin fold” of saposin D consists of five α-helices [64]. Its crystal structure demonstrates that saposin D is mainly in a monomeric and that it presents two conformational states [64, 128]. Unlike the other three saposins, saposin D has a weak propensity to form dimers [128], and there is a slow dynamic equilibrium between the two conformational states [64]. However the function of this equilibrium is not yet clear. Compared to the monomeric structures of saposin A and C, saposin D shows a slightly more compact hydrophobic cavity owing to a slight repositioning of the 'stem' and 'hairpin' regions of the protein [128].

1.2.2.4.2 Function

Saposin D is specifically required for the lysosomal breakdown of ceramide to a fatty acid and sphingosine by acid ceramidase [9, 128]. Ceramide is ubiquitously present in plasma membranes and, together with its hydrolytic product sphingosine, functions as lipid second messengers which is important for cell function and survival [129]. Ceramide is hydrolyzed by both acid and alkaline ceramidase [130]. However, saposin D only stimulates acid ceramidase [131]. Saposin D has also been reported as an activator protein for acid sphingomyelinase *in vitro*, which hydrolyzes sphingomyelin into ceramide and phospholipid molecules [9, 113, 132]. However, *in vivo*, the degradation of sphingomyelin by acid sphingomyelinase probably is not dependent on saposin D [133]. Acid sphingomyelinase itself contains a saposin-like domain, which functions in membrane destabilization [134].

The activity of saposin D is maximal at acidic pH and maximum binding of both Saposin D and acid ceramidase to lipid bilayer occurred at pH 4.0 [64, 135]. The lower pH causes conformational change and dramatically increases the superficial hydrophobicity of saposin D

[64, 136]. The increase of hydrophobicity is essential for the binding of saposin D to lipids and its destabilizing membrane ability [114]. The interaction of saposin D with membrane also requires acidic phospholipids [61]. The degradation of membrane-bound ceramide was significantly increased in the presence of three acidic phospholipids most abundant in the acidic endolysosomal compartment, lysobisphosphatidic acid (LBPA), phosphatidylinositol and phosphatidylserine [135, 137].

According to Linker et al., at the low pH of the late endosomal and lysosomal compartments, the increased superficial hydrophobicity of saposin D triggers the interaction of this saposin with anionic phospholipid-containing membrane. When the saposin D concentration on the lipid surface reaches a critical value, it solubilizes the intra-endosomal and intra-lysosomal membranes into smaller particles [136]. The increased membrane curvature of the small particles further results in higher ceramide degradation rates [135].

1.2.3 The precursor of sphingolipid activator proteins, prosaposin

Prosaposin is the common precursor of saposin A, B, C, and D [138]. After translation, prosaposin is glycosylated in the ER and the Golgi complex [139], and transported to the lysosomes where it is proteolytically cleaved into four saposins [140, 141].

1.2.3.1 Gene

1.2.3.1.1 Alignment

The prosaposin gene localizes in the chromosome 10 [142]. Bar-Am et al. precisely mapped the human prosaposin gene to the 10q22.1 for the first time [143]. According to Rorman et al., the human prosaposin gene is formed by 19,985 bp. The length of the exons ranges from 57 to 1200 bp while that of the introns from 91 to 3812 bp. The exons encodes the N-terminus, four saposin domains and the C-terminus of prosaposin [144]. Zhao et al. found that the prosaposin

gene contains15 exons. Among them, the exons 3, 4, and 5 encode saposin A, exons 6, 7, 8, and 9 encode saposin B, exons 10 and 11 encode saposin C, and exons 12, 13, and 14 encode saposin D. Exons 1, 2 and 15 encode the N- and C-terminus. In addition, the exon 11 of the mouse prosaposin gene has 93 extra base pairs compared to human prosaposin gene, which encode a proline-rich region located between saposin C and saposin D in the mouse prosaposin molecule [145]. The prosaposin gene is highly conserved. The interspecies identity between the mouse and human prosaposin genes is 77% [52], and 59% between the human and chicken genes [146]. Since all the four saposin domains share a common structure, it is deduced that the prosaposin gene evolved from an ancestral gene which duplicated twice to form the four saposin domains [85, 144].

1.2.3.1.2 Expression regulation

The expression of prosaposin is temporally and spatially regulated at transcriptional and post-translational levels [147]. According to Sun et al., the transcriptional start sites in mouse prosaposin gene are located 87 and 94 bp upstream of the start ATG codon in exon 1. The 5' promoter region lies within 2,400 bp upstream of the transcription start site and contains positive and negative regulatory elements. The negative regulatory element is located between 742 and 310 bp upstream of the transcription start site [148]. This negative regulatory element is composed of a 3' Sp1 site, a 5' Sp1/U cluster binding sites and a RORE (retinoic acid-receptor-related orphan receptor α subunit-binding element), which binds to Sp1 (the member of the Sp family), the retinoic acid-receptor-related orphan receptor α (RORα), and a U factor (an unknown transcription factor) [149]. The factors that bind to the Sp1/U cluster site and RORE interact negatively to diminish promoter activity to a background level, which is determined primarily by the 3' Sp1 site [149]. The Sp1 and RORE residing sites mediate developmental

regulation in the central nervous system and eye [147, 150, 151]. The positive regulatory elements, containing the transcription-factor-binding sites Brn-2 and Oct-6, localize within 742-2400 bp upstream of the transcriptional start site, which is mainly responsible for prosaposin expression in visceral tissues (e.g. liver, spleen, lung, kidney, thymus and heart) [147].

Compared to mouse prosaposin, the transcription initiation sites of human prosaposin gene is localized to 23, 27, 31 and 83bp 5' to ATG and the negative regulatory region existed between -813 and -2500bp [152]. The human promoter does not contain a Sp1 cluster, but it has AP-1, Oct-1 and two ROR α sites [152]. In addition, the human prosaposin promoter was shown to be TATA-less. Therefore, the human prosaposin gene belongs to the TATA-less housekeeping gene family [152].

1.2.3.1.3 Alternative splicing

The exon 8 of prosaposin gene contains nine base pairs (CAG GAT CAG), encoding three amino acids (QDQ) that are implicated in the sphingolipid binding affinity of saposin B [52, 145]. This exon is alternatively spliced in the prosaposin mRNA [145]. Most of prosaposin mRNA of brain, heart, and muscle contains exon 8, whereas the mRNA from testis, lung, pancreas, spleen, and kidney does not [145, 153]. The alternative splicing of exon 8 does not affect prosaposin secretion or the metabolism of sphingolipids, including gangliosides, sulfatides, neutral glycosphingolipids, neutral phospholipids, other neutral lipids, and ceramide [154]. However, the ratio of the mRNA transcription with and without exon 8 changes in the nervous system after ischemic injury [155, 156]. Normally, the two prosaposin transcripts (with and without the exon 8) are expressed at a ratio of 85:15 in normal brain. But this ratio is changed to 5:95 following ischemic injury, suggesting that the alternative splicing of prosaposin mRNA is associated with

the nervous injury-repair mechanism [155]. In contrast, the expression of mRNA with exon 8 is constant throughout the regenerative period [156].

1.2.3.2 Protein structure

Human prosaposin is composed of 524, 526 or 527 amino acids depending on the alternative splicing of its mRNA. These numbers include a signal peptide of 16 residues [157]. Mouse prosaposin presents a 70% sequence similarity to the human prosaposin amino acid sequence and has an extra proline-rich region of 31 residues between the saposin B and C domains [138, 145].

Prosaposin contains four central and two peripheral domains [9-12]. The four central domains, termed saposin A-D domains, which are arranged in tandem, are delimited by three linker regions [138]. The saposin domains correspond to the mature saposin proteins and they are termed by some investigators as B-type domains [13, 14]. Subsequent to the lysosomal transport of prosaposin, the linker regions of the central domains are proteolytically cleaved to liberate saposins into the lumen of the lysosomes [15]. The peripheral domains, referred as A-type domains, are situated at the N-terminus and C-terminus of prosaposin [14]. While the B-type domains are composed of 80-84 amino acid residues, the A-type domains comprise 34 amino acid residues [13, 14].

Prosaposin neurotrophic activity resides in a linear 12-mer region located in the N-terminal sequence of the saposin C domain [158]. The neurotrophic sequence of human prosaposin is LIDNNRTEEILY [159].

As indicated above, according to the alternatively spliced exon 8, there are three prosaposin forms: one with three extra amino acid residues (QDQ), one with two extra residues (DQ) and a third form with no extra residues [160]. In addition, the post-translational glycosylation, of prosaposin can yield two other forms: the fully glycosylated 70kD prosaposin and the partially

glycosylated 65kD prosaposin [139].

Prosaposin is synthesized as a 53kD protein in the cytoplasm first and glycosylated into 65kD and 70kD prosaposins [17]. The 65kD prosaposin is intracellularly targeted to the lysosomes by a sorting receptor, sortilin [161]. After transport to the lysosome, the 65kD prosaposin is proteolytically processed to the mature saposins, by cathepsin D and possibly by some other proteases [157]. Cathepsin D cleaves prosaposin into 35 to 53kD intermediate molecules and other proteases trim them to the mature 8-11kD forms of individual saposin molecules [157]. Instead, the 70kD prosaposin can be secreted to the extracellular space and re-endocytosed by the mannose-6-phosphate receptors and/or by the low-density lipoprotein receptor-related protein (LRP) on cell surface [162].

While mature saposins are found mainly in liver, lung, kidney, and spleen, prosaposin is detected mainly in brain, heart, and muscle [163]. It is also found in body fluids such as milk, semen, cerebrospinal fluid, bile, and pancreatic juice [36]. Especially, prosaposin is present in high concentrations in the luminal fluids of the seminiferous tubules and epididymis, where it is thought to be involved in degradation of lipids of residual bodies and/or in the modification of membrane lipids during sperm maturation [164].

In summary, prosaposin can be considered a multi-functional protein [165] involved in the following functions: 1) The lysosomal 65kD prosaposin participates in sphingolipid catabolism via the production of saposins. 2) The secreted 70kD prosaposin protein, involved in the activation of MAPK- and PI3K/Akt-signalling pathways [166], exerts neurotrophic activities in cell growth, development, and maintenance of the nervous system, nerve regeneration and plasticity, as well as the protection of neurons from cell-death or apoptosis [159, 167]. 3) The

secreted 70kD isoform is also suggested to be involved in membrane biogenesis [78], and in the development and maintenance of the male reproductive system [168].

1.2.3.3 Distribution in tissues

Prosaposin exhibits a unique tissue distribution [169]. Compared to saposins, which are dominant in spleen, lung, liver, and kidney, prosaposin is mainly found as an intact protein in skeletal muscle, heart, and brain [169]. In human blood, leukocytes contain mainly saposins, while plasma contains primarily prosaposin [169]. Human platelets contain both prosaposin and saposins, without much difference in amount [169]. However, prosaposin is released from human platelets in response to stimulation by thrombin, but mature saposins are not [170]. Prosaposin also exists in human secretory fluids, including cerebrospinal fluid, semen, milk, pancreatic juice and bile [170].

In the various tissues that contain prosaposin, the expression levels are also different [171]. The nervous and reproductive systems, as well as upper trachea, lungs and esophagus, show high level expression of prosaposin while the heart, kidneys, liver, adrenals and lymphoid organs express lower amounts of prosaposin [172]. Interestingly, specific regions of the tissues where this protein is found in relatively lower levels, for instance, the cortical tubules of the kidney, liver hepatocytes, macrophages of lymph nodes, spleen and thymus, as well as pneumocytes type II, show high levels of prosaposin expression [171]. Prosaposin expression was also found in sense organs, such as in the organ of Corti, stria vascularis and spiral ganglion of ears, as well as the retinal pigment epithelium (RPE) cell monolayer and ganglion cells of eyes [173, 174].

In the central and peripheral nervous systems prosaposin is abundant in almost all neurons including the subcortical and spinal cord neurons [175, 176]. Prosaposin also exists as an integral component of the surface membranes of neuronal cells, including the membrane of dendrites,

axons and cell bodies [176]. In the central nervous system, prosaposin is abundant in the brainstem, hypothalamus, cerebellum, striatum, and hippocampus, and less abundant in the cerebral cortex [177]. In the ependymal lining and the secretory epithelial cells of the choroid plexus, the expression of prosaposin is also at high level [171]. In neurons of the cerebral cortex, cerebellar cortex, and lateral columns of the spinal cord, the expression of prosaposin mRNA shows discrete localization [171].

In the reproductive system, Sertoli cells, Leydig cells and peritubular cells of the testis have prosaposin expression while germ cells do not [172]. Igdoura et al. found that prosaposin exists in Sertoli cell lysosomes and in phagosomes containing the residual bodies released by late spermatids [178]. These authors suggested that prosaposin generates lysosomal saposins which play a role in the hydrolysis of membrane glycolipids present in the residual bodies [178]. Prosaposin also expresses in ovine endometrium during the oestrous cycle and during early pregnancy [179].

Kondoh et al. isolated prosaposin from human milk for the first time [180]. Prosaposin exists exclusively in the milk serum (whey) as a monomeric form [181]. In human milk the amount of prosaposin fluctuates during the lactating period. That is, prosaposin is in high concentration within a few days after delivery, in low concentration during the transitional milk lactating stage, and in high concentration again at the mature milk lactating stage [170].

1.2.3.4 Functions

1.2.3.4.1 Functions in glycolipid degradation

Prosaposin is the precursor of saposin A, B, C, and D, which are proteolytically cleaved off from prosaposin by cathepsin D in the lysosomes [157]. During its proteolytic processing in mammalian cells, the N-terminus of prosaposin is removed first followed by the excision of

saposin A. The remaining trisaposin B-C-D is then cleaved into disaposin B-C or C-D by removal of the B or D domains of the precursor [140]. Hiraiwa et al. reported that cathepsin D may also remove saposin D first, yielding an A-B-C trisaposin form. They also found that cathepsin D may directly cleave prosaposin into disaposins A-B and C-D. On the other hand, cathepsin D is unable to cleave the interdomain fragments of disaposins and trisaposins Therefore, it is accepted that an unknown protease must be involved in the lysosomal maturation of saposin B, C, and D [157]. Some investigators suggest that gangliosides might protect prosaposin from the proteolysis by cathepsin D *in vivo* [157]. Once the proteolysis processes are completed, saposins are involved in lysosomal hydrolysis of GM1 ganglioside, glucosylceramide, galactosylceramide, sulfatide, sphingomyelin and other sphingolipids [182].

Prosaposin itself has been implicated in the stimulation of sphingolipid degradation. Masao et al. has found that prosaposin binds tightly to gangliosides to form stable ganglioside-prosaposin complexes, and transfers gangliosides from donor membranes to acceptor membranes *in vitro*. This observation suggests that secretory prosaposin may transfer gangliosides to target membranes and that integral membrane prosaposin may change the cytoplasmic location of gangliosides [182]. Prosaposin also stimulates the activity of glucosylceramidase, ganglioside GM1 galactosylceramidase, and sphingomyelinase. [183].

1.2.3.4.2 Functions as a neurotrophic factor

Prosaposin, as well as saposin C, stimulates axon outgrowth and acts as a neurotrophic factor by preventing neuronal apoptosis, by elongating axons, and/or by facilitating myelination and increasing choline acetyltransferase (ChAT) activity [184, 185]. The mechanism of prosaposin neurotrophic activity is independent of nerve growth factor (NGF), brain-derived neurotrophic factor (BDNF) and neurotrophin 3 (NT3) [184].

Prosaposin exists either as a component of the surface membranes of neural cells or as a secreted protein in body fluids to mediate trophic signalling transduction [186]. Sorice et al. found that exogenous prosaposin bound to the lipid rafts on plasma membrane, triggered a signal cascade, induced extracellular signal-regulated kinase phosphorylation and sphingosine kinase activation, and prevented consequent cell death [186]. Prosaposin rescued mature cerebellar granule neurons from apoptosis probably through a similar way to that of IGF-1 rather than BDNF [187].

Prosaposin was found to increase sulfatide concentrations in primary and transformed Schwann cells and oligodendrocytes, suggesting that this protein is involved in promoting myelin lipid synthesis and in prolonging neuron survival. Prosaposin may also function as a myelinotrophic factor *in vivo* during development and repair of myelinated nerves [167].

In addition, prosaposin was found to increase the level of gangliosides GM3, GM2, GD1a in the plasma membrane of NS20Y neuroblastoma cells, suggesting that the neurotrophic activity of prosaposin may affect the composition of cell surface gangliosides [188].

Investigations on brain injury also provided evidence for the neurotrophic activity of prosaposin. For example, prosaposin was found to be involved in the process of facial nerve regeneration after experimental slicing of the facial nerve [185]. Prosaposin was also found to protect the brain after stab wounds [189], to protect hippocampal CA1 neurons from ischemia-induced learning disability and neuronal loss [190] and to prevent the atrophy of cholinergic large neurons in the anterior horn [191].

1.2.3.4.3 Roles of prosaposin in other tissues

Prosaposin is involved in the development of the male reproductive system through maintaining the differentiation of reproductive organs, spermatogenesis, and fertilization [192].

Hammerstedt et al. found that prosaposin increased the binding of rooster sperm to the perivitelline membrane of chicken eggs *in vitro* and substantially raised fertility after artificial insemination. Moreover, these authors found that a fragment of 60 amino acids between saposins A and B was involved in promoting sperm-egg binding [193].

Guo et al. found that prosaposin was able to bind Rhox5 [192]. Rhox genes are a cluster of more than 30 homeobox genes on the X chromosome, selectively expressed in male and female reproductive tissues, especially in Sertoli cells [194]. Rhox5 belongs to a subset of Rhox genes that mediate androgen-dependent steps during spermatogenesis and Rhox5 decreases male germ cell apoptosis and increases sperm production, sperm motility, and fertility [195]. Therefore, the interaction between Rhox5 and prosaposin might regulate the development of male reproductive organs dynamically [192]. These authors also suggested that the C-terminus of prosaposin might be essential for the interaction with Rhox5 [192].

In the literature it was also reported that the homozygous inactivation of prosaposin in mice led to the development of a number of abnormalities in the male reproductive system, including the atrophy of the prostate gland [196]. Interestingly, prosaposin is expressed at a higher level by androgen-independent (AI) prostate cancer cells [124]. Koochekpour et al. found that prosaposin is an androgen-regulated gene (ARG), which may be implicated in the normal and neoplastic growth of the prostate. In fact, prosaposin appears to up-regulate the expression/activity of androgen receptor (AR) and AR-target genes in LNCaP cells. They also found that the proximal region of the prosaposin gene promoter contains a hormone-responsive element, which is capable of associating with the AR [197].

Prosaposin is also required for epidermal barrier formation [198]. Ceramide, the main lipid constituent of the intercellular matrix of the skin's stratum corneum, derives from the hydrolysis

of glucosylceramide by glucosylceramidase [199]. Prosaposin deficiency in the epidermis causes accumulation of glucosylceramide, reduction of ceramide in epithelium and abnormal stratum corneum formation [198, 200]. In the skins of both atopic dermatitis and psoriasis patients, the expression of prosaposin is abnormally low [201, 202].

1.2.3.4.4 Roles of prosaposin in MAPK signalling pathways

Prosaposin has been found to trigger some MAPK pathways and exert their functions through those signalling cascades [196].

Misasi et al. found that prosaposin induced extracellular signal-regulated kinases (ERKs), which is required for the stimulation of DNA synthesis. Moreover, prosaposin increased sphingosine kinase (SK) activity, prevented cell apoptosis and induced pheochromocytoma cells (PC12) to enter the S phase of the cell cycle [203].

These authors also found that prosaposin has similar functions in death prevention, reducing necrosis and apoptosis through ERKs and SK pathways in both human histiocytic U937 cell and peripheral blood mononuclear cells. In these cells, prosaposin acted as a protective factor on tumor necrosis factor α (TNFα) induced cell death [204]. Prosaposin also led to rapid ERK phosphorylation in U937 cells and increased sphingosine kinase activity [204].

In addition, prosaposin may trigger G-protein-coupled receptor (GPCR)-mediated Akt phosphorylation cascades to exert its neurotrophic and myelinotrophic activity [205, 206]. Ochiai et al. found that prosaposin protected PC-12 cells from cell death not only through the activation of an ERK phosphorylation cascade, but also through blocking Akt phosphorylation to down-regulate caspase-3 activation. Prosaposin also blocked the phosphorylation of c-Jun N-terminal kinase (JNK) and p38 stress-activated protein kinase through decrease of the levels of c-Jun and ATF-3 [205]. Thus, these authors suggested that the prosaposin functions in anti-apoptosis not

only by reducing the phosphorylation levels of JNK and p38, but also by regulating the c-Jun/AP-1 pathway [205].

1.2.3.4.5 Roles in cancer and metastasis

Koochekpour et al. found that prosaposin was overexpressed in prostate cancer cells and that it was capable to activate the p42/44 and SAPK/JNK members of the MAPK superfamily and PI3K/Akt signalling pathways [207]. They also found that dihydrotestosterone (DHT) treatment of prostate stromal (PrSt) cells increased prosaposin expression through the hormone-responsive element (HRE) located in the proximal region of the prosaposin gene promoter [208]. They concluded that prosaposin is a pleiotrophic growth factor for prostate cancer, contributing to prostate carcinogenesis and progression at an early stage [208]. In addition, prosaposin may function as an androgen-agonist by increasing androgen receptor (AR) expression and phosphorylation in an androgen-independent manner [165, 197].

Prosaposin may also function in eliminating barriers to tumor metastasis by facilitating hydrolysis of membrane glycolipids [209]. The preliminary evidence suggests that it may play a role in tamoxifen resistance [210].

1.2.3.5 Peptides derived from prosaposin

1.2.3.5.1 Prosaptide TX14(A)

A series of peptides derived from prosaposin have been synthesized for potential therapeutic functions [211, 212]. The best studied peptide, the TX14(A), exhibits neurotrophic activity. TX14(A) is also known as “prosaptide”, the trademark of Myelos Corporation, San Diego, USA [211]. Since the neurotrophic activity of prosaposin is located in a linear 12-mer sequence (LIDNNKTEKEIL) in the N-terminal of saposin C domain [158], TX14(A) is synthesized as a 14-mer peptide containing this 12-mer sequence [167].

Campana et al. found that TX14(A) was a potent neuritogenic factor for both sensory and motor neurons of peripheral nerves. TX14(A) increased the number and elongation of neuroblastoma cells, as well as of explanted primary sensory neurons. TX14(A) also induced sprouting at the motor endplate in the mouse gluteus muscle [213]. Furthermore, they found that TX14(A) rapidly enhanced phosphorylation of ERK1 and ERK2 through a pertussis toxin-sensitive G-protein pathway in both Schwann cells and an immortalized Schwann cell line. Through this pathway, TX14(A) enhanced the sulfatide synthesis in Schwann cells [166].

According to Koochekpour et al., TX14(A) also stimulates the proliferation/survival, migration, and invasion of prostate cancer cells by activating the Raf-MEK-ERK-RSK-Elk-1 signalling cascade of the MAPK pathway [214].

TX14(A) is a small peptide capable of crossing the blood-brain barrier. Therefore it could be used as a potential drug in the treatment of CNS disorders [211]. Since TX14(A) also prevents nerve degeneration and improves nerve regeneration, this peptide may be also used as therapeutic agent in the treatment of peripheral nerve system diseases [215, 216]. In this respect, Calcutt et al. used TX14(A) to treat streptozotocin-diabetic rats, a model of insulin-deficient diabetes in which hyperglycemia results in severe nerve injury. They found that TX14(A) prevented degeneration and promoted regeneration of peripheral nerves [217]. In diabetic rats, TX14(A) prevented the progressive of nerve fiber malfunction, preserved sodium-potassium ATPase activity, and attenuated the decline of nerve substance P levels [217, 218]. TX14(A) also prevented the decline of large sensory fiber conduction velocity in the sciatic nerve and the development of paw thermal hypoalgesia [215, 219].

In addition to all these benefits, TX14(A) has anti-allodynic properties in diverse models of neuropathic pain [212]. The mechanism of these anti-allodynic properties may include

modulation of spinal nociceptive processing [212, 220]. Therefore, TX14(A) also could be used in the therapy of both degenerative neuropathy and neuropathic pain [212].

TX14(A) has been shown to have effects in muscular tissues and in the prostate [221]. TX14(A) attenuated the decline of muscle mass loss following nerve injury induced by a constricting ligature [221]. TX14A also stimulated cell proliferation, migration and invasion via the activation of the MAPK signalling pathway in prostate cancer cells [214]. In addition, TX14A decreases the growth-inhibitory effect, caspase-3/7 activity, and apoptotic cell death induced by anti-cancer drug etoposide [124]. TX14(A) probably prevents the neurotoxic effects of another chemotherapeutic drug paclitaxel, which has been reported to induce a predominantly sensory neuropathy, without interfering with its anti-tumor activity [222].

1.2.3.5.2 Prosaptide D5

Since TX14(A) was not stable in blood, other prosaptides derived from the original neurotrophic sequence have been produced and investigated, such as the 11-mer prosaptides D1-D5 [223], the 15-mer prosaptide TX15-2 [211], the 18-mer peptide [224], and the 22-mer prosaptide 769 [225]. Among all of them, the retro-inverso 11-mer prosaptide D5 (D-amino acids LLEETANNDLL) was found to be a good therapeutic agent for central nervous system diseases [223].

Prosaptide D5, with more stability in blood than TX14(A), can cross the brain-blood barrier [223]. However, its properties in the nerve system are still questionable. Yan et al. found that prosaptide D5 induced axon outgrowth in NS20Y neuroblastoma cells, ameliorated thermal hyperalgesia in the Seltzer rat model of neuropathic pain, and modulated voltage-dependent calcium channels (VDCC) probably through a pertussis toxin-sensitive G-protein coupled receptor [226]. Lu et al. indicated that prosaptide D5 reduced brain infarction in a rat ischemic

model [227]. Hiraiwa et al. investigated the myelinotrophic action of prosaptide D5 in developing rats and found that D5 significantly increased sulfatide concentrations in both brain and sciatic nerve by promoting ERK phosphorylation [228]. However, Lapchak et al. contradicted these findings and reported that D5 was not neurotrophic and neuroprotectant *in vivo* and that the peptide even worsened the ischemia-induced behavioral deficits [229].

1.2.3.5.3 FertPlus peptide

A 60-residue polypeptide derived from prosaposin was synthesized by Hammerstedt et al. [230]. This polypeptide is commercially known as FertPlus and contains the sequence CQSLQEYLAEQNQRQLESNKIPEVDLARVVAPFMSNIPLLLYPQDRPRS QPQPKANEDC [230].

FertPlus enhanced significantly the sperm-egg binding ability in human, boar and bull [230]. Amann et al. claimed that the treatment of sperms with FertPlus peptide before artificial insemination (AI) increased the pregnancy rate of bulls [231].

1.2.4 Deficiencies of activator proteins and their precursor

Since sphingolipid activator proteins play essential roles in stimulating lysosomal enzymes, the deficiency of activator proteins results in lysosomal catabolism dysfunction with the consequence of various severe lysosomal storage disorders (LSDs) [15]. LSDs are a group of over 40 rare human genetic diseases [232]. Due to a deficiency of activator protein and/or lysosomal hydrolytic enzymes involved the digestion of macromolecules, LSDs share a common characteristic: the abnormal accumulation of lipids, glycoproteins or mucopolysaccharides inside the lysosomes [233, 234].

By the accumulated storage material or the defected proteins, all of the LSDs are classified into several groups: glycosaminoglycan degradation defects; glycoprotein degradation defects;

glycolipid degradation defects; glycogen degradation defects; polypeptide degradation defects; cholesterol and lipid transport defects; multiple lysosomal enzyme defects; lysosomal transport defects; unknown defects; and activator protein defects [235, 236]. Within the activator protein defects group, the GM2 activator deficiency causes GM2-gangliosidosis AB variant [237], and the deficiencies of saposins and prosaposin result in different LSDs, such as metachromatic leukodystrophy, Krabbe disease and Gaucher disease [15].

LSDs cause substantial morbidity and mortality and produce a broad clinical phenotypic spectrum, such as dementia, major psychiatric illness, developmental delay, or cerebral palsy from conception with a progressive course [238, 239]. But the clinical phenotypes of various LSDs show differences in the age of onset, involved organs, clinical severity or occurrence of central nervous system regression [238, 239].

1.2.4.1 Deficiency in prosaposin

1.2.4.1.1 Prosaposin deficiency in human

Prosaposin deficiency results in an elevation of multiple glycolipids, especially extensive glycosphingolipid storage in central nervous system [240, 241]. Until now, six prosaposin deficiency cases have been found.

The first patient diagnosed with prosaposin deficiency was reported in 1989. The clinical phenotype of that patient, who died at 16-week postnatally, included hyperkinetic behaviour, myoclonia, respiratory insufficiency and hepatosplenomegaly. Gaucher-like storage cells were found in the bone marrow. Biochemical tests showed partial activity deficiencies of galactosylceramidase, glucosylceramidase and ceramidase, but the sphingomyelinase activity was normal. Glucosylceramide and ceramide were elevated in liver tissue because of the profound defect in ceramide catabolism [242]. The fetus sibling of that patient from his mother's

next pregnancy also died of similar pathology at pregnancy week 20 [242]. Bradova et al. found that the concentrations of neutral glycolipids, including glucosylceramide, galactosylceramide, lactosylceramide, digalactosylceramide, tri- and tetrahexosylceramide, were elevated in liver, kidney and cultured skin fibroblasts from the patient. The kidney also showed increase in the concentration of sulfatide, galactosylceramide and digalactosylceramide and the liver presented increase of GM3 and GM2 gangliosides. Skin biopsies from both sibs showed massive lysosomal storage with vesicular and membranous materials [243]. Further investigation demonstrated that the turnover of cerebroside sulfate and globotriaosylceramide were both impaired. However, the activities of arylsulfatase A and globotriaosylceramide α-galactosidase were normal. In addition, there was an increase in cerebroside sulfate concentration in the kidney of the affected fetus. These defects were clear indications that the death of the patient and his fetal sibling were due to the deficiency of prosaposin [244]. The research on prosaposin cDNA from the two sibs showed an A to T mutation in the initiation codon and their parents were both heterozygous carriers for this defect [245].

Hulkova et al. investigated a new patient with prosaposin deficiency in 2001. In addition to the pathological alteration described above, the patient presented severe neuropathology, featuring neuronal storage, massive depopulation of cortical neurons and pronounced fibrillary astrocytosis. Active demyelination occurred in the white matter. They found that the patient was homozygous for a 1 bp deletion (c.803delG) on the prosaposin gene within the saposin B domain, which caused a frame shift and a premature stop codon, and his parents were both heterozygous carriers of this deletion [246]. They also reviewed a case found in 1984, in which a female patient died during the neonatal period. Originally the patient was diagnosed to suffer a variant form of Niemann-Pick disease (NPD) with enhanced glycolipid storage [247]. After the revision

of this case the authors found a prosaposin deficiency with the same deletion to the one described above (c.803delG). Her mother was a heterozygous carrier of the same deletion [246].

In 2005, Elleder et al. found a prosaposin deficient infant, who presented multifocal myoclonus, cyanotic hypoxemia, enteropathy, massive ascites and epilepsy. The patient, who died at 17 weeks after birth, had a homozygous c.1A to T mutation in the prosaposin gene, resulting in the complete loss of prosaposin expression [248].

Kuchar et al. reported a prosaposin-D deficient case with severe neurovisceral dystrophy in 2009. The patient was homozygous for a point mutation c.1006-2A to G and died at neonatal age. This mutation was located in an acceptor splice site two bases upstream of exon 10, which led to an insertion of 70 bases and resulted in a premature stop codon. Both parents were heterozygous carriers of this mutation [249].

1.2.4.1.2 PSAP-/- mouse model

Fujita et al. created a homozygous mouse model with a null allele prosaposin [241]. They found abnormally increased levels of lactosylceramide, glucosylceramide, galactosylceramide, globotriaosylceramide, ceramide and sulfatide in brain, liver and kidney. The PSAP-/- mice presented two clinical phenotypes: a neonatally fatal and a late onset. The late onset mice developed rapidly progressive neurological pathology, including severe hypomyelination and periodic acid-Schiff-positive materials throughout the nervous system, and died at the age of 35-38 days [241]. Chu et al. found a massive accumulation of multivesicular bodies (MVBs) in CNS neurons. In addition, the cortical and hippocampal neurons of these animals exhibit poor survival and display an axon degenerative pattern [250]. Sun et al. found that the neuropathology of PSAP-/- mice also included neuronal glycosphingolipid storage and Purkinje cell loss, as well as impairment of neuronal function [240].

Our laboratory reported that the prosaposin deficient mouse also presents reproductive system abnormalities, such as involution of the prostate, seminal vesicles, epididymis and testis. The decrease in testis size was concomitant to reduced spermiogenesis [168, 196]. The involution of the prostate gland and the decrease of testis size was independent of testosterone levels and androgen receptor expression, indicating that extracellular prosaposin may have trophic functions [251]. Akil et al. found that prosaposin deficiency also resulted in progressive deafness. The histology of the organ of Corti shows cellular hypertrophy of the inner hair cells (IHCs) and greater epithelial ridge and a loss and vacuolization of the outer hair cells (OHCs) [252].

1.2.4.2 Deficiency in saposin A

1.2.4.2.1 Krabbe disease

Saposin A defect results in the classic globoid cell leukodystrophy (Krabbe disease) [253]. Krabbe disease is a genetic demyelinating disorder with infantile onset and rapid clinical course, although late-onset forms may also exist [254]. Neurologic pathologies are prominent and unique, consisting of a rapid and almost complete disappearance of myelin and oligodendrocytes in both the central and peripheral nervous system. These lesions are accompanied with reactive astrocytic gliosis and the presence of unique and often multinucleated macrophages (globoid cells) [254]. A cytotoxic metabolite, galactosylsphingosine, normally degraded by galactosylceramidase, is considered to play a critical role in the pathogenesis [255]. Krabbe disease normally is caused by defects of this galactosylceramidase [254]. However, saposin A facilitates the degradation of galactosylsphingosine by galactosylceramidase [53] and saposin A defects may cause a late-onset variant form of Krabbe disease [253].

Spiegel et al. reported a six-month-old female patient with progressive neurological deterioration and abnormal myelination in the cerebral white matter, diagnosed as Krabbe disease. They found a deletion of three base pair, c.207del TGT, in the saposin A domain of the prosaposin gene, which led to the deletion of a conserved valine. The mutation resulted in the malfunction of saposin A [58].

1.2.4.2.2 Saposin A-/- mouse model

Matsuda et al. created a saposin A deficiency mouse model by introducing a mutation (C106F) into the saposin A domain by the Cre/loxP system to break one conserved disulfide bond. The saposin A-/- mice exhibited a progressive hind leg paralysis at approximately 2.5 months after birth and died at the age of 5 months. The pathology and clinical phenotypes were identical to but milder than Krabbe disease caused by a galactosylceramidase defect [63]. The average lifetime (134.4+/-29.1 days) was also longer than that of twitcher mice, an animal model of galactosylceramidase deficiency (47.5+/-3.9 days) [256].

1.2.4.3 Deficiency in saposin B

1.2.4.3.1 Metachromatic leukodystrophy

Metachromatic leukodystrophy (MLD) is an autosomal recessive inherited lysosomal storage disease, resulted from the impaired catabolism of cerebroside sulfate [257]. Deficiency of arylsulfatase A or saposin B leads to the accumulation of cerebroside sulfate, causing a lethal progressive demyelination, extensive white matter damage and loss of both cognitive and motor functions [258]. Mutations in the arylsulfatase A are far more frequent than those of saposin B [259]. So far fifteen patients with saposin B deficiency have been described.

Shapiro et al. were the first authors to report two MLD patients with saposin B deficiency. Those patients were siblings with developmentally delayed spasticity and progressive central

nervous system degeneration. Sulfated glycolipid catabolism was impaired but the activities of arylsulfatase A were near normal [260]. The siblings were carriers of a point mutation in the saposin B domain, C650T (counted from the initiation ATG of the prosaposin gene) and their mother was a heterozygous carrier of this mutation [56, 261]. This mutation resulted in the change of residues from threonine (ACC) to isoleucine (ATC) [56, 261]. Since the consensus sequence of a glycosylation site of a glycoprotein is Asn-Xxx-Ser/Thr, this point mutation disabled the glycosylation site of saposin B [262].

Hahn et al. reported a patient with a sulfatide lipidosis but normal activities of arylsulfatase A. This patient showed slow development and died at 22 years of age. The nerve conduction was slow due the sulfatide lipidosis [263, 264]. This patient presented a 33-base-pair insertion between nucleotides 777 and 778 (counted from the initiation codon ATG of the prosaposin gene) while her sister and one of her parents were heterozygous carriers [265]. Zhang et al. found the mechanism of this 33 nucleotides insertion. The 33 nucleotides were originally present near the middle of a 4-kb intron, preceded by a string of pyrimidines and followed by a dinucleotide gt. However, a single base mutation just preceding the 33 nucleotides, c.C775A, occurred in the prosaposin DNA sequence of this patient. This mutation changed a trinucleotide ccg to cag, which coupled with the string of pyrimidines and the dinucleotide gt, created a new splice junction and led to the expression of these 33 nucleotides as a new exon. Consequently, the insertion of 11 additional amino acids resulted in the unstable protein structure and led to the degradation of saposin B [266].

Wenger et al. reported in 1989 that a 28-month-old infant patient died with severe mental and motor deterioration, seizures, and aspiration. His liver was moderately enlarged while testes were small. The patient had normal spleen and kidneys. The ratio of galactosylceramide to

sulfatide was decreased in brain. GM2 and GM3 gangliosides were increased and the activities of arylsulfatase A and galactosylceramidase were normal. This patient was confirmed to suffer of metachromatic leukodystrophy caused by saposin B deficiency [267].

Schlote et al. described in 1991 a MLD in a 7-year-old boy that resulted from saposin B deficiency. Metachromatic staining of lysosomal storage in macrophages and PAS-positive submucosal neurons were reported in this patient [268]. Holtschmidt et al. found that this youngster had a mutation c.G722C in saposin B domain, which resulted in the substitution of serine for Cys241. In addition, the prosaposin gene of the patient contained a polymorphism 1389C to T, which did not change the amino acid sequence of the final translation product [269].

Landrieu et al. reported a 2-year-old saposin-B deficiency patient who presented a metachromatic leukodystrophy-variant phenotype mainly involving the peripheral nervous system (PNS). Magnetic resonance imaging also showed persistent white matter lesions and progressive pontocerebellar atrophy [270].

Regis et al. also found a male patient living more than 5 years in 1999. The psychomotor development of the patient was delayed. He presented spasticity, axial hypotonia, depressed deep tendon reflexes and mental deterioration. Nerve conduction velocities were markedly slowed. Sulfatide deposited macrophages and endothelial cells were found. The activity of arylsulfatase A was normal. These researchers identified a mutation (p.N215K) in the saposin B domain of the prosaposin, which abolished the only N-glycosylation site of saposin B [271].

Wrobe et al. reported two cases in 2000. A 4 years old Spanish girl showed severe motor deterioration, hypotonia, weakness and signs of CNS demyelination and polyneuropathy, active demyelination and metachromatic deposits in macrophages. The patient died before she became 5 years old. Her 2 years old sister showed moderate hypotonia and initial occipital demyelination.

Both of them bore the same mutation in the saposin B domain of prosaposin gene, A643C, resulting in the exchange of asparagine (N215) to histidine and eliminating the single glycosylation site of saposin B. Their parents were all heterozygous carriers of this point mutation [272].

A new case in a 2-year-old Italian girl with mutations in the prosaposin was reported in 2008. The patient was diagnosed with MLD due to saposin B deficiency. Two mutations were identified in this case: p.N215K in the saposin B domain (originated from her father) and p.M1V in the first residue of prosaposin (originated from her mother) [273].

In 2008, Grossil et al. described four saposin B deficiency cases from 21 Italian MLD patients. Three of them were homozygous carriers of the mutation c. C645A, which resulted in p.N215K. One of them carried a homozygous mutation c.577-1G>A [274].

Kuchar et al. reported a saposin B deficiency patient in 2009. The patient was a compound heterozygote with two mutations on alleles. The first mutation on one allele, c.577-2A>G, was a splicing mutation located in the acceptor splice site of intron 5, resulting in the loss of exon 6 and therefore leading to non-functional saposin B. The second mutation on the other allele was a 2bp deletion, c.828-829delGA, located in exon 8, leading to a frameshift and a premature stop codon. The mother was the carrier of c.577-2A>G mutation and the father was heterozygous for c.828-829delGA mutation [249].

1.2.4.3.2 Saposin B-/- mouse model

Sun et al. created a saposin B-/- mouse model by a knock-in mutation of an essential cysteine in exon 7 of the prosaposin gene in 2008. The saposin B-/- mouse showed slowly progressive neuromotor deterioration and minor head tremor by 15 months. The sulfatide level in brain and kidney was elevated, with the presence of sulfatide storage cells. The levels of

lactosylceramide and globotriaosylceramide were also increased in various tissues. The mouse died at the age of 23 month [275].

1.2.4.4 Deficiency in saposin C

1.2.4.4.1 Gaucher disease

Gaucher disease (GD) is an inherited autosomal recessive LSD caused by a deficiency of glucosylceramidase or saposin C, characterized by accumulation of glucosylceramide in the liver, spleen, and bones [276]. According to clinical phenotypes, patients with Gaucher disease are categorized into three types: Gaucher disease type 1 exhibits variable hepatosplenomegaly, anemia, thrombocytopenia, and skeletal/pulmonary/kidney abnormalities while the central nervous system is not involved in this variant. Gaucher disease type 2 shows hepatosplenomegaly and extensive central nervous system damage at early childhood and patients usually die of devastating neurological disease between 1 and 2 years of age. Gaucher disease type 3 is subclassified into types 3a and 3b. Type 3a exhibits mild-to-moderate hepatosplenomegaly and slowly progressive neurologic deterioration with recurrent myoclonic seizures while type 3b shows horizontal supranuclear gaze paresis, splenomegaly, extensive hepatomegaly and esophageal varices [277]. Normally, GD type 1 is caused by partial deficiency of glucosylceramidase while both type 2 and type 3 are resulted from profound enzyme deficiency [278]. So far, six GD patients with saposin C deficiency have been found.

Christomanou et al. identified the first patient with Gaucher disease caused by saposin C deficiency in 1986. The patient presented Gaucher disease type 1 with normal glucosylceramidase activity and absence of saposin C [279]. Schnabel et al. identified in this patient a mutation (c.G1154T, counted from A of the initiation codon ATG) in prosaposin gene, resulting in the substitution of Phe for Cys385 in the mature saposin C [280].

Christomanou et al. reported another patient with saposin C deficiency in 1989. A 15-year-old boy with a neuronopathic form of Gaucher disease contained cells with storage of glucosylceramide but with normal activity of glucosylceramidase and lacked of an sphingolipid activator protein [281]. Rafi et al. found that the patient presented a c.T1144G mutation in the saposin C domain of the prosaposin gene, changing cysteine382 to glycine. His father and unaffected brother were heterozygous carriers. The mother of the patient contained only half of the normal amount of mRNA for prosaposin without any noticeable mutation in the saposin C domain [282]. However, Diaz-Font et al. found that the mother of the patient carried a different mutation, c.C1288T (counted from the A of the ATG initiation codon), which was localized in the saposin D domain of prosaposin gene and resulted in a premature stop codon. This premature stop codon probably led to the degradation of prosaposin mRNA by a process termed nonsense mediated decay (NMD) [283].

Amsallem et al. reported the third GD case of saposin C deficiency in 2005. The female patient developed normally before the age of 7 years old but with enlarged spleen and mile leucopenia. Since the age of 11, nocturnal epileptic fits developed. At age of 16, school performance slowly decreased. Dysmetria, myoclonic jerks and frequent seizures appeared. The level of glucosylceramidase activity was normal. However two mutations were found in the prosaposin alleles. One allele had p.C315S mutation and the other a M1V mutation [284].

Stirnemann et al. claimed the discovery of a new GD patient with saposin C in France in 2007 but details of this case are lacking [285]. Tylki-Szymanska et al. reported two new cases in 2007, a 36-year-old man and his 30-year-old sister with Gaucher disease type 1 due to saposin C deficiency. Both patients had very high levels of chitotriosidase activity, chemokine CCL18, and increased concentration of glucosylceramide in plasma and normal glucosylceramidase activity.

They carried compound heterozygous mutations. One mutation, p.L349P, was identified in the saposin C domain of one allele and another mutation, p.M1L, in the initiation codon of the prosaposin gene on another allele [59].

1.2.4.4.2 Saposin C-/- mouse model

Sun et al. created a mouse model of Gaucher disease in 2005 by backcrossing mice expressing low levels of prosaposin and saposins to mice with glucosylceramidase mutations [286]. In 2007, the same authors created a CD-/- mouse model, which has both saposin C and D deficiencies, by introducing genomic point mutations into critical cysteines in the saposin C and D domains. These mice presented severe neurological phenotype with ataxia, kyphotic posturing and hind limb paralysis. Loss of Purkinje cells was evident after 6 weeks. Glucosylceramide and α-hydroxy ceramide were accumulated in brain and kidney with the presence of storage bodies in neurons of the spinal cord, brain and dorsal root ganglion. Skin fibroblasts and tissues from CD-/- mice showed increased intracellular prosaposin, impaired prosaposin secretion, deficiencies of saposins C and D and decreases in saposins A and B. The life span of the mice was about 56 days [287].

1.2.4.5 Deficiency in saposin D

Any case of saposin D deficiency in human has never been reported. In addition to the saposin CD-/- mouse model generated by Sun et al. [288], Matsuda et al. generated a specific saposin D(-/-) mouse in 2004 by introducing a mutation (p.C509S) into the saposin D domain of the prosaposin gene. The saposin D(-/-) model showed progressive polyuria in 2 months old mice and ataxia in 4 months old animals. Renal tubular degeneration and hydronephrosis occurred in the kidneys. A progressive loss of the cerebellar Purkinje cells was also observed in

the central nervous system. Almost all Purkinje cells disappeared in 12 months old mice. In addition, ceramide accumulated in the kidneys, brain, and cerebellum [57].

1.2.5 The receptor protein for the lysosomal trafficking of prosaposin

Most newly synthesized lysosomal hydrolases are tagged with a mannose-6-phosphate group by a phosphotransferase in Golgi apparatus, which is recognized by the mannose 6-phosphate receptor (MPR) in the trans-Golgi network (TGN) [289]. After binding to the Golgi-associated, γ-adaptin homologous, ARF binding proteins (GGAs), MPRs lead their cargos to the lysosomes through clathrin-coated vesicles (CCVs) [290]. However, in the fibroblasts of Inclusion-cell disease (ICD), which is resulted from a mutation in the phosphotransferase, prosaposin is still transported to the lysosomes while most of hydrolases are secreted to the extracellular space [291]. This observation suggested that the lysosomal trafficking of prosaposin is independent of MPR system [289]. Our laboratory demonstrated that the trafficking of prosaposin from Golgi to the lysosomes is mediated by sortilin [161].

1.2.5.1 Structure of sortilin

Sortilin is a 100kD, 833-residue type-I membrane protein, which was first purified by Petersen et al. in 1997 using RAP affinity chromatography [4]. Receptor-associated protein (RAP) is an ER chaperon involved in the binding of low density lipoprotein receptors [292]. These investigators found a novel RAP associated sorting receptor designated sortilin [4].

Sortilin is expressed in a variety of tissues, including fat, brain, spinal cord, muscle and lung [293-295]. Its gene maps to chromosome 1p and the protein contains a luminal segment at the N-terminal region, a single transmembrane segment and a cytoplasmic tail on its C-terminus [4]. Most part of the luminal segment is composed of a large domain designated Vps10 domain, because it is extensively homologous to the luminal domain of the yeast vacuolar protein-sorting

10 protein, Vps10p [4]. The N-terminus of newly synthesised premature sortilin contains a furin cleavage site, $R_{41}WRR_{44}$, preceding the Vps10 domain [4]. Therefore, the premature sortilin becomes the mature form after the elimination of a 44-residue propeptide by furin [296]. Since this propeptide is able to bind mature sortilin and to inhibit the binding of other sortilin ligands, Petersen et al. suggested that the propeptide plays a chaperon role in the ER to protect premature sortilin from abnormal binding to their ligands [296]. Westergaard et al. found that, in addition to the protection of premature sortilin, the propeptide facilitates receptor transport in the early Golgi compartments [297]. They also suggested that Vps10 domain of sortilin contains a segment (10CC) characterized by 10 conserved cysteines, which form 5 disulfide bonds. This 10CC segment is adjacent to the transmembrane domain and contains the major ligand binding site [297]. By means of computational analysis Paiardini et al. suggested that the Vps10 domain of sortilin contains a β-propeller fold, which is probably important for the ligand binding [298].

The cytoplasmic tail of sortilin contains several sorting signals, suggesting that sortilin is a multifunctional sorting protein [4]. One of the signals is a nine-residue sequence HDDSDEDLL. This sequence contains the dileucine acidic sorting motif (DXXLL), which is essential for the protein trafficking pathway from TGN to the lysosomes [4]. During the lysosomal trafficking, the dileucine signal is recognized by GGAs [299]. GGAs are ubiquitous coat proteins associated with TGN, belonging to the family of ADP Ribosylation Factor (ARF)-binding Proteins [300]. They are consisting of an N-terminal VHS domain, a GAT domain, a linker segment, and a C-terminal ear domain [300]. GGAs bind to the acidic dileucine signal of sortilin through the VHS domain and therefore lead sortilin and its cargo to the lysosomes from TGN [299, 301] (Figure I).

The sequence YSVL, which belongs to the consensus motif YXXØ [4], has been shown to be present in the cytoplasmic tail of sortilin, to bind adaptor proteins AP-1 and AP-2, and to

mediate both endocytosis and lysosomal trafficking pathway through clathrin-coated vesicles [302, 303]. The motif FLVHRY, which belongs to the internalization sorting signal (F/Y)XXXX(F/Y), was also found in the sortilin C-terminus [4, 302, 304]. These signals share extensive homology with the similar motifs in MPR, demonstrating that sortilin is involved both in endocytosis and in lysosomal trafficking from TGN [5, 305].

1.2.5.2 Ligands of sortilin

In addition to prosaposin, sortilin mediates both the lysosomal trafficking pathway from TGN and endocytosis pathway of many other ligands.

1.2.5.2.1 Ligands in the intracellular trafficking from TGN

Sortilin mediates the trafficking of newly synthesized glucose transporter isoform 4 (GLUT4) to a specialized compartment, GLUT4 storage vesicles (GSVs) [306]. GLUT4 protein functions in clearance of blood glucose through facilitating glucose across plasma membrane for intracellular storage in responsive to insulin [307]. It was found to be colocalized with sortilin in GSVs, which probably derive from endosomes in fat and skeletal muscle cells [293, 308]. Through the binding to GGAs on TGN membrane, sortilin leads GLUT4 to GSVs under the stimulation of insulin [306].

Sortilin is also involved in the lysosomal trafficking of some cathepsins [309]. Until now, it has been know that cathepsin H is exclusively transported from the TGN to the lysosomes by sortilin whereas cathepsin D is transported by both sortilin and the MPRs [310].

The lysosomal trafficking of acid sphingomyelinase (ASM) is also partially dependent on sortilin [7]. Although its transport depends primarily on MPRs, our lab found that sortilin may also function as an alternative receptor for ASM trafficking [7].

1.2.5.2.2 Ligands in the endocytosis pathway

Less than ten percent of sortilin can reach the plasma membrane in neurons. Therein it is believed to be a neurotensin (NT) receptor, mediating the efficient internalization of NT [311, 312]. In addition, sortilin has been implicated in some NT mediated actions, such as in microglia cell migration, by facilitating the phosphorylation of the extracellular signal-regulating kinases 1/2 and Akt in the PI3-kinase and MAPK pathways [313]. The evidence suggests that NT binds to the β-propeller region in the Vps10 domain of sortilin [314].

Sortilin is also suspected to be a co-receptor of the precursor of nerve growth factor, proNGF. Together with another receptor p75NTR, sortilin stimulates proNGF to selectively induce apoptosis [294]. Since proNGF is neurotoxic for aged people and associated with Alzheimer's disease, increased sortilin level is proposed to result in age-related neuronal atrophy and degeneration [315].

Similarly to proNGF, the precursor of brain-derived neurotrophic factor, proBDNF, is believed to bind to sortilin and p75NTR to induce cell apoptosis [316]. Chen et al. found that sortilin was colocalized with BDNF in the secretory granules of neurons and that the truncation and low expression level of sortilin result in BDNF missorting, suggesting that sortilin plays a role in the subcellular trafficking of BDNF [317].

Nielsen et al. found that about 8% sortilin localized on cell surface partly bound to lipoprotein lipase (LPL). Thus, these authors suggested that sortilin may also function in the endocytosis and degradation of LPL [318]. Sortilin and LPL have been implicated in osteogenesis. While LPL negatively regulates osteogenesis, overexpression of sortilin increased osteogenesis by triggering the degradation of LPL [319].

Sortilin also binds to apolipoprotein A-V (apoA-V), a 39kD apolipoprotein that reduces triacylglycerol levels in blood [320]. After binding to sortilin, apoA-V is rapidly internalized and delivered to early endosomes [320]. It is believed that during this process sortilin is recycled to TGN while apoA-V reaches the lysosomes for degradation [320].

Additionally, sortilin has been implicated in thyroglobulin (Tg) recycling in thyroid epithelial cells (thyrocytes) in a TSH-dependent manner [321]. Tg is the precursor of thyroid hormones and is synthesized by thyrocytes and secreted into the lumen of thyroid follicles [322]. Sortilin binds to Tg with high affinity, induces its endocytosis and transports it to the Golgi apparatus where Tg is fully glycosylated and secreted back to the colloid [321].

In conclusion, sortilin is a multifunctional receptor mediating various cell processes. However, it is accepted that one of the main functions of this protein is the sorting and trafficking of soluble lysosomal proteins to the endolysosomal compartment [15]. In fact, sortilin binds primarily to prosaposin, the GM2 activator protein (GM2AP) and cathepsin H and to a lesser extend cathepsin D and acid sphingomyelinase (ASM) [7, 289, 309]. In addition, the cytoplasmic region of sortilin contains all the sorting and trafficking motifs to cycle between the TGN and endosomes [4]. Finally, inhibition of sortilin via dominant-negative constructs and RNAi severely impairs the transport of these lysosomal proteins [323].

Thus, the main objective of the present investigation was to identify the critical domain within prosaposin that is responsible for the binding to and transport by sortilin to the lysosomes.

Chapter 2

Materials and Methods

2.1 Materials

2.1.1 Reagents

All of the primers and DH-5α E.Coli competent cells were purchased from Bio S&T (Montreal, QC). All restriction enzymes were from New England Biolabs (Pickering, ON). T4 DNA ligase was from Roche (Laval, QC). Dulbecco's modified eagle medium (DMEM), fetal bovine serum, trypsin, ProLong Gold antifade reagent, DAPI and Hoechst 33342 were from Invitrogen (Carlsbad, CA). Protease inhibitor cocktail was from Roche (Laval, QC). StrataClone Ultra PCR Cloning Kit, QuikChange II Site-Directed Mutagenesis Kit and QuikChange Lightning Site-Directed Mutagenesis Kit were from Stratagene (La Jolla, CA). Long Range PCR Kit, Taq PCR Kit, QIAquick Gel Extraction Kit, QIAprep Spin Miniprep Kit, Hispeed Plasmid Midi Kit and PolyFect Transfection Reagent were all from Qiagen (Mississauga, ON). Protein A Sepharose 4 Fast Flow, ECL Plus Western Blotting Detection Reagents and Amersham Hyperfilm MP autoradiography films were from GE Healthcare (Piscataway, NJ). MG132 (Z-Leu-Leu-Leu-al), citric acid and Na_2HPO_4 were from Sigma (Oakville, ON). BlokHen was from Aves Labs (Tigard, OR)

2.1.2 Antibodies

2.1.2.1 Primary Antibodies

The rabbit polyclonal anti-prosaposin antibody was generated in our laboratory [161] and validated in several studies [161, 305, 323]. Monoclonal anti-c-myc antibody was from Sigma (Oakville, ON). Rabbit polyclonal anti-sortilin antibodies were purchased from Alomone Labs

(Jerusalem, Israel). Monoclonal anti-LAMP-1 antibody was from BD Biosciences (Mississauga, ON). Monoclonal anti-Golgin-97 antibody was from Invitrogen (Carlsbad, CA). Chicken polyclonal anti-myc antibody was from Aves Labs (Tigard, OR).

2.1.2.2 Secondary Antibodies

Goat anti-mouse IgG antibodies conjugated to HRP were from Sigma (Oakville, ON). Goat anti-rabbit IgG antibodies conjugated to HRP was from Santa Cruz Biotechnology (Santa Cruz, CA). Goat anti-mouse IgG antibody conjugated to Alexa 594 was from Invitrogen (Carlsbad, CA). Chicken polyclonal anti-myc antibody, fluorescein-labeled goat anti-chicken IgY antibody was from Aves Labs (Tigard, OR).

2.1.3 Vectors and Wild-type Constructs

The pcDNA 3.1A/Myc-His vector was from Invitrogen (Carlsbad, CA). The pGEM-T Easy Vector System II was from Promega (Madison WI). The wild-type prosaposin cDNA construct linked to a myc tag, designated as PSAP-WT, was generated in our laboratory (Figure II A) [17]. The primers PSAP-F (5'-aagcttatgtacgccctcgccctcttcgccag-3') and PSAP-R (5'-gaattcgttccacacatggcgtttg-3') were used for its amplification. The sortilin-myc construct was a gift from Dr. C. Petersen (University of Aarhus) (Figure II A).

2.1.4 Truncation Constructs and Primers

We have also produced six truncated prosaposin constructs (Figure II B). The first truncated prosaposin construct was designated P-75, where 25% of the DNA sequence encoding the A-type domain of the C-terminus was deleted from the 3'-end. This truncated prosaposin contained 75% of the C-terminus, lacking aa552-557. To achieve this deletion, a pair of primers, PSAP-F (5'-aagcttatgtacgccctcgccctcttcgccag-3') and P75-R (5'-cgccgtgaattcgcaatgatcgacagcattgcatc-3'), was used for PCR amplification.

The second truncated construct, P-50, lacked aa541-557 representing 50% of the DNA sequence encoding the C-terminus. The primers PSAP-F and P50-R (5'-gaattcctccatgttctgacaccagtag-3') were employed to attain the truncation.

The third construct, P-25, lacked 75% of the C-terminal end (aa532-557). The primers used for the amplification of P-25 were PSAP-F and P25-R (5'-agaagtgaattcgccccagacacacttctcggttc-3').

The fourth truncated construct P-0 lacked the entire A-type domain excluding the linker region (aa524-557). The primers used for the PCR amplification were PSAP-F and P0-R (5'-gaattccagcagcagcttataggcagaag-3').

The final truncated construct P-ΔC lacked the whole C-terminus (aa518-557), including the linker region connecting this domain to saposin D. The primers for P-ΔC amplification were PSAP and PΔC-R (5'-gaattcagaagggcaaactccaattttc-3'). All of the above constructs were produced following the same protocol employed for the generation of PSAP-WT.

Additionally, we engineered a truncated construct designated P-L50. Contrary to P-50, in which 50% of the DNA sequence encoding the A-type domain was deleted from the 3'-end, P-L50 lacked the first half of A-type domain on C-terminus (aa524-540). That is, the 50% of the DNA sequence was removed from the 5'-end of A-type domain. To generate P-L50 we employed the QuikChange Lightning Site-Directed Mutagenesis Kit. The pair of primers for P-L50 amplification was designed with the QuikChange Primer Design Program. The primers for P-L50 mutagenesis, which were complementary to each other, were PL50-1 (5'-tgcccttctgcctataagctgctgctgactgccgcccgatgcaatgctgtcgat-3') and PL50-2 (5'-atcgacagcattgcatcgggcggcagtcagcagcagcttataggcagaagggca-3').

2.1.5 Site-Directed Mutations of Hydrophilic Residues

Six site-directed mutations of hydrophilic residues in the C-terminus of prosaposin were generated by QuikChange II Site-Directed Mutagenesis (Figure III). For each mutation, one of the hydrophilic amino acids within the first half of the C-terminus was changed to the disfavoured substitute residue [324]. The site-directed mutations were K520F, E526F, K527F, Q537F, N538W, and E540F. The pairs of primers were designed with the QuikChange Primer Design Program. In each pair, the primers were complementary to each other. The pairs of primers for those mutations were as follow:

K520F: K520F-1 (5'-gtttgcccttctgcctatttcctgctgctgggaaccg-3') and K520F-2 (5'-cggttcccagcagcaggaaataggcagaagggcaaac-3')

E526F: E526F-1 (5'-gctgctgctgggaaccttcaagtgtgtctggggcc-3') and E526F-2 (5'-ggccccagacacacttgaaggttcccagcagcagc-3')

K527F: K527F-1 (5'-ctgctgggaaccgagttctgtgtctggggccct-3') and K527F-2 (5'-agggccccagacacagaactcggttcccagcag-3')

Q537F: Q537F-1 (5'-gccctagctactggtgtttcaacatggagactgccgc-3') and Q537F-2 (5'-gcggcagtctccatgttgaaacaccagtagctagggc-3')

N538W: N538W-1 (5'-ctagctactggtgtcagtggatggagactgccgcccg-3') and N538W-2 (5'-cgggcggcagtctccatccactgacaccagtagctag-3')

E540F: E540F-1 (5'-ctactggtgtcagaacatgttcactgccgcccgatgcaat-3') and E540F-2 (5'-attgcatcgggcggcagtgaacatgttctgacaccagtag-3')

2.1.6 Site-Directed Mutations of Hydrophobic Residues

Eight site-directed mutations in the C-terminus of prosaposin were generated by QuikChange Lightning Site-Directed Mutagenesis Kits (Figure VI). For each mutation, one of

the hydrophobic amino acids within the first half of the C-terminus was changed to the disfavoured substitute residue [324]. The site-directed mutations were C528D, W530A, W530P, P532W, P532H, W535A, W535P, and C536D. The pairs of primers were designed with the QuikChange Primer Design Program. In each pair, the primers were complementary to each other. The pairs of primers for those mutations were as follow:

C528D: C528D-1 (5'-ctgggaaccgagaaggatgtctggggccctag-3') and C528D-2 (5'-ctagggccccagacatccttctcggttcccag-3')

W530A: W530A-1 (5'-accgagaagtgtgtcgcgggccctagctactg-3') and W530A-2 (5'-cagtagctagggcccgcgacacacttctcggt-3')

W530P: W530P-1 (5'-gaaccgagaagtgtgtccctggccctagctactggtg-3') and W530P-2 (5'-caccagtagctagggccagggacacacttctcggttc-3')

P532W: P532W-1 (5'-gagaagtgtgtctggggctggagctactggtgtcagaac-3') and P532W-2 (5'-gttctgacaccagtagctccagccccagacacacttctc-3')

P532H: P532H-1 (5'-gtgtgtctggggccatagctactggtgtc-3') and P532H-2 (5'-gacaccagtagctatggccccagacacac-3')

W535A: W535A-1 (5'-tggggccctagctacgcgtgtcagaacatggag-3') and W535A-2 (5'-ctccatgttctgacacgcgtagctagggcccca-3')

W535P: W535P-1 (5'-gtctggggccctagctacccttgtcagaacatggagact-3') and W535P-2 (5'-agtctccatgttctgacaagggtagctagggccccagac-3')

C536D: C536D-1 (5'-ggggccctagctactgggatcagaacatggagactg-3') and C536D-2 (5'-cagtctccatgttctgatcccagtagctagggcccc-3')

2.2 Methods

2.2.1 Generation of Truncated Prosaposin

For sequential deletion of the C-terminus, a prosaposin cDNA was amplified by PCR with the corresponding primers. A HindIII restriction site was added into the 5'-end of the primer PSAP-F and an EcoRI restriction site into the 5'-end of PSAP-R. Subsequently, the purified PCR product was subcloned into the pGEM-T vector and transformed into DH-5α competent cells. The resulting prosaposin TA clone was purified with QIAprep Miniprep Kit and digested with HindIII and EcoRI restriction enzymes. After purification with QIAquick Gel Extraction Kit, the truncated prosaposin cDNA was ligated with the pcDNA 3.1A vector digested with HindIII and EcoRI enzymes. After the second round of transformation and purification, the resulting truncated prosaposin-myc construct was harvested.

2.2.2 Site-Directed Mutagenesis

The point-mutated prosaposin constructs were generated and amplified by PCR with QuikChange Lightning Enzyme and corresponding primers. After amplification, Dpn I restriction enzyme was added into PCR product and incubated at 37°C for 5 minutes to digest the parental DNA. The digested product was transformed into DH-5α competent cells and harvested with QIAprep Midiprep Kit.

2.2.3 Cell Culture

COS-7 cells were cultured in DMEM supplemented with 10% FBS, 5% penicillin and streptomycin, and 0.03% L-glutamine, overnight with 5% CO_2 at 37ºC to 40% (for confocal microscopy) or 80% confluence (for co-immunoprecipitation). All transfections were done with the PolyFect Transfection kit and incubated for twenty four hours prior to the harvesting of the cells.

2.2.4 Co-Transfection

Approximately 4×10^5 COS7 cells were seeded on 6-well plates, or 1.6×10^6 cells on 100mm dishes, and incubated for 24 hours. 0.75μg sortilin DNA and 0.75μg prosaposin DNA were mixed with 10μl PolyFect transfection reagent in DMEM to the final volume 100 μl for 6-well plates while 2μg sortilin DNA and 2μg prosaposin DNA mixed with 25μl PolyFect transfection reagent in DMEM to 300μl for 100mm dishes. After 10 minutes incubation at room temperature, the mixture were diluted with 0.6ml or 1ml DMEM, and transferred into the 6-well plates or 100mm dishes respectively. Then the cells were incubated for another 24 hours at 37°C and 5% CO_2 to allow for gene expression. Finally, the cells were subjected to confocal microscopy or harvested for Western-blotting and co-immunoprecipitation (CO-IP).

2.2.5 Sortilin-Prosaposin Binding Assay

COS-7 cells were co-transfected with the sortilin-myc plasmid and one of the following constructs: PSAP-WT, P-75, P-50, P-25, P-0, P-ΔC, P-L50, K520F, E526F, K527F, Q537F, N538W, E540F, or pcDNA3.1A empty vector. Twenty four hours after transfection the cells were harvested and lysed (50 mM Tris-HCl, 0.15M NaCl, 0.5% NP-40, and protease inhibitor cocktail, pH6.0). The cellular supernatants were incubated with protein A Sepharose beads coupled to anti-sortilin antibody at 4ºC overnight. The resulting protein-beads complexes were washed three times with washing buffer (50 mM Tris–HCl, 0.15M NaCl, pH6.0) and boiled in 3X SDS–PAGE loading buffer. Proteins were separated on a 10% SDS-PAGE gel, transferred to a nitrocellulose membrane and immunoblotted with anti-myc antibody diluted to 1:5,000. Anti-mouse secondary antibodies coupled to HRP were used at a dilution of 1:10,000. The desired protein bands were detected with ECL Plus Western Blotting Detection Reagents. This experiment was repeated three times.

2.2.6 Immuno-Confocal Microscopy

COS-7 cells were seeded onto cover slips in 6-well plates and cultured 24 hours. The cells were then transfected with PSAP-WT, P-70, P-50, P-25, P-0, P-ΔC, P-L50, K520F, E526F, K527F, C528D, W530A, W530P, P532W, P532H, W535A, W535P, C536D, Q537F, N538W, E540F, or pcDNA3.1A empty vector. After 24 hours, the cells were washed with 1 X PBS, fixed for 10 min in 4% paraformaldehyde, and then permeabilized with 0.25% Triton X-100 for 5 min. Subsequently, the cells were incubated for 1 h with 3% goat serum, 1:10 diluted BlokHen, and 0.1% Triton X-100. The incubation of double primary antibodies was performed at a 1:200 dilution overnight at 4 °C with chicken anti-myc antibody and mouse anti-LAMP-1 or anti-Golgin-97 antibody. The cells were washed with PBS and incubated with mixed secondary antibodies diluted to 1:400 (i.e., goat anti-mouse IgG antibody conjugated to Alexa 594 and fluorescein-labeled goat anti-chicken IgY antibody) for 1 h at RT. Then the cells were washed again with PBS and the nuclei were counter stained with 300 µl Hoechst 33342 (0.007 µg/µl). Finally, the cells were rinsed with PBS and water and mounted onto slides using ProLong Gold antifade reagent with DAPI. The immunofluorescent staining was visualized with an LSM 510 META confocal microscope from Carl Zeiss (Toronto, ON). These experiments were repeated at least five times.

2.2.7 Sortilin-Prosaposin pH-dependent Binding Assay

COS-7 cells were co-transfected with sortilin-myc and wild-type prosaposin-myc constructs. Twenty four hours after transfection the cells were harvested and lysed in lysis buffer (0.5% NP-40 and protease inhibitor cocktail in citric acid/Na_2HPO_4 buffer, pH 4.0, or 5.0, or 5.5, or 6.0, or 6.5, or 7.0). The supernatants were incubated with protein A Sepharose beads coupled to anti-prosaposin antibody 4ºC overnight. The beads were washed three times with washing buffer

(Citric acid/Na_2HPO_4 buffer, pH 4.0, 5.0, 5.5, 6.0, 6.5 or 7.0) and boiled in 3X SDS-PAGE loading buffer. After separation on a 10% SDS-PAGE gel, the proteins were transferred to a nitrocellulose membrane and immunoblotted with anti-sortilin antibody at a 1:2500 dilution. Anti-rabbit secondary antibody coupled to HRP was used at a 1:10,000 dilution. This experiment was repeated three times.

2.2.8 MG132 Proteasome Inhibition Assay

COS-7 cells were transfected with one of the following constructs: P532W, P532H, W535P, PSAP-WT, or pcDNA3.1A empty vector. After incubation with 5% CO_2 at 37ºC overnight, the cells were washed and incubated in DMEM containing 10 μM MG132 for additional 6 hours to inhibit the proteasome degradation pathway. After washing, the cells were lysed and the integrity of the prosaposin mutants was examined by SDS-PAGE detection. This experiment was repeated three times.

2.2.9 Statistic Analysis

The results of confocal microscopy were statistically analyzed using the SPSS 16.0 package. First, the number of vesicles stained by the LAMP-1 antibody (red) and the number of overlaid vesicles (yellow) stained by both anti-LAMP-1 and anti-myc antibodies in transfected cells were counted. Subsequently, the percentage of overlaid structures for each construct was calculated and analyzed with several statistic tests to determine whether the difference between the means of wild-type prosaposin and truncated/mutated prosaposin constructs were significant or not.

Before choosing a test to examine the statistical difference of the means, we performed One-Sample Kolmogorov-Smirnov analysis to examine the distributions of the data and the Levene test to check the homogeneity of variances. The application of both analytical methods allowed us to select either One-way ANOVA or Weltch t-test.

Chapter 3

Results

3.1 Effects of sequential truncations of the prosaposin C-terminus

3.1.1 Co-immunoprecipitation results

COS7 cells were co-transfected with sortilin and each one of the truncated prosaposin constructs P-ΔC, P-0, P-25, P-50, P-75, P-L50, and PSAP-WT. The cells were homogenized in lysis buffer (pH 6.0) and subjected to immunoprecipitation. The sortilin-prosaposin complexes were pulled down with anti-sortilin antibody and resolved on a 10% acrylamide gel. Anti-myc antibody was used in immunoblotting. In Figure 1A, the upper panel shows the bands of truncated and wild-type prosaposin pulled down by CO-IP. The lower two panels show the 2% input of sortilin and prosaposin proteins as loading controls. The middle panel shows sortilin in the crude cell lysates detected by Western-blotting while the bottom panel shows truncated and wild-type prosaposin in the crude lysates. In the middle panel, the sortilin bands were observed in each lane and all of them showed similar density, demonstrating that the protein loading amounts of all samples was roughly the same. The bottom panel shows that all of the truncated prosaposin constructs were expressed in the COS7 cells. The small variation in the migration of the bands was a reflection of the truncation sizes.

The upper panel demonstrates that the sequential truncations of prosaposin affected the bands of prosaposin pulled down by sortilin. In the lanes of P-ΔC, P-0 and P-25, no prosaposin bands were observed. On the other hand, in the lanes corresponding to P-50, P-75 and PSAP-WT

prosaposin bands were ostensible. The lane in the right (NC) was loaded with the lysate of cells co-transfected with wild-type sortilin and empty vectors as negative control.

Figure 1B illustrates the co-immunoprecipitation result of truncated prosaposin construct P-L50. In this figure, the lower two panels show the 2% input of sortilin and prosaposin in the crude lysates. The sortilin loading controls in the middle panel of Figure 1B showed similar densities, demonstrating that the amounts of protein in the three samples were the same. The bottom panel shows that P-L50 has a smaller size than PSAP-WT. The left lane corresponds to the negative control (NC) from cells co-transfected with PSAP-WT and empty vector.

The upper panel of Figure 1B shows the bands of prosaposin pulled down by sortilin. As expected, no band was observed in the negative control lane (NC). In the left lane, there was no P-L50 band either whereas in the middle lane the wild-type prosaposin band was ostensibly present.

3.1.2 Confocal microscopy observations

To verify whether or not the truncations affected the transport of prosaposin to the lysosomes, COS7 cells transfected with each prosaposin construct were examined by confocal microscopy after immunofluorescence labeling. Both the wild-type and truncated prosaposin constructs were stained in green with anti-myc antibody. The TGN and lysosomes were stained in red with anti-Golgin 97 antibody or anti-LAMP1 antibody respectively. The nuclei were counter stained in blue with Hoechst 33342.

Figure 2 shows the result obtained in COS7 cells transfected with wild type prosaposin (PSAP-WT). The micrographs of the top panels are representative fields of several experiments illustrating the vesicular and perinuclear staining of PSAP-WT in the cytoplasm of COS7 cells. The mid left micrograph shows a representative immunostaining of the Golgi apparatus of the

cultured cells which appear as globular perinuclear structures. The bottom left panel shows that the perinuclear Golgi staining of the TGN overlaids with PSAP-WT staining yielding discrete areas of glowing yellow. The mid right micrograph shows a representative vesicular staining of lysosomes with anti-LAMP1 antibody in the cytoplasm of COS7 cells. The bottom right panel shows that several of the green vesicular structures stained by the anti-myc antibody overlaid in yellow with the anti-LAMP1 immunostained lysosomes.

Figure 3 illustrates that transfection of COS7 cells with P75 produced similar staining patterns to that of PSAP-WT. Thus, the top micrographs are representative fields showing the vesicular and perinuclear staining of P75. The mid left micrograph illustrates the staining of the Golgi apparatus with the anti-Golgin 97 antibody. The bottom left panel showed that the perinuclear Golgi staining of the TGN overlaids with P75. Similarly, the mid right micrograph shows a representative vesicular staining of lysosomes with anti-LAMP1 antibody and the bottom right panel shows that several of the green vesicular structures stained by the anti-myc antibody overlaid in yellow with the anti-LAMP1 immunostained lysosomes.

Figure 4 demonstrates that transfection of COS7 cells with P50 also produced similar results to those of PSAP-WT and P75, since the perinuclear Golgi staining of the TGN overlaids with P50 (bottom left micrograph) and the vesicular lysosomes stained with the anti-LAMP1 antibody overlaid with several of the punctuate structures stained by the anti-myc antibody (bottom right micrograph).

When the COS7 cells were transfected with P-25, the recombinant truncated prosaposin was localized in the perinuclear region of these cells (Figure 5, top micrographs). The bottom pictures show that P-25 overlaid only with anti-Golgin 97 (left) but not with anti-LAMP1 staining (right).

Figure 6 illustrates representative fields of COS7 cells transfected with P-0. The staining pattern produced by the anti-myc antibody was similar to that of P50. In consequence, P0 immunostaining was only observed in the perinuclear region of transfected COS7 cells (top micrographs). The bottom images show that P0 overlaid only with anti-Golgin 97 (left) but not with anti-LAMP1 staining (right).

Figure 7 shows representative images of several experiments where COS7 cells were transfected with the negative control probe P-ΔC. As expected, P-ΔC was only observed in the perinuclear region of transfected cells (top images) and overlaid with anti-Golgin 97 antibody (bottom left micrograph) but not with anti-LAMP1 antibody (bottom right micrograph).

Figure 8 displays the confocal microscope results obtained in COS7 cells transfected with the construct P-L50. The images are representative of several experiments. P-L50 exhibited a similar distribution to those of P-25, P-0 and P-ΔC. Thus, P-L50 was observed in the perinuclear region of transfected COS7 cells (top micrographs) and was co-stained with anti-Golgin 97 (bottom left micrograph) but not with anti-LAMP1 (bottom right micrograph).

3.1.3 Statistical analysis of confocal microscope results

The confocal microscope studies were analyzed statistically. We first counted the number of overlaid vesicles (yellow granular structures) and the total number of LAMP-1 vesicles (both red and yellow granular structures) in the cells transfected with truncated or wild-type constructs. The overlaid yellow vesicles were regarded as endosomes and/or lysosomes containing both LAMP-1 (red) and prosaposin (green). The counting allowed us to calculate the percentage of overlaid LAMP-1/prosaposin for each cell. To analyze these results we performed first the One-Sample Kolmogorov-Smirnov Test to examine the distribution of the data before choosing the

appropriate statistical tests. The result showed that the data of both truncated and wild-type prosaposin constructs belonged to a Gaussian distribution (normal distribution). In statistical terms this was an indication that our data clustered around the mean values. Then we performed the Levene Test to check homoscedasticity and the analysis showed that the variances of the wild-type prosaposin data and truncated prosaposin data were different ($P<0.01$). Based on these two assumptions, we applied the Weltch t-test to determine whether or not the difference between the means of wild-type prosaposin construct and each of the truncated constructs was significant (Figure 9). The results showed that while P-ΔC, P-0, P-25 and P-L50 were significantly different from PSAP-WT ($P<0.01$), P-50 and P-75 were not ($P>0.05$) (Table 1).

3.2 Effect of pH on the Interaction of Prosaposin and Sortilin

The binding and dissociation between a soluble hydrolase and its sorting receptor are pH-dependant processes [325]. While a mild acidic compartment, such as the lumen of the TGN (pH 6.0), favours the binding of soluble hydrolases to the MPRs, the strong acidic environment of the endosomes and lysosomes (pH 5.0 or lower) induces their release from the MPRs [326-329].

To test the hypothesis that the binding of prosaposin to sortilin is also pH-dependent, we performed an *in vivo* pH-dependent assay. Since the amount of endogenous prosaposin and sortilin in the COS-7 cells is insufficient for co-immunoprecipitation assays, the cells were co-transfected with wild-type prosaposin and sortilin constructs. The transfected cells were homogenized in lysis buffer at pH 4.0, 5.0, 5.5, 6.0, 6.5 or 7.0. Non-transfected COS-7 cells were lysed at pH 6.0 and used as negative control. All samples were subjected to immunoprecipitation and contained equal concentration of lysate. The washing buffer for each sample had the same pH to that of the lysis buffer to keep the sample in a stable pH condition. The complexes pulled down by anti-prosaposin antibody were resolved on a 10% acrylamide gel. After transferring to a

nitrocellulose membrane, the samples were immunoblotted for both prosaposin and sortilin using anti-myc antibodies. In Figure 10, the lower bands correspond to the prosaposin pulled down by the anti-prosaposin antibody. Prosaposin was pulled down between pH 7.0 and pH 5.0 but not at pH 4.0, demonstrating that the immunoprecipitation was infective at pH 4.0. The upper bands correspond to co-immunoprecipitated sortilin. The results demonstrated that the presence and/or intensity of the sortilin bands varied at different pHs. Thus, the sortilin bands were intense at pH 7.0, pH 6.5 and pH6.0. The intensity of the sortilin band decreased at pH 5.5, and no sortilin bands were detected at pH 5.0 and pH 4.0.

3.3 Effects of site-directed mutations in the C-terminus of prosaposin

3.3.1 Site-directed mutations of hydrophilic residues

In this experiment we introduced six point mutations to hydrophilic amino acid residues in the first half of the C-terminus of prosaposin, bearing in mind that those residues might play key roles in the pH-dependent binding of prosaposin to sortilin. The point mutations were directed to several conserved polar amino acids in the first half of the A-type domain (Figure III) [52].

Each mutant probe (K520F, E526F, K527F, Q537F, N538W, and E540F) was co-transfected to COS-7 cells with the wild type sortilin construct and subjected to co-immunoprecipitation. After being pulled down with anti-sortilin antibody, the protein complexes were immunoblotted with anti-myc antibody. In Figure 11, the lower two panels show 1.5% input of sortilin and prosaposin in the crude lysates as loading controls. Both of them showed similar sizes and densities, demonstrating that the same amounts of proteins were loaded. The upper panel shows the prosaposin mutations pulled down by CO-IP. The last two lanes on the right correspond to a negative control (NC), which was loaded with the lysate of cells co-transfected with the empty vector and a positive control which was loaded with the lysate of cells co-transfected with the

wild type prosaposin construct (PSAP-WT). Our results showed that each of the prosaposin mutants (K520F, E526F, K527F, Q537F, N538W, and E540F) was pulled down by sortilin.

To investigate if the hydrophilic mutations affected the transport of prosaposin to the lysosomes, the COS7 cells were transfected with the mutated prosaposin constructs and immunostained with the anti-myc, the anti-Golgin 97 and the anti-LAMP-1 antibodies. Afterwards, the cells were examined by confocal microscopy.

Figure 12 shows a representative result of several experiments obtained with the K520F prosaposin mutant. The top panels illustrate the distribution of K520F stained with the anti-myc antibody. The middle panels show the staining of the TGN by anti-Golgin 97 antibody (left) or the staining of lysosomes by anti-LAMP1 antibody(right). The bottom panels are the overlaid images of the myc and Golgin 97 or the myc and LAMP1 immunostaining. The results demonstrated that K520F exhibited both vesicular and perinuclear staining and that it overlaids with both TGN and lysosomal staining.

Figure 13 is a representative result of several experiments obtained with the E526F prosaposin mutant. The results were similar to that of the K520F mutation. Thus, the E525 prosaposin mutant overlaid with structures stained by both Golgin 97 and LAMP1 antibodies.

In Figure 14, the K527F mutant also showed a granular and a perinuclear staining in the cytoplasm of the transfected COS7 cells. Similarly, the anti-myc stained structures overlaid with the same structures stained by the Golgin 97 and LAMP1 antibodies.

Figure 15 shows that Q537F mutant overlaid with both TGN and lysosomal structures too. Figure 16 and Figure 17 also show that the N538W and E540F point mutations did not alter the

distribution of prosaposin. Thus, both mutants were localized in vesicular structures and in the perinuclear region and overlaid with anti-LAMP1 and anti-Golgin 97 staining.

In order to check whether or not there was a significant difference between wild-type prosaposin construct and each of these mutations, we calculated the percentage of overlaid LAMP-1/prosaposin for each cell transfected with those site-directed mutations. One-Sample Kolmogorov-Smirnov Test was performed to analyze the distribution of the data. The result confirmed that the collected values exhibited a Gaussian distribution. The application of the Levene Test showed that the variances of the data did not present significant difference ($P>0.05$), indicating that the values were homoscedastic. Based on these results, we chose One-way ANOVA to determine if the differences between the mean of data (i.e., the percentages of LAMP1 structures labelled with wild-type and each mutated prosaposin) were significant or not. The result of ANOVA demonstrated that all of the mutations (K520F, E526F, K527F, Q537F, N538W, and E540F) were not significantly different from PSAP-WT ($P>0.05$) (Figure 18, Table 2).

3.3.2 Site-directed mutations of hydrophilic residues

Since the hydrophilic residue mutations had no effect on the binding of prosaposin to sortilin, we further introduced eight additional point mutations to hydrophobic residues in the first half of the A-type domain, C528D, W530A, W530P, P532W, P532H, W535A, W535P and C536D (Figure VI).

We performed western blot analysis to check the expression of those mutations. The analysis did not detect bands for the mutations W535P, P532W and P532H, indicating that they

abolished the expression of prosaposin (Figure 19). On the other hand, the mutations C528D, W530A, W530P, W535A, and C536D generated normal prosaposin bands (Figure 19).

Next, we performed confocal microscopy to examine the intracellular distribution of the mutated prosaposin constructs.

Figure 20 illustrates that C528D was only present in the perinuclear region of transfected cells (top panels). The bottom panels show that the anti-myc perinuclear staining overlaid with anti-Golgin 97, but rarely with vesicular structures stained by anti-LAMP-1. In Figure 21-24, the distribution of W530A, W530P, W535A, and C536D were all similar to that of C528D, indicating that the hydrophobic mutations affected the sorting and targeting of prosaposin to the lysosomes.

We collected the data of the percentage of overlaid LAMP-1/prosaposin for each cell transfected with the mutations described above. After performing the One-Sample Kolmogorov-Smirnov Test and Levene Test, we found that the values were not homoscedastic, and presented significant variances ($P<0.05$) and a Gaussian distribution. Based on these results, we performed the Weltch t-test and found that all of the hydrophobic mutations C528D, W530A, W530P, W535A, and C536D presented significantly lower number of anti-myc/anti-LAMP-1 overlaid vesicles than that of PSAP-WT ($P<0.01$) (Figure 25, Table 3).

The cells transfected with mutant W535P, P532W and P532H did not produce fluorescence signal, confirming the lack expression of these constructs (Figure 26).

3.3.3 MG132 Proteasome Inhibition Assay

Since W535P, P532W and P532H were not expressed, we assumed that those mutations probably resulted in unstable protein structure degraded via the endoplasmic reticulum-

associated protein degradation (ERAD) pathway. To verify this assumption, we performed the MG132 proteasome inhibition assay, in which MG132 was used to inhibit the proteasome function and therefore to block ERAD pathway. In Figure 27, the upper panel showed the MG132-treated samples while the lower panel the samples without MG132 treatment. The cells transfected with empty vectors were used as negative controls. In the lower panel, the bands of W535P, P532W and P532H without MG132 treatment did not appear. However, after MG132 treatment, W535P, P532W and P532H generated bands (upper panel) and the intensity of PSAP-WT increased dramatically due to the proteasome inhibition. As expected the negative controls did not yield bands before or after MG132 treatment.

Chapter 4

Discussions

4.1 Intracellular trafficking of prosaposin

Prosaposin is the product of a single gene that has been shown to follow multiple intracellular pathways [144, 169, 330, 331]. In addition to its well known lysosomal trafficking pathway, prosaposin may be routed and secreted to the extracellular space and subsequently internalized to the lysosomes via endocytic flow [330, 331]. Igdoura et al. were the first to show that lysosomal prosaposin and secretory prosaposin have different molecular weights [332]. While the former possesses a size of 65kD the latter has a size of 70kD due to differences in glycosylation [332]. The size of unglycosylated prosaposin is approximately 55kD [332]. The 65kD lysosomal isomer is partially glycosylated and sensitive to Endo H treatment [17]. The lysosomal isomer also associates with inner leaflet of the TGN membrane and travels to the lysosomes [17, 139]. The 70kD prosaposin is terminally glycosylated and resistant to Endo H treatment [17]. This isoform aggregates in a distal compartment of the Golgi apparatus and is secreted to the extracellular space [139]. The aggregation of the 70kD prosaposin seems to depend on the mild acidic environment (~pH6.4) and on the calcium ion concentration [139]. In fact, this mechanism of aggregation has been observed in several regulated secretory proteins [333]. Nonetheless, the question on how glycosylation changes the fate of prosaposin targeting requires further elucidation.

The prosaposin gene has a small 9 bp exon (exon 8), which encodes three extra amino acid residues (QDQ) [52, 145]. Interestingly, this exon may be alternatively spliced in a tissue specific manner. According to Zhao et al. prosaposin found in muscle, heart and brain contained the QDQ insertion but not in testis, lung, pancreas, spleen, and kidney [145]. Madar-Shapiro et al. reported that the QDQ residues may affect the transport of prosaposin to the lysosomes or to the extracellular space. These authors suggested that a prosaposin with the extra residues is usually secreted out of the cells while a prosaposin without QDQ is transported to the lysosomes [160]. However, in brain tissues where the QDQ insertion is present, prosaposin was also found in the lysosomes of neurons [175]. Thus, the real function of the QDQ residues in the trafficking of prosaposin requires further clarification.

Sphingomyelin is thought to be involved in the lysosomal trafficking of prosaposin [334]. Our laboratory found that fumonisin B1 and D609, which block the synthesis of ceramide and sphingomyelin respectively, decreased the content of prosaposin in the lysosomes [334]. Conversely, the addition of sphingomyelin to fumonisin B1 and D609 treated cells restored the trafficking prosaposin to the lysosomes [335]. It is accepted that sphingomyelin is one of the main components of lipid rafts, which confers resistance to detergent extraction to discrete regions of biological membranes [336]. These detergent-resistant membranes (DRMs) are organized microdomains of cell membrane bilayer enriched in cholesterol, saturated phospholipids, sphingolipids and specific proteins [336]. Prosaposin was found to be transported to the lysosomes through DRMs [335]. This observation was supported by the presence of prosaposin in the DRMs along with its sorting protein, sortilin [18].

In addition, Grassel et al. found that prosaposin was associated with the precursor of cathepsin D, procathepsin D (proCD), *in vivo* [337]. Both 70kD and 65kD prosaposin

specifically bind to proCD after synthesis and their association is maintained during the intracellular trafficking, either during the secretory pathway or during the MPR-independent lysosomal targeting pathway [141, 338]. The association of prosaposin and cathepsin D during the secretory pathway was also reported by Campana et al., who demonstrated that the secretion pattern of both prosaposin and proCD over time were similar [209]. However, during the endocytosis process, prosaposin and proCD are internalized separately, mediated by different cell surface receptors. The endocytosis of prosaposin is mainly mediated by the low density lipoprotein receptor-related protein-1 (LRP) while the internalization of proCD is mediated by MPRs [339]. Recently prosaposin was found to spontaneously bind to proCD with strong affinity at acidic pH. Under this condition prosaposin is in an oligomer form while proCD maintains a monomer form [340]. Although this spontaneous and strong interaction might play an important role in the intracellular trafficking of these molecules [340], more studies are required to unfold the significance of this process.

Burkhardt et al. found that secreted prosaposin was endocytosed by fibroblasts and transported to the lysosomes, where it was cleaved into mature saposins, in a similar fashion to the classical processing of prosaposin delivered from the Golgi apparatus [341]. The endocytosis of prosaposin also occurs in testis, where the prosaposin secreted by Sertoli cell is internalized by nonciliated cells in the efferent ducts [342]. Prosaposin internalization is mediated by the multifunctional cell surface receptor, the low density lipoprotein receptor-related protein-1 and -2 (LRP) [162]. The trafficking of prosaposin by LRP is negatively regulated by LRP adaptor protein, GULP [343]. Overexpression of GULP resulted in the mistargeting of prosaposin into all kinds of intracellular compartments while the knockdown of GULP enhanced the targeting of prosaposin to the lysosomes [343]. In addition to LRP, the mannose-6-phosphate receptor is also

involved in the endocytosis of secreted prosaposin [162]. Hence, the intracellular trafficking of prosaposin may follow distinct pathways.

4.2 Role of prosaposin C-terminus

Sphingolipid activator proteins (SAPs) are soluble co-factors involved in the lysosomal degradation of glycosphingolipids [50]. SAPs act as biological detergents by facilitating the interaction of glycosphingolipid substrates with their respective enzymes for degradation, since glycosphingolipids with short saccharide chains are unable to interact directly with their hydrolytic enzymes in a hydrosoluble milieu [15, 39, 50, 344]. SAPs include 5 activator proteins, the GM_2 activator protein (GM_2AP) and saposins A, B, C, and D [50]. Saposins resemble each other in that they are all composed of approximately 80 amino acids, that they are glycosylated, and that they all have six conserved cysteines forming three internal disulfide bridges [9, 15, 345]. Unlike the $G_{M2}AP$, saposins A-D derive from the common precursor prosaposin [157]. Since each saposin constitutes a functional unit within the prosaposin molecule, they are classified as B-type domains before prosaposin is hydrolyzed into four smaller mature proteins, saposins [14].

In addition to B-type domains, prosaposin possesses two smaller peripheral regions in the N- and C-terminus referred as A-type domains [14]. A-type domains contain 34 amino acids, i.e., approximately half length of B-type domains [13, 14]. Each A-type domain contains 4 conserved cysteines. To our knowledge the crystal structure of the A-type domains are not known. Therefore the structural role of the four cysteines has not been assessed. Experimental data generated by another lab suggested that prosaposin may form complexes *in vivo* [340]. Thus, we performed experiments to examine whether prosaposin forms oligomers or not. Through reducing and non-reducing SDS-PAGE, we found that prosaposin oligomers were broken down

by the reducing reagent 2-ME, suggesting that intermolecular disulphide bonds may be involved in the oligomerization of prosaposin. Since all of the cysteines in the B-type domains form intramolecular disulphide bonds [9, 15, 345], we proposed that the cysteines presented in the N- and/or C-termini of the molecule might contribute to the formation of the intermolecular bridges.

In a previous comparative study on the structure of human, mouse and rat prosaposin our lab found that the D-domain and the C-terminus were the most conserved regions among the three species with more than 90% of sequence identity [52]. Thus, the high level of conservation suggests that this region carries a critical function. In fact, our laboratory showed that the C-terminus is required for the transportation of prosaposin to the lysosomes [17].

It is accepted that soluble lysosomal proteins are sorted within the TGN by a sorting receptor and that the ligand-receptor complex is tethered to the lysosomes by accessory proteins that interact with the sorting receptor [346, 347]. Recently, our laboratory demonstrated that unlike the majority of soluble hydrolases, which are transported via the MPRs, prosaposin is translocated to endosomes via the alternative receptor, sortilin [161].

Interestingly, deletion of the C-terminus of prosaposin blocked its lysosomal targeting without disturbing its secretion. On the other hand, the deletion of N-terminal domain or any saposin domain did not affect either the lysosomal trafficking or secretion. A chimeric albumin linked with the C terminus and saposin D domain of prosaposin could be transported to the lysosomes. The addition of the prosaposin C-terminus to albumin induced the binding of the chimeric protein to sortilin, the penetration of the complex within detergent resistant microdomains and the targeting of albumin to the lysosomes [17]. Therefore, preliminary evidence suggests that the lysosomal trafficking of prosaposin requires the C terminus and at least one saposin domain [17].

This observation led us to propose a model in which a specific domain within the C-terminal region of prosaposin interacts with the luminal domain of sortilin [161]. However, the precise nature of this interaction, as well as the intervening domains of these molecules, is still unknown. Interestingly, the saposin-like motif of prosaposin C-terminus is similar to the A-type domain found in the N-terminus of the surfactant B associated protein [14], which has been implicated in the transport of this protein to the lamellar bodies of type II pneumocytes [348]. Therefore, the elucidation of the recognition process between prosaposin and sortilin is important to understand the mechanism of this interaction.

4.3 Effects of sequential truncations of the prosaposin C-terminus

The objective of this investigation was to identify the specific domain within the C-terminus of prosaposin implicated in its binding to sortilin. To accomplish this objective, six truncated prosaposin constructs were generated by deleting specific regions of the C-terminus. Before engineering these constructs, we analyzed the predicted secondary structure of the C-terminus using EMBOSS Garnier [349]. The EMBOSS output file predicted the existence of two α-helices within the C-terminus. The first helix is localized to the linker region between aa518-523, and the second between aa540-550. Between the two helixes there were several turns (aa524-539). Based on the predicted secondary structure we proposed that prosaposin C-terminus might form a "hairpin" structure.

Thus, the generation of the truncated constructs was based on the information obtained from the EMBOSS Garnier program. For the first construct P-75, we deleted the C-terminal region immediately after C551 to prevent the disruption of the potential α-helixes and the elimination of cysteines. In construct P-50, the deleted sequence spanned between aa541-557. In this case, the second helix (E540 to H550) was eliminated. In P-25, the deletion spanned between aa531-557,

with the elimination of two cysteine residues. The construct P-0 lacked the entire A-type domain (aa524-557). The final construct, P-ΔC, was a truncated prosaposin lacking the entire C-terminus and the linker that connects this region to saposin D (aa518-557).

The effect of these truncations on the binding to sortilin was examined by co-immunoprecipitation. The results surprisingly showed that P-75 and P-50 were able to bind to sortilin. The confocal microscopy results also demonstrated that P-75 and P-50 were both transported to lysosomes. Therefore, it was suggested that the second helix was not responsible for the binding of prosaposin to sortilin. The elimination of the terminal half of the A-type domain (aa541-557), including the second α-helix, did not affect the binding of prosaposin to sortilin and/or its transport to the lysosomes.

On the other hand, the co-immunoprecipitation assays demonstrated that P-25, P-0 and P-ΔC could not be pulled-down by sortilin. The confocal microscopy also showed that none of the three truncated prosaposins were transported to the lysosomes, confirming that the elimination of the first half of the A-type domain (aa524-540), which contains 17 amino acids located between the two α-helices, abolished the trafficking of this protein to the lysosomal compartment.

Furthermore, we generated an additional construct P-L50 to confirm or discard this conclusion. In P-L50, the terminal half of the A-type domain was directly linked to the D-domain. Therefore this prosaposin construct also lacked the first half part of the A-type domain. We found that P-L50 was not able to bind to sortilin or to be transported to the lysosomes.

Therefore, we concluded that the stretch of 17 amino acids (aa524-540) on the C-terminus, which is formed by several turns according to the predicted structure, is responsible for the lysosomal transportation of prosaposin.

4.4 Effect of pH on the interaction of prosaposin and sortilin

Most of the organelles of the intracellular vacuolar system, including the Golgi apparatus, endosomes, lysosomes and coated vesicles, are acidic and the pH of those organelles varies from neutral to extreme acidic pHs [325]. The Golgi apparatus has a mildly acidic pH, which is progressively decreased from the cis-Golgi network (CGN) to the trans-Golgi network (TGN) [350]. For example, the average pH of the Golgi complex is 6.4 while the pH of the TGN is 5.91 in Hela cell [328, 351]. Although the pH of the TGN varies within a small range in different cell lines, most cells have a pH value of 6.0 [352]. The endosomes, consisting of heterogeneous vacuolar and tubular vesicles in the peripheral and perinuclear cytoplasm[353], are also acidic with an average pH 5.5-6.0, which is decreased to pH 5.0 when they are transformed in lysosomes [325, 354]. The lysosomes are the most acidic subcellular compartments, the pH of which ranges from 4.5 to 5.0 [327, 329, 355].

The acidic environment is critical for maintaining a number of cell biological processes, including protein modifications within the Golgi apparatus, intracellular trafficking in endocytic and exocytic pathways, and lysosomal digestion [325]. The binding and dissociation of ligand and receptors are also affected by the pH of endosomes. The acidic pH induces conformational changes of receptors and ligands to facilitate their dissociation [356]. Generally, receptors bind to their ligands with high affinity at neutral pH and with lower affinity in mildly acidic pH like in the late recycling endosomes, where they dissociate from the ligands to be sent to the cell surface. On the other hand, the ligands are incorporated into the lysosomes for their degradation [325]. Therefore the acidic pH of endosomes regulates the recycling of receptors and the elimination of ligands [325].

Based on the fact that most ligand-receptor interactions depend on small pH shifts [325], we proposed that the pH also regulated the binding of prosaposin to sortilin in the Golgi apparatus and its dissociation in the endosomes. Thus, we tested whether or not the binding of prosaposin to sortilin was pH-dependent through a co-immunoprecipitation assay. The result of CO-IP demonstrated that the binding of prosaposin to sortilin occurred at a pH higher than 6.0. A substantial decrease in binding affinity was detected at pH 5.5, where prosaposin was weakly associated with sortilin. Conversely, at the pH 5.0, both proteins did not form complexes. This result indicated that the binding of prosaposin to sortilin was pH-dependent. Therefore, our findings suggested that the mild acidic environment of the TGN (pH 6.0) favours the association of prosaposin to sortilin, whereas the strong acidic environment of the endosomes (pH 5.5) promotes the dissociation of prosaposin from sortilin. Our results also suggest that in the lysosomes (pH 5.0), prosaposin is completely liberated from its receptor to produce mature saposins by proteolysis.

4.5 Effects of hydrophilic residue mutations in prosaposin C-terminus

It is accepted that hydrophilic amino acids found at the surface of water-soluble proteins contribute to their solubility and form binding sites for charged molecules [357]. A soluble globular protein requires the interaction of polar residues on the surface with water molecules for solubility [358]. As a consequence, small shifts of cellular pH may affect the charge of hydrophilic amino acids and modulate the binding properties of soluble proteins [357]. Since prosaposin is a soluble globular protein and its binding to sortilin appears to be a pH-dependent process, we presupposed that the acidic pH affects their binding through the hydrophilic amino acids. Thus, the acidic pH shifts may affect the surface charge of prosaposin C-terminus, induce its conformational change and result in the dissociation of this domain to sortilin.

The sequence analysis of the C-terminus revealed the presence of a saposin-like motif composed of two α-helices separated by several turns. Our sequential deletion experiments demonstrated that the first half of C-terminus formed by those turns is essential for its binding to sortilin. Therefore, the tertiary structure of this 17-residue stretch is probably modulated by pH shifts affecting the hydrophilic amino acids of this stretch that appear to be responsible for the binding of prosaposin to sortilin. Based on this assumption, we generated six point mutations of conserved polar amino acid residues within this stretch, replacing a hydrophilic amino acid with a hydrophobic residue, to examine whether a peripheral polar amino acid is essential for the lysosomal transport of prosaposin.

To our surprise, the introduction of hydrophilic residue mutations did not alter the binding of prosaposin to sortilin and did not affect the trafficking of prosaposin to the lysosomes. A recent study on the N-terminus of surfactant protein B (SP-B) precursor, which contains a saposin A-type domain responsible for the intracellular sorting of SP-B [348], suggested that this region is susceptible to pH-dependent conformational changes [359, 360]. In fact, pH variations have been shown to induce conformational changes in all four saposins [114]. Therefore these studies indicated that saposin domains, including both A-type domain and B-type are susceptible to conformational changes by acidic pH shifts. In this context, a plausible interpretation of our results is that the conformation of prosaposin C-terminus was also affected by acidic pH. But this conformational change was probably mediated by an effect on the total surface charge on the 17-residue stretch of C-terminus and not by a one amino acid. Thus, a single hydrophilic residue mutation was probably insufficient to elicit an effect on the binding of prosaposin to sortilin and on the lysosomal trafficking of prosaposin.

4.6 Effects of hydrophobic residue mutations in prosaposin C-terminus

In addition to the distribution of charged hydrophilic residues on the protein surface, which may be responsible for pH-induced conformational changes, hydrophobic amino acids are also important for the stabilization of protein structure and protein-protein interaction [324]. One of the most important amino acids is tryptophan. Tryptophan is a relatively rare bulky aromatic residue. In most proteins tryptophan is located at one or a few highly conserved positions [361]. The N-terminus and the saposin A domain of prosaposin contain a single conserved tryptophan respectively while saposins B, C and D domains lack tryptophan residues [73]. Interestingly prosaposin C-terminus possesses three tryptophans residues and two of them are localized in the first half of the A-type domain.

Tryptophans are often found buried inside of protein forming a hydrophobic core [362]. Hydrophobic core are implicated in the maintenance of native structure and function of proteins [363-365]. However, tryptophan residues may be found on the surface of certain proteins participating in protein interactions [362, 366-368]. In fact, tryptophan is the top ranking residue in hot spots of protein-protein binding [324, 369]. Its unique roles in the stabilization of protein tertiary structure and in protein-protein interactions are attributed to its aromatic side chain and bulky size [370]. Existing evidence suggest that tryptophan residues within the saposin A-type domain on N-terminus of the SP-B precursor are responsible for the conformational change of this protein induced by low pH [359].

Based on this information we hypothesized that the tryptophan residues within the 17-residue stretch of prosaposin A-type domain on C-terminus may be critical for the lysosomal targeting of this protein. According to our hypothesis subtle pH changes may induce a conformational change in the C-terminus of prosaposin affecting its binding to sortilin. To test

this hypothesis we introduced four mutations to the highly conserved tryptophan residues 530 and 535 in this region (W530A, W530P, W535A and W535P). We replaced the tryptophans with either alanines or prolines, which are smaller amino acids without aromatic side chains. The intracellular targeting of the mutated prosaposins was examined confocal microscopy. The results showed that W530A, W530P and W535A mutations blocked the lysosomal trafficking of prosaposin. Surprisingly, the W535P mutant was not expressed by the COS-7 cells.

Our results demonstrated that W530 and W535 were critical for the lysosomal trafficking of prosaposin. Tryptophans have been implicated in the pH-dependent conformational change of SP-B precursor [359], and it is plausible that W530 and W535 may play a similar role in the C-terminus of prosaposin. Based on our results we propose that the C-terminus is susceptible to a pH-dependent conformational change via W530 and W535 that favours or disfavours the binding of prosaposin to sortilin.

In addition to tryptophan, cysteine is also an important amino acid. Cysteine contains a thiol group on the side chain which is implicated in the formation of disulphide bonds [324]. The formation of disulfide bonds is essential for proper folding and stability of proteins [371]. Within the reducing intracellular environment, cysteine is usually found at protein active and binding site [324].

Consequently, we introduced two mutations C528D and C536D by replacing the cysteines in the C-terminus of prosaposin with aspartates and examined whether or not these cysteine residues were critical for prosaposin targeting. As expected, both of the mutations significantly decreased the transport of prosaposin to the lysosomes, indicating that both cysteines were essential for the lysosomal trafficking of prosaposin. Although cysteines are usually not directly involved in protein-protein interactions, these amino acid residues might form disulfide bonds

that stabilize the tertiary structure of prosaposin C-terminus and contribute to the formation of the recognition site for sortilin. Thus, the cysteine mutations probably changed the conformation of the C-terminus and resulted in the abrogation of prosaposin binding to sortilin and in the inhibition of prosaposin targeting to the lysosomes.

We also mutated the only proline of the C-terminus. Proline is considered very important for protein structure. Proline has a nitrogen-containing cyclic structure, in which the side chain connects to the protein backbone twice. This distinctive five-membered ring gives proline an exceptional conformational rigidity. Therefore, proline often acts as a structural disruptor and introduces tight turns on protein backbones [324, 372]. During protein synthesis, proline also plays a key role in the proper folding of newly formed proteins [373]. We introduced two mutations to the proline residues (P532W and P532H) on the C-terminus by replacing the prolines with either the bulky amino acid residue tryptophan or with the positively charged amino acid histidine [324]. Both mutations abolished the expression of prosaposin and were not detected by either Western-blot analysis or by immunofluorescence microscopy.

Our results suggest that both mutations induced the misfolding of the defective prosaposins in the endoplasmic reticulum. Misfolded proteins are usually recognized by a quality control system in ER, which is called ER-Associated Degradation (ERAD) system [374], and transported from ER lumen back to the cytoplasm. After ubiquitination in the cytoplasm, these proteins are conveyed to proteasomes for degradation [375]. Considering the unique function of proline in protein structure, we tested the hypothesis that the lack of prosaposin expression was the result of misfolding and proteasome degradation. To test this hypothesis, we performed the MG132 Proteasome Inhibition Assay, in which the transfected cells with the mutant probes were treated with the proteasome inhibitor, MG132 [376]. As expected, we visualized the presence of

the mutated prosaposins by Western blot analysis after MG132 treatment. Thus, the result confirmed that proline 532 was critical for the stability of prosaposin and that the proline mutations resulted in the rapid degradation of the defective prosaposins.

4.7 General conclusions

For a number of years the main interest of our laboratory has been the identification of the mechanism of prosaposin targeting to the lysosomes. A previous investigation showed that the prosaposin C-terminus is responsible for the binding of this protein to the sorting receptor sortilin in the Golgi apparatus and that this interaction results in the lysosomal targeting of prosaposin [17].

The objective of the present research was the identification of the actual binding site of prosaposin to sortilin. We have determined that the binding region of prosaposin is located within a 17-residue peptide stretch (aa524-540), localized on the first half of the C-terminus.

Furthermore, our research demonstrated that this region binds to sortilin in a pH-dependent manner. We showed that the C-terminus is probably susceptible to pH-induced conformational changes, by which prosaposin might expose or bury the binding site for sortilin to favor or disfavor the interaction with this receptor. Unexpectedly we found that the hydrophilic residues were not critical for this interaction.

We observed that tryptophans W530 and W535 were essential for the lysosomal trafficking of prosaposin, suggesting that they might be involved in pH-induced conformational change that appears to affect the interaction between prosaposin and sortilin.

And finally, our research demonstrated that the proline P532, the cysteines C528 and C536 were indispensable for prosaposin expression and trafficking. We found that proline 532 probably plays a role in proper folding of prosaposin in the ER and that its mutation leads to the

degradation of the molecule. On the other hand, our research suggested that the cysteines probably function in the stabilization of the prosaposin tertiary structure by forming disulfide bridges.

In conclusion, our investigation identified the binding region of prosaposin to sortilin and disclosed the essential residues implicated in the formation of ligand-receptor complexes. These observations will contribute to the identification of the sortilin binding site by computational methods.

4.8 Future Directions

The combination of protein truncation, site-directed mutagenesis and *in silico* analysis will allow us to identify the potential recognition site of sortilin and to design small prosaposin molecules with homogeneous structure that will be used to test the binding model.

Original Contributions

We have shown for the first time that the binding of prosaposin to sortilin is pH dependent. At pH 6.0 and above prosaposin binds to sortilin and at pH 5.5 and lower prosaposin dissociates from sortilin.

We have demonstrated that a region of 17 amino acids (aa524-540) located in the first half of the prosaposin C-terminus is critical for its binding to sortilin and its targeting to the lysosomes.

Using mutational analyses we have provided the following original information:

1) Deletion of the first half of prosaposin C-terminus abolished the binding of prosaposin to sortilin and the trafficking of prosaposin to the lysosomal compartment.

2) Deletion of the last half of prosaposin C-terminus did not affect the binding of prosaposin to sortilin and the trafficking of prosaposin to the lysosomal compartment.

3) Replacement of the active region of 17 amino acids with the second half of prosaposin C-terminus did not restore the trafficking of prosaposin to the lysosomes.

4) Site-directed mutagenesis of single hydrophilic amino acids in in the first half of the prosaposin C-terminus did not affect the trafficking of prosaposin to the lysosomes.

5) Site-directed mutagenesis of five single hydrophobic residues in the same segment produced the following effects:

A) Mutations of tryptophans W530A and W535A and cysteines C528D and C536D blocked lysosomal transport to prosaposin.

B) Mutation of proline P532H affected the stability of prosaposin during its synthesis and induced its degradation via the endoplasmic reticulum-associated protein degradation (ERAD) pathway.

Reference

1. Dahms, N.M., P. Lobel, and S. Kornfeld, *Mannose 6-phosphate receptors and lysosomal enzyme targeting.* J Biol Chem, 1989. **264**(21): p. 12115-8.
2. Geuze, H.J., et al., *Possible pathways for lysosomal enzyme delivery.* J Cell Biol, 1985. **101**(6): p. 2253-62.
3. Gabel, C.A., D.E. Goldberg, and S. Kornfeld, *Identification and characterization of cells deficient in the mannose 6-phosphate receptor: evidence for an alternate pathway for lysosomal enzyme targeting.* Proc Natl Acad Sci U S A, 1983. **80**(3): p. 775-9.
4. Petersen, C.M., et al., *Molecular identification of a novel candidate sorting receptor purified from human brain by receptor-associated protein affinity chromatography.* J Biol Chem, 1997. **272**(6): p. 3599-605.
5. Nielsen, M.S., et al., *The sortilin cytoplasmic tail conveys Golgi-endosome transport and binds the VHS domain of the GGA2 sorting protein.* Embo J, 2001. **20**(9): p. 2180-90.
6. Marcusson, E.G., et al., *The sorting receptor for yeast vacuolar carboxypeptidase Y is encoded by the VPS10 gene.* Cell, 1994. **77**(4): p. 579-86.
7. Ni, X. and C.R. Morales, *The lysosomal trafficking of acid sphingomyelinase is mediated by sortilin and mannose 6-phosphate receptor.* Traffic, 2006. **7**(7): p. 889-902.
8. Canuel, M., et al., *AP-1 and retromer play opposite roles in the trafficking of sortilin between the Golgi apparatus and the lysosomes.* Biochem Biophys Res Commun, 2008. **366**(3): p. 724-30.
9. Morimoto, S., et al., *Saposin D: a sphingomyelinase activator.* Biochem Biophys Res Commun, 1988. **156**(1): p. 403-10.
10. Morimoto, S., et al., *Saposin A: second cerebrosidase activator protein.* Proc Natl Acad Sci U S A, 1989. **86**(9): p. 3389-93.

11. Stastny, J.J., et al., *Production and characterization of a monoclonal antibody to human saposin C.* Hybridoma, 1992. **11**(3): p. 351-9.

12. Hiraiwa, M., et al., *The effect of carbohydrate removal on stability and activity of saposin B.* Arch Biochem Biophys, 1993. **303**(2): p. 326-31.

13. Kishimoto, Y., M. Hiraiwa, and J.S. O'Brien, *Saposins: structure, function, distribution, and molecular genetics.* J Lipid Res, 1992. **33**(9): p. 1255-67.

14. Patthy, L., *Homology of the precursor of pulmonary surfactant-associated protein SP-B with prosaposin and sulfated glycoprotein 1.* J Biol Chem, 1991. **266**(10): p. 6035-7.

15. O'Brien, J.S. and Y. Kishimoto, *Saposin proteins: structure, function, and role in human lysosomal storage disorders.* Faseb J, 1991. **5**(3): p. 301-8.

16. Sandhoff, K., T. Kolter, and G. Van Echten-Deckert, *Sphingolipid metabolism. Sphingoid analogs, sphingolipid activator proteins, and the pathology of the cell.* Ann N Y Acad Sci, 1998. **845**: p. 139-51.

17. Zhao, Q. and C.R. Morales, *Identification of a novel sequence involved in lysosomal sorting of the sphingolipid activator protein prosaposin.* J Biol Chem, 2000. **275**(32): p. 24829-39.

18. Canuel, M., et al., *Sortilin and prosaposin localize to detergent-resistant membrane microdomains.* Exp Cell Res, 2009. **315**(2): p. 240-7.

19. Hakomori, S., *Glycosphingolipids in cellular interaction, differentiation, and oncogenesis.* Annu Rev Biochem, 1981. **50**: p. 733-64.

20. Hannun, Y.A. and L.M. Obeid, *The Ceramide-centric universe of lipid-mediated cell regulation: stress encounters of the lipid kind.* J Biol Chem, 2002. **277**(29): p. 25847-50.

21. Spiegel, S. and A.H. Merrill, Jr., *Sphingolipid metabolism and cell growth regulation.* Faseb J, 1996. **10**(12): p. 1388-97.

22. Hakomori, S., *Structure, organization, and function of glycosphingolipids in membrane.* Curr Opin Hematol, 2003. **10**(1): p. 16-24.

23. Stoffel, W., *Sphingolipids.* Annu Rev Biochem, 1971. **40**: p. 57-82.

24. Stults, C.L., C.C. Sweeley, and B.A. Macher, *Glycosphingolipids: structure, biological source, and properties.* Methods Enzymol, 1989. **179**: p. 167-214.

25. Macher, B.A. and C.C. Sweeley, *Glycosphingolipids: structure, biological source, and properties.* Methods Enzymol, 1978. **50**: p. 236-51.

26. Curatolo, W., *The physical properties of glycolipids.* Biochim Biophys Acta, 1987. **906**(2): p. 111-36.

27. Steinman, R.M., et al., *Endocytosis and the recycling of plasma membrane.* J Cell Biol, 1983. **96**(1): p. 1-27.

28. Sandhoff, K. and T. Kolter, *Biosynthesis and degradation of mammalian glycosphingolipids.* Philos Trans R Soc Lond B Biol Sci, 2003. **358**(1433): p. 847-61.

29. Luzio, J.P., P.R. Pryor, and N.A. Bright, *Lysosomes: fusion and function.* Nat Rev Mol Cell Biol, 2007. **8**(8): p. 622-32.

30. Peters, C. and K. von Figura, *Biogenesis of lysosomal membranes.* FEBS Lett, 1994. **346**(1): p. 108-14.

31. Carlsson, S.R., et al., *Isolation and characterization of human lysosomal membrane glycoproteins, h-lamp-1 and h-lamp-2. Major sialoglycoproteins carrying polylactosaminoglycan.* J Biol Chem, 1988. **263**(35): p. 18911-9.

32. Schulze, H., T. Kolter, and K. Sandhoff, *Principles of lysosomal membrane degradation Cellular topology and biochemistry of lysosomal lipid degradation.* Biochim Biophys Acta, 2008.

33. Wilkening, G., T. Linke, and K. Sandhoff, *Lysosomal degradation on vesicular membrane surfaces. Enhanced glucosylceramide degradation by lysosomal anionic lipids and activators.* J Biol Chem, 1998. **273**(46): p. 30271-8.

34. Umebayashi, K., *The roles of ubiquitin and lipids in protein sorting along the endocytic pathway.* Cell Struct Funct, 2003. **28**(5): p. 443-53.

35. Frederick, T.E., et al., *Bis(monoacylglycero)phosphate forms stable small lamellar vesicle structures: insights into vesicular body formation in endosomes.* Biophys J, 2009. **96**(5): p. 1847-55.

36. Kolter, T. and K. Sandhoff, *Principles of lysosomal membrane digestion: stimulation of sphingolipid degradation by sphingolipid activator proteins and anionic lysosomal lipids.* Annu Rev Cell Dev Biol, 2005. **21**: p. 81-103.

37. Meier, E.M., et al., *The human GM2 activator protein. A substrate specific cofactor of beta-hexosaminidase A.* J Biol Chem, 1991. **266**(3): p. 1879-87.

38. Wright, C.S., S.C. Li, and F. Rastinejad, *Crystal structure of human GM2-activator protein with a novel beta-cup topology.* J Mol Biol, 2000. **304**(3): p. 411-22.

39. Furst, W. and K. Sandhoff, *Activator proteins and topology of lysosomal sphingolipid catabolism.* Biochim Biophys Acta, 1992. **1126**(1): p. 1-16.

40. Hechtman, P. and D. LeBlanc, *Purification and properties of the hexosaminidase A-activating protein from human liver.* Biochem J, 1977. **167**(3): p. 693-701.

41. Morimoto, S., et al., *Interaction of saposins, acidic lipids, and glucosylceramidase.* J Biol Chem, 1990. **265**(4): p. 1933-7.

42. Sandhoff, K., *The GM2-gangliosidoses and the elucidation of the beta-hexosaminidase system.* Adv Genet, 2001. **44**: p. 67-91.

43. Burg, J., et al., *Mapping of the gene coding for the human GM2 activator protein to chromosome 5.* Ann Hum Genet, 1985. **49**(Pt 1): p. 41-5.

44. Conzelmann, E. and K. Sandhoff, *Purification and characterization of an activator protein for the degradation of glycolipids GM2 and GA2 by hexosaminidase A.* Hoppe Seylers Z Physiol Chem, 1979. **360**(12): p. 1837-49.

45. Hama, Y., Y.T. Li, and S.C. Li, *Interaction of GM2 activator protein with glycosphingolipids.* J Biol Chem, 1997. **272**(5): p. 2828-33.

46. Wu, Y.Y., et al., *Expression and specificity of human GM2 activator protein.* J Biol Chem, 1994. **269**(23): p. 16276-83.

47. Li, S.C., et al., *Specific recognition of N-acetylneuraminic acid in the GM2 epitope by human GM2 activator protein.* J Biol Chem, 1995. **270**(41): p. 24246-51.

48. Wilkening, G., et al., *Degradation of membrane-bound ganglioside GM1. Stimulation by bis(monoacylglycero)phosphate and the activator proteins SAP-B and GM2-AP.* J Biol Chem, 2000. **275**(46): p. 35814-9.

49. Conzelmann, E. and K. Sandhoff, *AB variant of infantile GM2 gangliosidosis: deficiency of a factor necessary for stimulation of hexosaminidase A-catalyzed degradation of ganglioside GM2 and glycolipid GA2.* Proc Natl Acad Sci U S A, 1978. **75**(8): p. 3979-83.

50. Schuette, C.G., et al., *Sphingolipid activator proteins: proteins with complex functions in lipid degradation and skin biogenesis.* Glycobiology, 2001. **11**(6): p. 81R-90R.

51. Ahn, V.E., et al., *Crystal structure of saposin B reveals a dimeric shell for lipid binding.* Proc Natl Acad Sci U S A, 2003. **100**(1): p. 38-43.

52. Zhao, Q., et al., *Mouse testicular sulfated glycoprotein-1: sequence analysis of the common backbone structure of prosaposins.* J Androl, 1998. **19**(2): p. 165-74.

53. Harzer, K., M. Hiraiwa, and B.C. Paton, *Saposins (sap) A and C activate the degradation of galactosylsphingosine.* FEBS Lett, 2001. **508**(1): p. 107-10.

54. Ho, M.W. and J.S. O'Brien, *Gaucher's disease: deficiency of 'acid' -glucosidase and reconstitution of enzyme activity in vitro.* Proc Natl Acad Sci U S A, 1971. **68**(11): p. 2810-3.

55. Klein, A., et al., *Sphingolipid activator protein D (sap-D) stimulates the lysosomal degradation of ceramide in vivo.* Biochem Biophys Res Commun, 1994. **200**(3): p. 1440-8.

56. Kretz, K.A., et al., *Characterization of a mutation in a family with saposin B deficiency: a glycosylation site defect.* Proc Natl Acad Sci U S A, 1990. **87**(7): p. 2541-4.

57. Matsuda, J., et al., *Mutation in saposin D domain of sphingolipid activator protein gene causes urinary system defects and cerebellar Purkinje cell degeneration with accumulation of hydroxy fatty acid-containing ceramide in mouse.* Hum Mol Genet, 2004. **13**(21): p. 2709-23.

58. Spiegel, R., et al., *A mutation in the saposin A coding region of the prosaposin gene in an infant presenting as Krabbe disease: first report of saposin A deficiency in humans.* Mol Genet Metab, 2005. **84**(2): p. 160-6.

59. Tylki-Szymanska, A., et al., *Non-neuronopathic Gaucher disease due to saposin C deficiency.* Clin Genet, 2007. **72**(6): p. 538-42.

60. Sano, A., et al., *Saposin-C from bovine spleen; complete amino acid sequence and relation between the structure and its biological activity.* Biochim Biophys Acta, 1992. **1120**(1): p. 75-80.

61. Tatti, M., et al., *Structural and membrane-binding properties of saposin D.* Eur J Biochem, 1999. **263**(2): p. 486-94.

62. Liepinsh, E., et al., *Saposin fold revealed by the NMR structure of NK-lysin.* Nat Struct Biol, 1997. **4**(10): p. 793-5.

63. Matsuda, J., et al., *A mutation in the saposin A domain of the sphingolipid activator protein (prosaposin) gene results in a late-onset, chronic form of globoid cell leukodystrophy in the mouse.* Hum Mol Genet, 2001. **10**(11): p. 1191-9.

64. John, M., et al., *Characterization of human saposins by NMR spectroscopy.* Biochemistry, 2006. **45**(16): p. 5206-16.

65. Munford, R.S., P.O. Sheppard, and P.J. O'Hara, *Saposin-like proteins (SAPLIP) carry out diverse functions on a common backbone structure.* J Lipid Res, 1995. **36**(8): p. 1653-63.

66. Simoes, I. and C. Faro, *Structure and function of plant aspartic proteinases.* Eur J Biochem, 2004. **271**(11): p. 2067-75.

67. Pena, S.V. and A.M. Krensky, *Granulysin, a new human cytolytic granule-associated protein with possible involvement in cell-mediated cytotoxicity.* Semin Immunol, 1997. **9**(2): p. 117-25.

68. Andersson, M., et al., *NK-lysin, structure and function of a novel effector molecule of porcine T and NK cells.* Vet Immunol Immunopathol, 1996. **54**(1-4): p. 123-6.

69. Zhai, Y. and M.H. Saier, Jr., *The amoebapore superfamily.* Biochim Biophys Acta, 2000. **1469**(2): p. 87-99.

70. Bornhauser, B.C. and D. Lindholm, *MSAP enhances migration of C6 glioma cells through phosphorylation of the myosin regulatory light chain.* Cell Mol Life Sci, 2005. **62**(11): p. 1260-6.

71. Weaver, T.E. and J.A. Whitsett, *Structure and function of pulmonary surfactant proteins.* Semin Perinatol, 1988. **12**(3): p. 213-20.

72. Vaccaro, A.M., et al., *Saposins and their interaction with lipids.* Neurochem Res, 1999. **24**(2): p. 307-14.

73. Qi, X. and G.A. Grabowski, *Differential membrane interactions of saposins A and C: implications for the functional specificity.* J Biol Chem, 2001. **276**(29): p. 27010-7.

74. Ahn, V.E., et al., *Crystal structures of saposins A and C.* Protein Sci, 2006. **15**(8): p. 1849-57.

75. Ito, K., et al., *Structural study of the oligosaccharide moieties of sphingolipid activator proteins, saposins A, C and D obtained from the spleen of a Gaucher patient.* Eur J Biochem, 1993. **215**(1): p. 171-9.

76. Harzer, K., et al., *Saposins (sap) A and C activate the degradation of galactosylceramide in living cells.* FEBS Lett, 1997. **417**(3): p. 270-4.

77. Fabbro, D. and G.A. Grabowski, *Human acid beta-glucosidase. Use of inhibitory and activating monoclonal antibodies to investigate the enzyme's catalytic mechanism and saposin A and C binding sites.* J Biol Chem, 1991. **266**(23): p. 15021-7.

78. Soeda, S., et al., *Binding of cerebrosides and sulfatides to saposins A-D.* J Biol Chem, 1993. **268**(25): p. 18519-23.

79. Alattia, J.R., et al., *Direct visualization of saposin remodelling of lipid bilayers.* J Mol Biol, 2006. **362**(5): p. 943-53.

80. Locatelli-Hoops, S., et al., *Saposin A mobilizes lipids from low cholesterol and high bis(monoacylglycerol)phosphate-containing membranes: patient variant Saposin A lacks lipid extraction capacity.* J Biol Chem, 2006. **281**(43): p. 32451-60.

81. Zhou, D., et al., *Lysosomal glycosphingolipid recognition by NKT cells.* Science, 2004. **306**(5702): p. 1786-9.

82. Cox, D., et al., *Determination of cellular lipids bound to human CD1d molecules.* PLoS ONE, 2009. **4**(5): p. e5325.

83. Yuan, W., et al., *Saposin B is the dominant saposin that facilitates lipid binding to human CD1d molecules.* Proc Natl Acad Sci U S A, 2007. **104**(13): p. 5551-6.

84. Whitelegge, J.P., et al., *Methionine oxidation within the cerebroside-sulfate activator protein (CSAct or Saposin B).* Protein Sci, 2000. **9**(9): p. 1618-30.

85. Hazkani-Covo, E., et al., *The evolutionary history of prosaposin: two successive tandem-duplication events gave rise to the four saposin domains in vertebrates.* J Mol Evol, 2002. **54**(1): p. 30-4.

86. Waring, A.J., et al., *Porcine cerebroside sulfate activator (saposin B) secondary structure: CD, FTIR, and NMR studies.* Mol Genet Metab, 1998. **63**(1): p. 14-25.

87. Fluharty, A.L., et al., *Preparation of the cerebroside sulfate activator (CSAct or saposin B) from human urine.* Mol Genet Metab, 1999. **68**(3): p. 391-403.

88. Remmel, N., et al., *Saposin B mobilizes lipids from cholesterol-poor and bis(monoacylglycero)phosphate-rich membranes at acidic pH. Unglycosylated patient variant saposin B lacks lipid-extraction capacity.* FEBS J, 2007. **274**(13): p. 3405-20.

89. Champagne, M.J., S. Lamontagne, and M. Potier, *Binding of GM1 ganglioside to a synthetic peptide derived from the lysosomal sphingolipid activator protein saposin B.* FEBS Lett, 1994. **349**(3): p. 439-41.

90. Lamontagne, S. and M. Potier, *Modulation of human saposin B sphingolipid-binding specificity by alternative splicing. A study with saposin B-derived synthetic peptides.* J Biol Chem, 1994. **269**(32): p. 20528-32.

91. Stokeley, D., et al., *Conformational dynamics of a lipid-interacting protein: MD simulations of saposin B.* Biochemistry, 2007. **46**(47): p. 13573-80.

92. Fluharty, C.B., et al., *Comparative lipid binding study on the cerebroside sulfate activator (saposin B).* J Neurosci Res, 2001. **63**(1): p. 82-9.

93. Kase, R., et al., *Only sphingolipid activator protein B (SAP-B or saposin B) stimulates the degradation of globotriaosylceramide by recombinant human lysosomal alpha-galactosidase in a detergent-free liposomal system.* FEBS Lett, 1996. **393**(1): p. 74-6.

94. Matzner, U., et al., *Saposin B-dependent reconstitution of arylsulfatase A activity in vitro and in cell culture models of metachromatic leukodystrophy.* J Biol Chem, 2009. **284**(14): p. 9372-81.

95. Ciaffoni, F., et al., *Saposin B binds and transfers phospholipids.* J Lipid Res, 2006. **47**(5): p. 1045-53.

96. Faull, K.F., et al., *Cerebroside sulfate activator protein (Saposin B): chromatographic and electrospray mass spectrometric properties.* J Mass Spectrom, 1999. **34**(10): p. 1040-54.

97. Jin, G., et al., *Coenzyme Q10-Binding/Transfer Protein Saposin B also Binds gamma-Tocopherol.* J Clin Biochem Nutr, 2008. **43**(2): p. 95-100.

98. Crane, F.L., et al., *Isolation of a quinone from beef heart mitochondria.* Biochim Biophys Acta, 1957. **25**(1): p. 220-1.

99. Jin, G., et al., *Saposin B is a human coenzyme q10-binding/transfer protein.* J Clin Biochem Nutr, 2008. **42**(2): p. 167-74.

100. Traber, M.G., et al., *Discrimination between forms of vitamin E by humans with and without genetic abnormalities of lipoprotein metabolism.* J Lipid Res, 1992. **33**(8): p. 1171-82.

101. Kayden, H.J. and M.G. Traber, *Absorption, lipoprotein transport, and regulation of plasma concentrations of vitamin E in humans.* J Lipid Res, 1993. **34**(3): p. 343-58.

102. Vaccaro, A.M., et al., *Structural analysis of saposin C and B. Complete localization of disulfide bridges.* J Biol Chem, 1995. **270**(17): p. 9953-60.

103. de Alba, E., S. Weiler, and N. Tjandra, *Solution structure of human saposin C: pH-dependent interaction with phospholipid vesicles.* Biochemistry, 2003. **42**(50): p. 14729-40.

104. Qi, X., et al., *Ex vivo localization of the mouse saposin C activation region for acid beta-glucosidase.* Mol Genet Metab, 2002. **76**(3): p. 189-200.

105. Qi, X., et al., *Functional organization of saposin C. Definition of the neurotrophic and acid beta-glucosidase activation regions.* J Biol Chem, 1996. **271**(12): p. 6874-80.

106. Qi, X., et al., *Conformational and amino acid residue requirements for the saposin C neuritogenic effect.* Biochemistry, 1999. **38**(19): p. 6284-91.

107. Liu, A., N. Wenzel, and X. Qi, *Role of lysine residues in membrane anchoring of saposin C.* Arch Biochem Biophys, 2005. **443**(1-2): p. 101-12.

108. Qi, X. and Z. Chu, *Fusogenic domain and lysines in saposin C.* Arch Biochem Biophys, 2004. **424**(2): p. 210-8.

109. Hawkins, C.A., E. de Alba, and N. Tjandra, *Solution structure of human saposin C in a detergent environment.* J Mol Biol, 2005. **346**(5): p. 1381-92.

110. Prence, E.M., *Effects of calcium on phosphatidylserine- and saposin C-stimulated glucosylceramide beta-glucosidase activity.* Biochem J, 1995. **310 (Pt 2)**: p. 571-5.

111. Alattia, J.R., et al., *Molecular imaging of membrane interfaces reveals mode of beta-glucosidase activation by saposin C.* Proc Natl Acad Sci U S A, 2007. **104**(44): p. 17394-9.

112. Sun, Y., X. Qi, and G.A. Grabowski, *Saposin C is required for normal resistance of acid beta-glucosidase to proteolytic degradation.* J Biol Chem, 2003. **278**(34): p. 31918-23.

113. Tayama, M., et al., *Effect of saposins on acid sphingomyelinase.* Biochem J, 1993. **290 (Pt 2)**: p. 401-4.

114. Vaccaro, A.M., et al., *pH-dependent conformational properties of saposins and their interactions with phospholipid membranes.* J Biol Chem, 1995. **270**(51): p. 30576-80.

115. Salvioli, R., et al., *Further studies on the reconstitution of glucosylceramidase activity by Sap C and anionic phospholipids.* FEBS Lett, 2000. **472**(1): p. 17-21.

116. Vaccaro, A.M., et al., *Saposin C induces pH-dependent destabilization and fusion of phosphatidylserine-containing vesicles.* FEBS Lett, 1994. **349**(2): p. 181-6.

117. Abu-Baker, S., et al., *Structural changes in a binary mixed phospholipid bilayer of DOPG and DOPS upon saposin C interaction at acidic pH utilizing 31P and 2H solid-state NMR spectroscopy.* Biochim Biophys Acta, 2005. **1717**(1): p. 58-66.

118. Wang, Y., G.A. Grabowski, and X. Qi, *Phospholipid vesicle fusion induced by saposin C.* Arch Biochem Biophys, 2003. **415**(1): p. 43-53.

119. You, H.X., et al., *Phospholipid membrane interactions of saposin C: in situ atomic force microscopic study.* Biophys J, 2003. **84**(3): p. 2043-57.

120. You, H.X., L. Yu, and X. Qi, *Phospholipid membrane restructuring induced by saposin C: a topographic study using atomic force microscopy.* FEBS Lett, 2001. **503**(1): p. 97-102.

121. Morita, F., et al., *Protective effect of a prosaposin-derived, 18-mer peptide on slowly progressive neuronal degeneration after brief ischemia.* J Cereb Blood Flow Metab, 2001. **21**(11): p. 1295-302.

122. Sun, Y., et al., *Prosaposin: threshold rescue and analysis of the "neuritogenic" region in transgenic mice.* Mol Genet Metab, 2002. **76**(4): p. 271-86.

123. Koochekpour, S., et al., *Saposin C stimulates growth and invasion, activates p42/44 and SAPK/JNK signaling pathways of MAPK and upregulates uPA/uPAR expression in prostate cancer and stromal cells.* Asian J Androl, 2005. **7**(2): p. 147-58.

124. Lee, T.J., et al., *Saposin C promotes survival and prevents apoptosis via PI3K/Akt-dependent pathway in prostate cancer cells.* Mol Cancer, 2004. **3**: p. 31.

125. Major, A.S., S. Joyce, and L. Van Kaer, *Lipid metabolism, atherogenesis and CD1-restricted antigen presentation.* Trends Mol Med, 2006. **12**(6): p. 270-8.

126. Winau, F., et al., *Saposin C is required for lipid presentation by human CD1b.* Nat Immunol, 2004. **5**(2): p. 169-74.

127. Roy, K.C., et al., *Involvement of secretory and endosomal compartments in presentation of an exogenous self-glycolipid to type II NKT cells.* J Immunol, 2008. **180**(5): p. 2942-50.

128. Popovic, K. and G.G. Prive, *Structures of the human ceramide activator protein saposin D.* Acta Crystallogr D Biol Crystallogr, 2008. **64**(Pt 5): p. 589-94.

129. Castillo, S.S. and D. Teegarden, *Ceramide conversion to sphingosine-1-phosphate is essential for survival in C3H10T1/2 cells.* J Nutr, 2001. **131**(11): p. 2826-30.

130. Momoi, T., Y. Ben-Yoseph, and H.L. Nadler, *Substrate-specificities of acid and alkaline ceramidases in fibroblasts from patients with Farber disease and controls.* Biochem J, 1982. **205**(2): p. 419-25.

131. Azuma, N., et al., *Stimulation of acid ceramidase activity by saposin D.* Arch Biochem Biophys, 1994. **311**(2): p. 354-7.

132. Ferlinz, K., et al., *Stimulation of lysosomal sphingomyelin degradation by sphingolipid activator proteins.* Chem Phys Lipids, 1999. **102**(1-2): p. 35-43.

133. Marchesini, N. and Y.A. Hannun, *Acid and neutral sphingomyelinases: roles and mechanisms of regulation.* Biochem Cell Biol, 2004. **82**(1): p. 27-44.

134. Kolzer, M., et al., *Functional characterization of the postulated intramolecular sphingolipid activator protein domain of human acid sphingomyelinase.* Biol Chem, 2004. **385**(12): p. 1193-5.

135. Linke, T., et al., *Interfacial regulation of acid ceramidase activity. Stimulation of ceramide degradation by lysosomal lipids and sphingolipid activator proteins.* J Biol Chem, 2001. **276**(8): p. 5760-8.

136. Ciaffoni, F., et al., *Saposin D solubilizes anionic phospholipid-containing membranes.* J Biol Chem, 2001. **276**(34): p. 31583-9.

137. Ciaffoni, F., et al., *Interaction of saposin D with membranes: effect of anionic phospholipids and sphingolipids.* Biochem J, 2003. **373**(Pt 3): p. 785-92.

138. Tsuda, M., et al., *The primary structure of mouse saposin.* Biochem Biophys Res Commun, 1992. **184**(3): p. 1266-72.

139. Igdoura, S.A., A. Rasky, and C.R. Morales, *Trafficking of sulfated glycoprotein-1 (prosaposin) to lysosomes or to the extracellular space in rat Sertoli cells.* Cell Tissue Res, 1996. **283**(3): p. 385-94.

140. Leonova, T., et al., *Proteolytic processing patterns of prosaposin in insect and mammalian cells.* J Biol Chem, 1996. **271**(29): p. 17312-20.

141. Zhu, Y. and G.E. Conner, *Intermolecular association of lysosomal protein precursors during biosynthesis.* J Biol Chem, 1994. **269**(5): p. 3846-51.

142. Kozak, C.A., M.C. Adamson, and M. Horowitz, *Genetic mapping of the mouse prosaposin gene (Psap) to mouse chromosome 10.* Genomics, 1994. **23**(2): p. 508-10.

143. Bar-Am, I., L. Avivi, and M. Horowitz, *Assignment of the human prosaposin gene (PSAP) to 10q22.1 by fluorescence in situ hybridization. Giraffidae, okapi (Okapiajohnstoni), and giraffe (Giraffa camelopardalis): evidence for ancestral telomeres at the okapi polymorphic rob (4;26) fusion site.* Cytogenet Cell Genet, 1996. **72**(4): p. 316-8.

144. Rorman, E.G., V. Scheinker, and G.A. Grabowski, *Structure and evolution of the human prosaposin chromosomal gene.* Genomics, 1992. **13**(2): p. 312-8.

145. Zhao, Q., N. Hay, and C.R. Morales, *Structural analysis of the mouse prosaposin (SGP-1) gene reveals the presence of an exon that is alternatively spliced in transcribed mRNAs.* Mol Reprod Dev, 1997. **48**(1): p. 1-8.

146. Azuma, N., et al., *Cloning, expression and map assignment of chicken prosaposin.* Biochem J, 1998. **330 (Pt 1)**: p. 321-7.

147. Sun, Y., et al., *Prosaposin: promoter analysis and central-nervous-system-preferential elements for expression in vivo.* Biochem J, 2000. **352 Pt 2**: p. 549-56.

148. Sun, Y., P. Jin, and G.A. Grabowski, *The mouse prosaposin locus: promoter organization.* DNA Cell Biol, 1997. **16**(1): p. 23-34.

149. Jin, P., Y. Sun, and G.A. Grabowski, *Role of Sp proteins and RORalpha in transcription regulation of murine prosaposin.* J Biol Chem, 1998. **273**(21): p. 13208-16.

150. Jin, P., Y. Sun, and G.A. Grabowski, *In vivo roles of RORalpha and Sp4 in the regulation of murine prosaposin gene.* DNA Cell Biol, 2001. **20**(12): p. 781-9.

151. Sun, Y., et al., *Analyses of temporal regulatory elements of the prosaposin gene in transgenic mice.* Biochem J, 2003. **370**(Pt 2): p. 557-66.

152. Sun, Y., et al., *Isolation and characterization of the human prosaposin promoter.* Gene, 1998. **218**(1-2): p. 37-47.

153. Cohen, T., et al., *Conservation of expression and alternative splicing in the prosaposin gene.* Brain Res Mol Brain Res, 2004. **129**(1-2): p. 8-19.

154. Cohen, T., et al., *The exon 8-containing prosaposin gene splice variant is dispensable for mouse development, lysosomal function, and secretion.* Mol Cell Biol, 2005. **25**(6): p. 2431-40.

155. Hiraiwa, M., et al., *Regulation of gene expression in response to brain injury: enhanced expression and alternative splicing of rat prosaposin (SGP-1) mRNA in injured brain.* J Neurotrauma, 2003. **20**(8): p. 755-65.

156. Chen, J., et al., *Expression patterns in alternative splicing forms of prosaposin mRNA in the rat facial nerve nucleus after facial nerve transection.* Neurosci Res, 2008. **60**(1): p. 82-94.

157. Hiraiwa, M., et al., *Lysosomal proteolysis of prosaposin, the precursor of saposins (sphingolipid activator proteins): its mechanism and inhibition by ganglioside.* Arch Biochem Biophys, 1997. **341**(1): p. 17-24.

158. O'Brien, J.S., et al., *Identification of the neurotrophic factor sequence of prosaposin.* Faseb J, 1995. **9**(8): p. 681-5.

159. Kotani, Y., et al., *A hydrophilic peptide comprising 18 amino acid residues of the prosaposin sequence has neurotrophic activity in vitro and in vivo.* J Neurochem, 1996. **66**(5): p. 2197-200.

160. Madar-Shapiro, L., et al., *Importance of splicing for prosaposin sorting.* Biochem J, 1999. **337 (Pt 3)**: p. 433-43.

161. Lefrancois, S., et al., *The lysosomal trafficking of sphingolipid activator proteins (SAPs) is mediated by sortilin.* Embo J, 2003. **22**(24): p. 6430-7.

162. Hiesberger, T., et al., *Cellular uptake of saposin (SAP) precursor and lysosomal delivery by the low density lipoprotein receptor-related protein (LRP).* Embo J, 1998. **17**(16): p. 4617-25.

163. Kolter, T., et al., *Lipid-binding proteins in membrane digestion, antigen presentation, and antimicrobial defense.* J Biol Chem, 2005. **280**(50): p. 41125-8.

164. Sylvester, S.R., et al., *Sulfated glycoprotein-1 (saposin precursor) in the reproductive tract of the male rat.* Biol Reprod, 1989. **41**(5): p. 941-8.

165. Koochekpour, S., et al., *Prosaposin upregulates AR and PSA expression and activity in prostate cancer cells (LNCaP).* Prostate, 2007. **67**(2): p. 178-89.

166. Campana, W.M., M. Hiraiwa, and J.S. O'Brien, *Prosaptide activates the MAPK pathway by a G-protein-dependent mechanism essential for enhanced sulfatide synthesis by Schwann cells.* Faseb J, 1998. **12**(3): p. 307-14.

167. Hiraiwa, M., et al., *Cell death prevention, mitogen-activated protein kinase stimulation, and increased sulfatide concentrations in Schwann cells and oligodendrocytes by prosaposin and prosaptides.* Proc Natl Acad Sci U S A, 1997. **94**(9): p. 4778-81.

168. Morales, C.R., et al., *Role of prosaposin in the male reproductive system: effect of prosaposin inactivation on the testis, epididymis, prostate, and seminal vesicles.* Arch Androl, 2000. **44**(3): p. 173-86.

169. Sano, A., et al., *Sphingolipid hydrolase activator proteins and their precursors.* Biochem Biophys Res Commun, 1989. **165**(3): p. 1191-7.

170. Hineno, T., et al., *Secretion of sphingolipid hydrolase activator precursor, prosaposin.* Biochem Biophys Res Commun, 1991. **176**(2): p. 668-74.

171. Sun, Y., D.P. Witte, and G.A. Grabowski, *Developmental and tissue-specific expression of prosaposin mRNA in murine tissues.* Am J Pathol, 1994. **145**(6): p. 1390-8.

172. Sprecher-Levy, H., et al., *Murine prosaposin: expression in the reproductive system of a gene implicated in human genetic diseases.* Cell Mol Biol (Noisy-le-grand), 1993. **39**(3): p. 287-99.

173. Van Den Berghe, L., et al., *Prosaposin gene expression in normal and dystrophic RCS rat retina.* Invest Ophthalmol Vis Sci, 2004. **45**(5): p. 1297-305.

174. Terashita, T., et al., *Localization of prosaposin in rat cochlea.* Neurosci Res, 2007. **57**(3): p. 372-8.

175. Hosoda, Y., et al., *Distribution of prosaposin in the rat nervous system.* Cell Tissue Res, 2007. **330**(2): p. 197-207.

176. Fu, Q., et al., *Occurrence of prosaposin as a neuronal surface membrane component.* J Mol Neurosci, 1994. **5**(1): p. 59-67.

177. Kondoh, K., et al., *Distribution of prosaposin-like immunoreactivity in rat brain.* J Comp Neurol, 1993. **334**(4): p. 590-602.

178. Igdoura, S.A. and C.R. Morales, *Role of sulfated glycoprotein-1 (SGP-1) in the disposal of residual bodies by Sertoli cells of the rat.* Mol Reprod Dev, 1995. **40**(1): p. 91-102.

179. Spencer, T.E., G.H. Graf, and F.W. Bazer, *Sulfated glycoprotein-1 (SGP-1) expression in ovine endometrium during the oestrous cycle and early pregnancy.* Reprod Fertil Dev, 1995. **7**(5): p. 1053-60.

180. Kondoh, K., et al., *Isolation and characterization of prosaposin from human milk.* Biochem Biophys Res Commun, 1991. **181**(1): p. 286-92.

181. Patton, S., et al., *Prosaposin, a neurotrophic factor: presence and properties in milk.* J Dairy Sci, 1997. **80**(2): p. 264-72.

182. Hiraiwa, M., et al., *Binding and transport of gangliosides by prosaposin.* Proc Natl Acad Sci U S A, 1992. **89**(23): p. 11254-8.

183. Hiraiwa, M., et al., *Isolation, characterization, and proteolysis of human prosaposin, the precursor of saposins (sphingolipid activator proteins).* Arch Biochem Biophys, 1993. **304**(1): p. 110-6.

184. O'Brien, J.S., et al., *Identification of prosaposin as a neurotrophic factor.* Proc Natl Acad Sci U S A, 1994. **91**(20): p. 9593-6.

185. Unuma, K., et al., *Changes in expression of prosaposin in the rat facial nerve nucleus after facial nerve transection.* Neurosci Res, 2005. **52**(3): p. 220-7.

186. Sorice, M., et al., *Neurotrophic signalling pathway triggered by prosaposin in PC12 cells occurs through lipid rafts.* FEBS J, 2008. **275**(19): p. 4903-12.

187. Tsuboi, K., M. Hiraiwa, and J.S. O'Brien, *Prosaposin prevents programmed cell death of rat cerebellar granule neurons in culture.* Brain Res Dev Brain Res, 1998. **110**(2): p. 249-55.

188. Misasi, R., et al., *Prosaposin and prosaptide, a peptide from prosaposin, induce an increase in ganglioside content on NS20Y neuroblastoma cells.* Glycoconj J, 1996. **13**(2): p. 195-202.

189. Hozumi, I., et al., *Administration of prosaposin ameliorates spatial learning disturbance and reduces cavity formation following stab wounds in rat brain.* Neurosci Lett, 1999. **267**(1): p. 73-6.

190. Sano, A., et al., *Protection by prosaposin against ischemia-induced learning disability and neuronal loss.* Biochem Biophys Res Commun, 1994. **204**(2): p. 994-1000.

191. Kotani, Y., et al., *Prosaposin facilitates sciatic nerve regeneration in vivo.* J Neurochem, 1996. **66**(5): p. 2019-25.

192. Guo, F., et al., *Identification of prosaposin as a novel interaction partner for Rhox5.* J Genet Genomics, 2007. **34**(5): p. 392-9.

193. Hammerstedt, R.H., et al., *A fragment of prosaposin (SGP-1) from rooster sperm promotes sperm-egg binding and improves fertility in chickens.* J Androl, 2001. **22**(3): p. 361-75.

194. Maclean, J.A., 2nd, et al., *Rhox: a new homeobox gene cluster.* Cell, 2005. **120**(3): p. 369-82.

195. Shanker, S., Z. Hu, and M.F. Wilkinson, *Epigenetic regulation and downstream targets of the Rhox5 homeobox gene.* Int J Androl, 2008. **31**(5): p. 462-70.

196. Morales, C.R., et al., *Targeted disruption of the mouse prosaposin gene affects the development of the prostate gland and other male reproductive organs.* J Androl, 2000. **21**(6): p. 765-75.

197. Koochekpour, S., et al., *Prosaposin is a novel androgen-regulated gene in prostate cancer cell line LNCaP.* J Cell Biochem, 2007. **101**(3): p. 631-41.

198. Doering, T., et al., *Sphingolipid activator proteins are required for epidermal permeability barrier formation.* J Biol Chem, 1999. **274**(16): p. 11038-45.

199. Holleran, W.M., Y. Takagi, and Y. Uchida, *Epidermal sphingolipids: metabolism, function, and roles in skin disorders.* FEBS Lett, 2006. **580**(23): p. 5456-66.

200. Cui, C.Y., et al., *Decreased level of prosaposin in atopic skin.* J Invest Dermatol, 1997. **109**(3): p. 319-23.

201. Alessandrini, F., et al., *The level of prosaposin is decreased in the skin of patients with psoriasis vulgaris.* J Invest Dermatol, 2001. **116**(3): p. 394-400.

202. Choi, M.J. and H.I. Maibach, *Role of ceramides in barrier function of healthy and diseased skin.* Am J Clin Dermatol, 2005. **6**(4): p. 215-23.

203. Misasi, R., et al., *Prosaposin treatment induces PC12 entry in the S phase of the cell cycle and prevents apoptosis: activation of ERKs and sphingosine kinase.* Faseb J, 2001. **15**(2): p. 467-74.

204. Misasi, R., et al., *Prosaposin: a new player in cell death prevention of U937 monocytic cells.* Exp Cell Res, 2004. **298**(1): p. 38-47.

205. Ochiai, T., et al., *Molecular mechanism for neuro-protective effect of prosaposin against oxidative stress: its regulation of dimeric transcription factor formation.* Biochim Biophys Acta, 2008. **1780**(12): p. 1441-7.

206. Campana, W.M., S.J. Darin, and J.S. O'Brien, *Phosphatidylinositol 3-kinase and Akt protein kinase mediate IGF-I- and prosaptide-induced survival in Schwann cells.* J Neurosci Res, 1999. **57**(3): p. 332-41.

207. Koochekpour, S., et al., *Amplification and overexpression of prosaposin in prostate cancer.* Genes Chromosomes Cancer, 2005. **44**(4): p. 351-64.

208. Koochekpour, S., et al., *Prosaposin is an AR-target gene and its neurotrophic domain upregulates AR expression and activity in prostate stromal cells.* J Cell Biochem, 2008. **104**(6): p. 2272-85.

209. Campana, W.M., et al., *Secretion of prosaposin, a multifunctional protein, by breast cancer cells.* Biochim Biophys Acta, 1999. **1427**(3): p. 392-400.

210. Meijer, D., et al., *TSC22D1 and PSAP predict clinical outcome of tamoxifen treatment in patients with recurrent breast cancer.* Breast Cancer Res Treat, 2009. **113**(2): p. 253-60.

211. Taylor, E.M., et al., *Designing stable blood-brain barrier-permeable prosaptide peptides for treatment of central nervous system neurodegeneration.* J Pharmacol Exp Ther, 2000. **293**(2): p. 403-9.

212. Jolivalt, C.G., et al., *Therapeutic efficacy of prosaposin-derived peptide on different models of allodynia.* Pain, 2006. **121**(1-2): p. 14-21.

213. Campana, W.M., et al., *Prosaposin-derived peptides enhanced sprouting of sensory neurons in vitro and induced sprouting at motor endplates in vivo.* J Peripher Nerv Syst, 2000. **5**(3): p. 126-30.

214. Koochekpour, S., et al., *Prosaptide TX14A stimulates growth, migration, and invasion and activates the Raf-MEK-ERK-RSK-Elk-1 signaling pathway in prostate cancer cells.* Prostate, 2004. **61**(2): p. 114-23.

215. Jolivalt, C.G., et al., *Impaired prosaposin secretion during nerve regeneration in diabetic rats and protection of nerve regeneration by a prosaposin-derived peptide.* J Neuropathol Exp Neurol, 2008. **67**(7): p. 702-10.

216. Hiraiwa, M., et al., *Prosaposin: a myelinotrophic protein that promotes expression of myelin constituents and is secreted after nerve injury.* Glia, 1999. **26**(4): p. 353-60.

217. Calcutt, N.A., et al., *Prosaposin gene expression and the efficacy of a prosaposin-derived peptide in preventing structural and functional disorders of peripheral nerve in diabetic rats.* J Neuropathol Exp Neurol, 1999. **58**(6): p. 628-36.

218. Mizisin, A.P., et al., *TX14(A), a prosaposin-derived peptide, reverses established nerve disorders in streptozotocin-diabetic rats and prevents them in galactose-fed rats.* J Neuropathol Exp Neurol, 2001. **60**(10): p. 953-60.

219. Calcutt, N.A., J.D. Freshwater, and J.S. O'Brien, *Protection of sensory function and antihyperalgesic properties of a prosaposin-derived peptide in diabetic rats.* Anesthesiology, 2000. **93**(5): p. 1271-8.

220. Jolivalt, C.G., et al., *Central action of prosaptide TX14(A) against gp120-induced allodynia in rats.* Eur J Pain, 2008. **12**(1): p. 76-81.

221. Rende, M., et al., *Prosaposin is immunolocalized to muscle and prosaptides promote myoblast fusion and attenuate loss of muscle mass after nerve injury.* Muscle Nerve, 2001. **24**(6): p. 799-808.

222. Campana, W.M., et al., *Prosaptide prevents paclitaxel neurotoxicity.* Neurotoxicology, 1998. **19**(2): p. 237-44.

223. Taylor, E.M., et al., *Retro-inverso prosaptide peptides retain bioactivity, are stable In vivo, and are blood-brain barrier permeable.* J Pharmacol Exp Ther, 2000. **295**(1): p. 190-4.

224. Igase, K., et al., *An 18-mer peptide fragment of prosaposin ameliorates place navigation disability, cortical infarction, and retrograde thalamic degeneration in rats with focal cerebral ischemia.* J Cereb Blood Flow Metab, 1999. **19**(3): p. 298-306.

225. Misasi, R., et al., *Colocalization and complex formation between prosaposin and monosialoganglioside GM3 in neural cells.* J Neurochem, 1998. **71**(6): p. 2313-21.

226. Yan, L., et al., *Prosaptide D5 reverses hyperalgesia: inhibition of calcium channels through a pertussis toxin-sensitive G-protein mechanism in the rat.* Neurosci Lett, 2000. **278**(1-2): p. 120-2.

227. Lu, A.G., et al., *Neuroprotective effect of retro-inverso Prosaptide D5 on focal cerebral ischemia in rat.* Neuroreport, 2000. **11**(8): p. 1791-4.

228. Hiraiwa, M., et al., *A retro-inverso Prosaptide D5 promotes a myelination process in developing rats.* Brain Res Dev Brain Res, 2001. **128**(1): p. 73-6.

229. Lapchak, P.A., et al., *Prosaptide exacerbates ischemia-induced behavioral deficits in vivo; an effect that does not involve mitogen-activated protein kinase activation.* Neuroscience, 2000. **101**(4): p. 811-4.

230. Amann, R.P., R.H. Hammerstedt, and R.B. Shabanowitz, *Exposure of human, boar, or bull sperm to a synthetic peptide increases binding to an egg-membrane substrate.* J Androl, 1999. **20**(1): p. 34-41.

231. Amann, R.P., G.E. Seidel, Jr., and Z.A. Brink, *Exposure of thawed frozen bull sperm to a synthetic peptide before artificial insemination increases fertility.* J Androl, 1999. **20**(1): p. 42-6.

232. Gieselmann, V., *Lysosomal storage diseases.* Biochim Biophys Acta, 1995. **1270**(2-3): p. 103-36.

233. Winchester, B., *Are there useful biochemical markers of disease activity in lysosomal storage diseases?* J Inherit Metab Dis, 2001. **24 Suppl 2**: p. 52-6; discussion 45-6.

234. Chen, C.S., et al., *Broad screening test for sphingolipid-storage diseases.* Lancet, 1999. **354**(9182): p. 901-5.

235. Wilcox, W.R., *Lysosomal storage disorders: the need for better pediatric recognition and comprehensive care.* J Pediatr, 2004. **144**(5 Suppl): p. S3-14.

236. Heese, B.A., *Current strategies in the management of lysosomal storage diseases.* Semin Pediatr Neurol, 2008. **15**(3): p. 119-26.

237. Suzuki, Y., *[Disorders of sphingolipid activator proteins].* Nippon Rinsho, 1995. **53**(12): p. 3025-7.

238. Beck, M., *Variable clinical presentation in lysosomal storage disorders.* J Inherit Metab Dis, 2001. **24 Suppl 2**: p. 47-51; discussion 45-6.

239. Wraith, J.E., *The clinical presentation of lysosomal storage disorders.* Acta Neurol Taiwan, 2004. **13**(3): p. 101-6.

240. Sun, Y., et al., *Temporal gene expression profiling reveals CEBPD as a candidate regulator of brain disease in prosaposin deficient mice.* BMC Neurosci, 2008. **9**: p. 76.

241. Fujita, N., et al., *Targeted disruption of the mouse sphingolipid activator protein gene: a complex phenotype, including severe leukodystrophy and wide-spread storage of multiple sphingolipids.* Hum Mol Genet, 1996. **5**(6): p. 711-25.

242. Harzer, K., et al., *Sphingolipid activator protein deficiency in a 16-week-old atypical Gaucher disease patient and his fetal sibling: biochemical signs of combined sphingolipidoses.* Eur J Pediatr, 1989. **149**(1): p. 31-9.

243. Bradova, V., et al., *Prosaposin deficiency: further characterization of the sphingolipid activator protein-deficient sibs. Multiple glycolipid elevations (including lactosylceramidosis), partial enzyme deficiencies and ultrastructure of the skin in this generalized sphingolipid storage disease.* Hum Genet, 1993. **92**(2): p. 143-52.

244. Paton, B.C., et al., *Additional biochemical findings in a patient and fetal sibling with a genetic defect in the sphingolipid activator protein (SAP) precursor, prosaposin. Evidence for a deficiency in SAP-1 and for a normal lysosomal neuraminidase.* Biochem J, 1992. **285 (Pt 2)**: p. 481-8.

245. Schnabel, D., et al., *Simultaneous deficiency of sphingolipid activator proteins 1 and 2 is caused by a mutation in the initiation codon of their common gene.* J Biol Chem, 1992. **267**(5): p. 3312-5.

246. Hulkova, H., et al., *A novel mutation in the coding region of the prosaposin gene leads to a complete deficiency of prosaposin and saposins, and is associated with a complex sphingolipidosis dominated by lactosylceramide accumulation.* Hum Mol Genet, 2001. **10**(9): p. 927-40.

247. Elleder, M., et al., *Niemann-Pick disease type C with enhanced glycolipid storage. Report on further case of so-called lactosylceramidosis.* Virchows Arch A Pathol Anat Histopathol, 1984. **402**(3): p. 307-17.

248. Elleder, M., et al., *Prosaposin deficiency -- a rarely diagnosed, rapidly progressing, neonatal neurovisceral lipid storage disease. Report of a further patient.* Neuropediatrics, 2005. **36**(3): p. 171-80.

249. Kuchar, L., et al., *Prosaposin deficiency and saposin B deficiency (activator-deficient metachromatic leukodystrophy): report on two patients detected by analysis of urinary sphingolipids and carrying novel PSAP gene mutations.* Am J Med Genet A, 2009. **149A**(4): p. 613-21.

250. Chu, Z., et al., *Saposin C: neuronal effect and CNS delivery by liposomes.* Ann N Y Acad Sci, 2005. **1053**: p. 237-46.

251. Morales, C.R. and H. Badran, *Prosaposin ablation inactivates the MAPK and Akt signaling pathways and interferes with the development of the prostate gland.* Asian J Androl, 2003. **5**(1): p. 57-63.

252. Akil, O., et al., *Progressive deafness and altered cochlear innervation in knock-out mice lacking prosaposin.* J Neurosci, 2006. **26**(50): p. 13076-88.

253. Suzuki, K., *Globoid cell leukodystrophy (Krabbe's disease): update.* J Child Neurol, 2003. **18**(9): p. 595-603.

254. Yagi, T., et al., *Hematopoietic cell transplantation ameliorates clinical phenotype and progression of the CNS pathology in the mouse model of late onset Krabbe disease.* J Neuropathol Exp Neurol, 2005. **64**(7): p. 565-75.

255. Inui, K., *[Krabbe disease, globoid cell leukodystrophy].* Ryoikibetsu Shokogun Shirizu, 2001(34 Pt 2): p. 56-8.

256. Yagi, T., et al., *Comparative clinico-pathological study of saposin-A-deficient (SAP-A-/-) and Twitcher mice.* J Neuropathol Exp Neurol, 2004. **63**(7): p. 721-34.

257. Hagberg, B., *Clinical aspects of globoid cell and metachromatic leukodystrophies.* Birth Defects Orig Artic Ser, 1971. **7**(1): p. 103-12.

258. Gieselmann, V. and K. von Figura, *Advances in the molecular genetics of metachromatic leukodystrophy.* J Inherit Metab Dis, 1990. **13**(4): p. 560-71.

259. Gieselmann, V., et al., *Molecular genetics of metachromatic leukodystrophy.* Hum Mutat, 1994. **4**(4): p. 233-42.

260. Shapiro, L.J., et al., *Metachromatic leukodystrophy without arylsulfatase A deficiency.* Pediatr Res, 1979. **13**(10): p. 1179-81.

261. Rafi, M.A., et al., *Detection of a point mutation in sphingolipid activator protein-1 mRNA in patients with a variant form of metachromatic leukodystrophy.* Biochem Biophys Res Commun, 1990. **166**(2): p. 1017-23.

262. Marshall, R.D., *Glycoproteins.* Annu Rev Biochem, 1972. **41**: p. 673-702.

263. Hahn, A.F., et al., *The AB-variant of metachromatic leukodystrophy (postulated activator protein deficiency). Light and electron microscopic findings in a sural nerve biopsy.* Acta Neuropathol, 1981. **55**(4): p. 281-7.

264. Hahn, A.F., et al., *A variant form of metachromatic leukodystrophy without arylsulfatase deficiency.* Ann Neurol, 1982. **12**(1): p. 33-6.

265. Zhang, X.L., et al., *Insertion in the mRNA of a metachromatic leukodystrophy patient with sphingolipid activator protein-1 deficiency.* Proc Natl Acad Sci U S A, 1990. **87**(4): p. 1426-30.

266. Zhang, X.L., et al., *The mechanism for a 33-nucleotide insertion in mRNA causing sphingolipid activator protein (SAP-1)-deficient metachromatic leukodystrophy.* Hum Genet, 1991. **87**(2): p. 211-5.

267. Wenger, D.A., et al., *Clinical, pathological, and biochemical studies on an infantile case of sulfatide/GM1 activator protein deficiency.* Am J Med Genet, 1989. **33**(2): p. 255-65.

268. Schlote, W., et al., *Sphingolipid activator protein 1 deficiency in metachromatic leucodystrophy with normal arylsulphatase A activity. A clinical, morphological, biochemical, and immunological study.* Eur J Pediatr, 1991. **150**(8): p. 584-91.

269. Holtschmidt, H., et al., *Sulfatide activator protein. Alternative splicing that generates three mRNAs and a newly found mutation responsible for a clinical disease.* J Biol Chem, 1991. **266**(12): p. 7556-60.

270. Landrieu, P., et al., *Bone marrow transplantation in metachromatic leukodystrophy caused by saposin-B deficiency: a case report with a 3-year follow-up period.* J Pediatr, 1998. **133**(1): p. 129-32.

271. Regis, S., et al., *An Asn > Lys substitution in saposin B involving a conserved amino acidic residue and leading to the loss of the single N-glycosylation site in a patient with metachromatic leukodystrophy and normal arylsulphatase A activity.* Eur J Hum Genet, 1999. **7**(2): p. 125-30.

272. Wrobe, D., et al., *A non-glycosylated and functionally deficient mutant (N215H) of the sphingolipid activator protein B (SAP-B) in a novel case of metachromatic leukodystrophy (MLD).* J Inherit Metab Dis, 2000. **23**(1): p. 63-76.

273. Deconinck, N., et al., *Metachromatic leukodystrophy without arylsulfatase A deficiency: a new case of saposin-B deficiency.* Eur J Paediatr Neurol, 2008. **12**(1): p. 46-50.

274. Grossi, S., et al., *Molecular analysis of ARSA and PSAP genes in twenty-one Italian patients with metachromatic leukodystrophy: identification and functional characterization of 11 novel ARSA alleles.* Hum Mutat, 2008. **29**(11): p. E220-30.

275. Sun, Y., et al., *Neurological deficits and glycosphingolipid accumulation in saposin B deficient mice.* Hum Mol Genet, 2008. **17**(15): p. 2345-56.

276. Beutler, E., *Gaucher disease.* Blood Rev, 1988. **2**(1): p. 59-70.

277. Brady, R.O., N.W. Barton, and G.A. Grabowski, *The role of neurogenetics in Gaucher disease.* Arch Neurol, 1993. **50**(11): p. 1212-24.

278. Germain, D.P. and K. Benistan, *[Prenatal diagnosis of Gaucher disease].* Rev Med Interne, 2007. **28 Suppl 2**: p. S193-7.

279. Christomanou, H., A. Aignesberger, and R.P. Linke, *Immunochemical characterization of two activator proteins stimulating enzymic sphingomyelin degradation in vitro. Absence of one of them in a human Gaucher disease variant.* Biol Chem Hoppe Seyler, 1986. **367**(9): p. 879-90.

280. Schnabel, D., M. Schroder, and K. Sandhoff, *Mutation in the sphingolipid activator protein 2 in a patient with a variant of Gaucher disease.* FEBS Lett, 1991. **284**(1): p. 57-9.

281. Christomanou, H., et al., *Activator protein deficient Gaucher's disease. A second patient with the newly identified lipid storage disorder.* Klin Wochenschr, 1989. **67**(19): p. 999-1003.

282. Rafi, M.A., et al., *Mutational analysis in a patient with a variant form of Gaucher disease caused by SAP-2 deficiency.* Somat Cell Mol Genet, 1993. **19**(1): p. 1-7.

283. Diaz-Font, A., et al., *A mutation within the saposin D domain in a Gaucher disease patient with normal glucocerebrosidase activity.* Hum Genet, 2005. **117**(2-3): p. 275-7.

284. Amsallem D, R.D., Vanier MT et al., *Third case of Gaucher disease with sap-C deficiency and evaluation of twelve months' therapy by miglustat.* J Inherit Metab Dis, 2005. **28 Suppl 1**: p. 152.

285. Stirnemann, J., T.B. de Villemeur, and N. Belmatoug, *[Organization of Gaucher disease management in France].* Rev Med Interne, 2007. **28 Suppl 2**: p. S198-201.

286. Sun, Y., et al., *Gaucher disease mouse models: point mutations at the acid beta-glucosidase locus combined with low-level prosaposin expression lead to disease variants.* J Lipid Res, 2005. **46**(10): p. 2102-13.

287. Sun, Y., et al., *Combined saposin C and D deficiencies in mice lead to a neuronopathic phenotype, glucosylceramide and alpha-hydroxy ceramide accumulation, and altered prosaposin trafficking.* Hum Mol Genet, 2007. **16**(8): p. 957-71.

288. Matsuda, J., A. Yoneshige, and K. Suzuki, *The function of sphingolipids in the nervous system: lessons learnt from mouse models of specific sphingolipid activator protein deficiencies.* J Neurochem, 2007. **103 Suppl 1**: p. 32-8.

289. Hassan, A.J., et al., *The trafficking of prosaposin (SGP-1) and GM2AP to the lysosomes of TM4 Sertoli cells is mediated by sortilin and monomeric adaptor proteins.* Mol Reprod Dev, 2004. **68**(4): p. 476-83.

290. Suzuki, Y., *[Lysosomal enzymes, sphingolipid activator proteins, and protective protein].* Nippon Rinsho, 1995. **53**(12): p. 2887-91.

291. Rijnboutt, S., et al., *Mannose 6-phosphate-independent membrane association of cathepsin D, glucocerebrosidase, and sphingolipid-activating protein in HepG2 cells.* J Biol Chem, 1991. **266**(8): p. 4862-8.

292. Bu, G., et al., *39 kDa receptor-associated protein is an ER resident protein and molecular chaperone for LDL receptor-related protein.* Embo J, 1995. **14**(10): p. 2269-80.

293. Lin, B.Z., P.F. Pilch, and K.V. Kandror, *Sortilin is a major protein component of Glut4-containing vesicles.* J Biol Chem, 1997. **272**(39): p. 24145-7.

294. Nykjaer, A., et al., *Sortilin is essential for proNGF-induced neuronal cell death.* Nature, 2004. **427**(6977): p. 843-8.

295. Sarret, P., et al., *Distribution of NTS3 receptor/sortilin mRNA and protein in the rat central nervous system.* J Comp Neurol, 2003. **461**(4): p. 483-505.

296. Munck Petersen, C., et al., *Propeptide cleavage conditions sortilin/neurotensin receptor-3 for ligand binding.* Embo J, 1999. **18**(3): p. 595-604.

297. Westergaard, U.B., et al., *Functional organization of the sortilin Vps10p domain.* J Biol Chem, 2004. **279**(48): p. 50221-9.

298. Paiardini, A. and V. Caputo, *Insights into the interaction of sortilin with proneurotrophins: a computational approach.* Neuropeptides, 2008. **42**(2): p. 205-14.

299. Takatsu, H., et al., *Golgi-localizing, gamma-adaptin ear homology domain, ADP-ribosylation factor-binding (GGA) proteins interact with acidic dileucine sequences within the cytoplasmic domains of sorting receptors through their Vps27p/Hrs/STAM (VHS) domains.* J Biol Chem, 2001. **276**(30): p. 28541-5.

300. Dell'Angelica, E.C., et al., *GGAs: a family of ADP ribosylation factor-binding proteins related to adaptors and associated with the Golgi complex.* J Cell Biol, 2000. **149**(1): p. 81-94.

301. Shiba, T., et al., *Structural basis for recognition of acidic-cluster dileucine sequence by GGA1.* Nature, 2002. **415**(6874): p. 937-41.

302. Trowbridge, I.S., J.F. Collawn, and C.R. Hopkins, *Signal-dependent membrane protein trafficking in the endocytic pathway.* Annu Rev Cell Biol, 1993. **9**: p. 129-61.

303. Braulke, T. and J.S. Bonifacino, *Sorting of lysosomal proteins.* Biochim Biophys Acta, 2009. **1793**(4): p. 605-14.

304. Sandoval, I.V. and O. Bakke, *Targeting of membrane proteins to endosomes and lysosomes.* Trends Cell Biol, 1994. **4**(8): p. 292-7.

305. Zeng, J., A.J. Hassan, and C.R. Morales, *Study of the mouse sortilin gene: Effects of its transient silencing by RNA interference in TM4 Sertoli cells.* Mol Reprod Dev, 2004. **68**(4): p. 469-75.

306. Hou, J.C. and J.E. Pessin, *Ins (endocytosis) and outs (exocytosis) of GLUT4 trafficking.* Curr Opin Cell Biol, 2007. **19**(4): p. 466-73.

307. Longo, N., et al., *Human fibroblasts express the insulin-responsive glucose transporter (GLUT4).* Trans Assoc Am Physicians, 1990. **103**: p. 202-13.

308. Kandror, K.V. and P.F. Pilch, *Multiple endosomal recycling pathways in rat adipose cells.* Biochem J, 1998. **331 (Pt 3)**: p. 829-35.

309. Canuel, M., et al., *Sortilin mediates the lysosomal targeting of cathepsins D and H.* Biochem Biophys Res Commun, 2008. **373**(2): p. 292-7.

310. Canuel, M., Y. Libin, and C.R. Morales, *The interactomics of sortilin: an ancient lysosomal receptor evolving new functions.* Histol Histopathol, 2009. **24**(4): p. 481-92.

311. Mazella, J., et al., *The 100-kDa neurotensin receptor is gp95/sortilin, a non-G-protein-coupled receptor.* J Biol Chem, 1998. **273**(41): p. 26273-6.

312. Navarro, V., et al., *Pharmacological properties of the mouse neurotensin receptor 3. Maintenance of cell surface receptor during internalization of neurotensin.* FEBS Lett, 2001. **495**(1-2): p. 100-5.

313. Martin, S., J.P. Vincent, and J. Mazella, *Involvement of the neurotensin receptor-3 in the neurotensin-induced migration of human microglia.* J Neurosci, 2003. **23**(4): p. 1198-205.

314. Quistgaard, E.M., et al., *Ligands bind to Sortilin in the tunnel of a ten-bladed beta-propeller domain.* Nat Struct Mol Biol, 2009. **16**(1): p. 96-8.

315. Al-Shawi, R., et al., *ProNGF, Sortilin, and Age-related Neurodegeneration.* Ann N Y Acad Sci, 2007. **1119**: p. 208-15.

316. Teng, H.K., et al., *ProBDNF induces neuronal apoptosis via activation of a receptor complex of p75NTR and sortilin.* J Neurosci, 2005. **25**(22): p. 5455-63.

317. Chen, Z.Y., et al., *Sortilin controls intracellular sorting of brain-derived neurotrophic factor to the regulated secretory pathway.* J Neurosci, 2005. **25**(26): p. 6156-66.

318. Nielsen, M.S., et al., *Sortilin/neurotensin receptor-3 binds and mediates degradation of lipoprotein lipase.* J Biol Chem, 1999. **274**(13): p. 8832-6.

319. Maeda, S., et al., *Sortilin is upregulated during osteoblastic differentiation of mesenchymal stem cells and promotes extracellular matrix mineralization.* J Cell Physiol, 2002. **193**(1): p. 73-9.

320. Nilsson, S.K., et al., *Endocytosis of apolipoprotein A-V by members of the low density lipoprotein receptor and the VPS10p domain receptor families.* J Biol Chem, 2008. **283**(38): p. 25920-7.

321. Botta, R., et al., *Sortilin is a putative postendocytic receptor of thyroglobulin.* Endocrinology, 2009. **150**(1): p. 509-18.

322. Degroot, L.J. and H. Niepomniszcze, *Biosynthesis of thyroid hormone: basic and clinical aspects.* Metabolism, 1977. **26**(6): p. 665-718.

323. Lefrancois, S., et al., *Inactivation of sortilin (a novel lysosomal sorting receptor) by dominant negative competition and RNA interference.* Biol Proced Online, 2005. **7**: p. 17-25.

324. M.J. Betts, R.B.R., *Amino acid properties and consequences of subsitutions.* In Bioinformatics for Geneticists, M.R. Barnes, I.C. Gray eds, Wiley, 2003: p. 289-316.

325. Mellman, I., R. Fuchs, and A. Helenius, *Acidification of the endocytic and exocytic pathways.* Annu Rev Biochem, 1986. **55**: p. 663-700.

326. Schindler, M., et al., *Defective pH regulation of acidic compartments in human breast cancer cells (MCF-7) is normalized in adriamycin-resistant cells (MCF-7adr).* Biochemistry, 1996. **35**(9): p. 2811-7.

327. Coffey, J.W. and C. De Duve, *Digestive activity of lysosomes. I. The digestion of proteins by extracts of rat liver lysosomes.* J Biol Chem, 1968. **243**(12): p. 3255-63.

328. Demaurex, N., et al., *Mechanism of acidification of the trans-Golgi network (TGN). In situ measurements of pH using retrieval of TGN38 and furin from the cell surface.* J Biol Chem, 1998. **273**(4): p. 2044-51.

329. van Weert, A.W., et al., *Transport from late endosomes to lysosomes, but not sorting of integral membrane proteins in endosomes, depends on the vacuolar proton pump.* J Cell Biol, 1995. **130**(4): p. 821-34.

330. Morales, C.R., et al., *Expression and tissue distribution of rat sulfated glycoprotein-1 (prosaposin).* J Histochem Cytochem, 1996. **44**(4): p. 327-37.

331. Collard, M.W., et al., *Biosynthesis and molecular cloning of sulfated glycoprotein 1 secreted by rat Sertoli cells: sequence similarity with the 70-kilodalton precursor to sulfatide/GM1 activator.* Biochemistry, 1988. **27**(12): p. 4557-64.

332. Igdoura, S.A., et al., *Nonciliated cells of the rat efferent ducts endocytose testicular sulfated glycoprotein-1 (SGP-1) and synthesize SGP-1 derived saposins.* Anat Rec, 1993. **235**(3): p. 411-24.

333. Chanat, E. and W.B. Huttner, *Milieu-induced, selective aggregation of regulated secretory proteins in the trans-Golgi network.* J Cell Biol, 1991. **115**(6): p. 1505-19.

334. Lefrancois, S., et al., *Role of sphingolipids in the transport of prosaposin to the lysosomes.* J Lipid Res, 1999. **40**(9): p. 1593-603.

335. Lefrancois, S., et al., *The lysosomal transport of prosaposin requires the conditional interaction of its highly conserved d domain with sphingomyelin.* J Biol Chem, 2002. **277**(19): p. 17188-99.

336. Foster, L.J. and Q.W. Chan, *Lipid raft proteomics: more than just detergent-resistant membranes.* Subcell Biochem, 2007. **43**: p. 35-47.

337. Grassel, S. and A. Hasilik, *Human cathepsin D precursor is associated with a 60 kDa glycosylated polypeptide.* Biochem Biophys Res Commun, 1992. **182**(1): p. 276-82.

338. Godbold, G.D., et al., *Biosynthesis and intracellular targeting of the lysosomal aspartic proteinase cathepsin D.* Adv Exp Med Biol, 1998. **436**: p. 153-62.

339. Laurent-Matha, V., et al., *Procathepsin D interacts with prosaposin in cancer cells but its internalization is not mediated by LDL receptor-related protein.* Exp Cell Res, 2002. **277**(2): p. 210-9.

340. Gopalakrishnan, M.M., et al., *Purified recombinant human prosaposin forms oligomers that bind procathepsin D and affect its autoactivation.* Biochem J, 2004. **383**(Pt. 3): p. 507-15.

341. Burkhardt, J.K., et al., *Accumulation of sphingolipids in SAP-precursor (prosaposin)-deficient fibroblasts occurs as intralysosomal membrane structures and can be completely reversed by treatment with human SAP-precursor.* Eur J Cell Biol, 1997. **73**(1): p. 10-8.

342. Morales, C.R., *Role of sialic acid in the endocytosis of prosaposin by the nonciliated cells of the rat efferent ducts.* Mol Reprod Dev, 1998. **51**(2): p. 156-66.

343. Kiss, R.S., et al., *The lipoprotein receptor-related protein-1 (LRP) adapter protein GULP mediates trafficking of the LRP ligand prosaposin, leading to sphingolipid and free cholesterol accumulation in late endosomes and impaired efflux.* J Biol Chem, 2006. **281**(17): p. 12081-92.

344. Mahuran, D.J., *The GM2 activator protein, its roles as a co-factor in GM2 hydrolysis and as a general glycolipid transport protein.* Biochim Biophys Acta, 1998. **1393**(1): p. 1-18.

345. O'Brien, J.S., et al., *Coding of two sphingolipid activator proteins (SAP-1 and SAP-2) by same genetic locus.* Science, 1988. **241**(4869): p. 1098-101.

346. Hirst, J. and M.S. Robinson, *Clathrin and adaptors.* Biochim Biophys Acta, 1998. **1404**(1-2): p. 173-93.

347. Rouille, Y., W. Rohn, and B. Hoflack, *Targeting of lysosomal proteins.* Semin Cell Dev Biol, 2000. **11**(3): p. 165-71.

348. Lin, S., et al., *Structural requirements for targeting of surfactant protein B (SP-B) to secretory granules in vitro and in vivo.* J Biol Chem, 1996. **271**(33): p. 19689-95.

349. Garnier, J., D.J. Osguthorpe, and B. Robson, *Analysis of the accuracy and implications of simple methods for predicting the secondary structure of globular proteins.* J Mol Biol, 1978. **120**(1): p. 97-120.

350. Wu, M.M., et al., *Mechanisms of pH regulation in the regulated secretory pathway.* J Biol Chem, 2001. **276**(35): p. 33027-35.

351. Chandy, G., et al., *Proton leak and CFTR in regulation of Golgi pH in respiratory epithelial cells.* Am J Physiol Cell Physiol, 2001. **281**(3): p. C908-21.

352. Machen, T.E., et al., *pH of TGN and recycling endosomes of H+/K+-ATPase-transfected HEK-293 cells: implications for pH regulation in the secretory pathway.* Am J Physiol Cell Physiol, 2003. **285**(1): p. C205-14.

353. Marsh, M., et al., *Three-dimensional structure of endosomes in BHK-21 cells.* Proc Natl Acad Sci U S A, 1986. **83**(9): p. 2899-903.

354. Anderson, R.G. and L. Orci, *A view of acidic intracellular compartments.* J Cell Biol, 1988. **106**(3): p. 539-43.

355. Ohkuma, S. and B. Poole, *Fluorescence probe measurement of the intralysosomal pH in living cells and the perturbation of pH by various agents.* Proc Natl Acad Sci U S A, 1978. **75**(7): p. 3327-31.

356. DiPaola, M. and F.R. Maxfield, *Conformational changes in the receptors for epidermal growth factor and asialoglycoproteins induced by the mildly acidic pH found in endocytic vesicles.* J Biol Chem, 1984. **259**(14): p. 9163-71.

357. Lodish, H., et al., *Chemical Foundations*, in *Molecular Cell Biology*. 2003, W H Freeman & Co. p. 29-58.

358. Schein, C.H., *Solubility as a function of protein structure and solvent components.* Biotechnology (N Y), 1990. **8**(4): p. 308-17.

359. Banares-Hidalgo, A., et al., *Self-aggregation of a recombinant form of the propeptide NH2-terminal of the precursor of pulmonary surfactant protein SP-B: a conformational study.* J Ind Microbiol Biotechnol, 2008. **35**(11): p. 1367-76.

360. Serrano, A.G., E.J. Cabre, and J. Perez-Gil, *Identification of a segment in the precursor of pulmonary surfactant protein SP-B, potentially involved in pH-dependent membrane assembly of the protein.* Biochim Biophys Acta, 2007. **1768**(5): p. 1059-69.

361. Padilla, C., et al., *Role of tryptophan residues in toxicity of Cry1Ab toxin from Bacillus thuringiensis.* Appl Environ Microbiol, 2006. **72**(1): p. 901-7.

362. Yamakura, F. and K. Ikeda, *Modification of tryptophan and tryptophan residues in proteins by reactive nitrogen species.* Nitric Oxide, 2006. **14**(2): p. 152-61.

363. Munson, M., et al., *What makes a protein a protein? Hydrophobic core designs that specify stability and structural properties.* Protein Sci, 1996. **5**(8): p. 1584-93.

364. Shortle, D., W.E. Stites, and A.K. Meeker, *Contributions of the large hydrophobic amino acids to the stability of staphylococcal nuclease.* Biochemistry, 1990. **29**(35): p. 8033-41.

365. Eriksson, A.E., et al., *Response of a protein structure to cavity-creating mutations and its relation to the hydrophobic effect.* Science, 1992. **255**(5041): p. 178-83.

366. Huntley, J.J., et al., *Role of a solvent-exposed tryptophan in the recognition and binding of antibiotic substrates for a metallo-beta-lactamase.* Protein Sci, 2003. **12**(7): p. 1368-75.

367. Ramakrishnan, B., E. Boeggeman, and P.K. Qasba, *Beta-1,4-galactosyltransferase and lactose synthase: molecular mechanical devices.* Biochem Biophys Res Commun, 2002. **291**(5): p. 1113-8.

368. Xie, Y. and J.B. Cohen, *Contributions of Torpedo nicotinic acetylcholine receptor gamma Trp-55 and delta Trp-57 to agonist and competitive antagonist function.* J Biol Chem, 2001. **276**(4): p. 2417-26.

369. Ma, B., et al., *Protein-protein interactions: structurally conserved residues distinguish between binding sites and exposed protein surfaces.* Proc Natl Acad Sci U S A, 2003. **100**(10): p. 5772-7.

370. Samanta, U., D. Pal, and P. Chakrabarti, *Environment of tryptophan side chains in proteins.* Proteins, 2000. **38**(3): p. 288-300.

371. Sevier, C.S. and C.A. Kaiser, *Formation and transfer of disulphide bonds in living cells.* Nat Rev Mol Cell Biol, 2002. **3**(11): p. 836-47.

372. Kay, B.K., M.P. Williamson, and M. Sudol, *The importance of being proline: the interaction of proline-rich motifs in signaling proteins with their cognate domains.* Faseb J, 2000. **14**(2): p. 231-41.

373. Wedemeyer, W.J., E. Welker, and H.A. Scheraga, *Proline cis-trans isomerization and protein folding.* Biochemistry, 2002. **41**(50): p. 14637-44.

374. Lord, J.M., L.M. Roberts, and C.J. Stirling, *Quality control: another player joins the ERAD cast.* Curr Biol, 2005. **15**(23): p. R963-4.

375. Vembar, S.S. and J.L. Brodsky, *One step at a time: endoplasmic reticulum-associated degradation.* Nat Rev Mol Cell Biol, 2008. **9**(12): p. 944-57.

376. Lee, D.H. and A.L. Goldberg, *Proteasome inhibitors: valuable new tools for cell biologists.* Trends Cell Biol, 1998. **8**(10): p. 397-403.

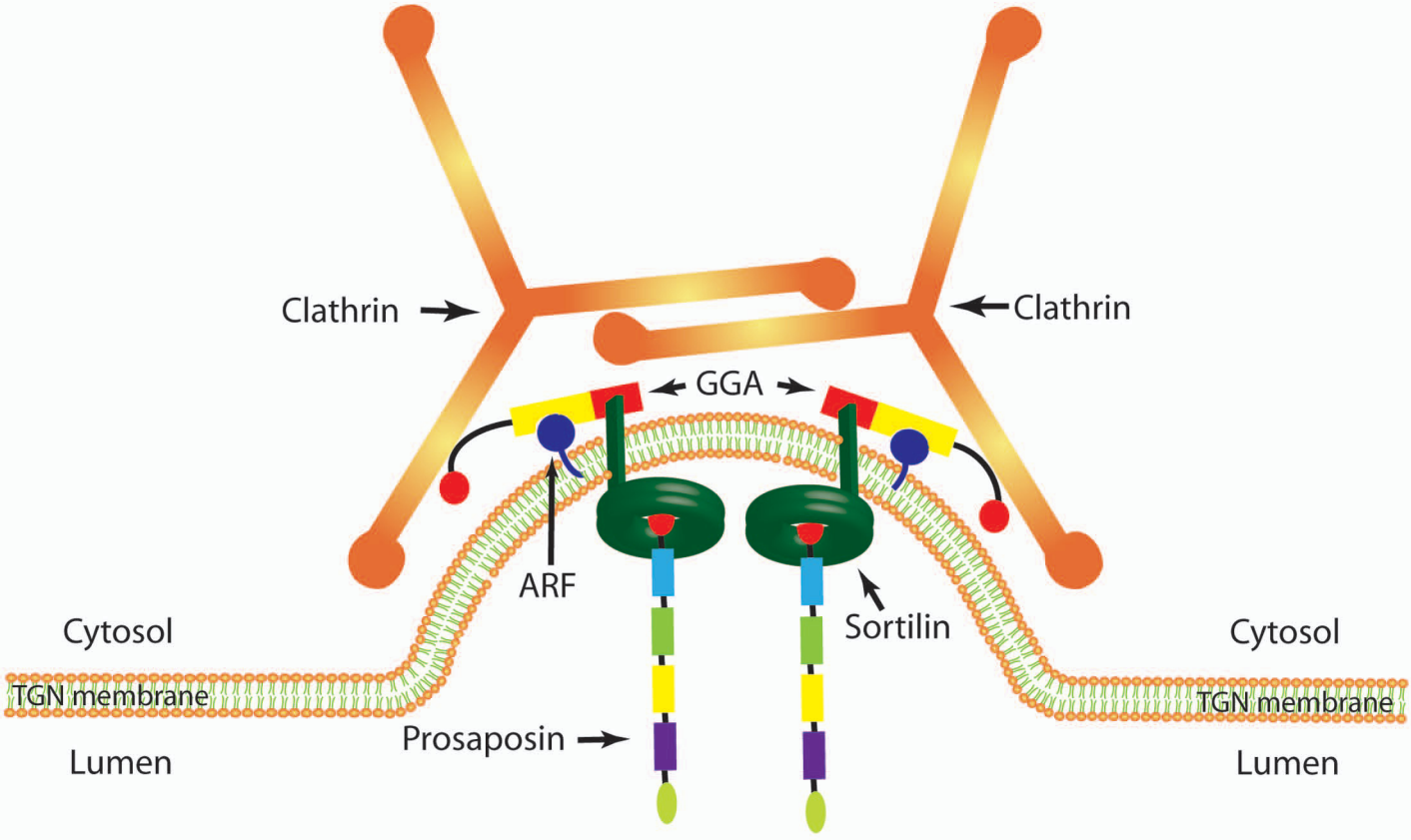

Figure I Schematic Representation of Prosaposin Sorting Model

Figure I Schematic Representation of Prosaposin Sorting Model

The binding of prosaposin to sortilin occurs in the lumen of Trans-Golgi Network. The large luminal segment of sortilin interacts with prosaposin C-terminus and the dileucine signal on its cytoplasmic domain is recognized by GGA, which is recruited onto the TGN membrane by ARF. Through the interaction with the ear domain of GGA, clathrin incorporates prosaposin into a clathrin-coated vesicle, which carries prosaposin to the lysosomes.

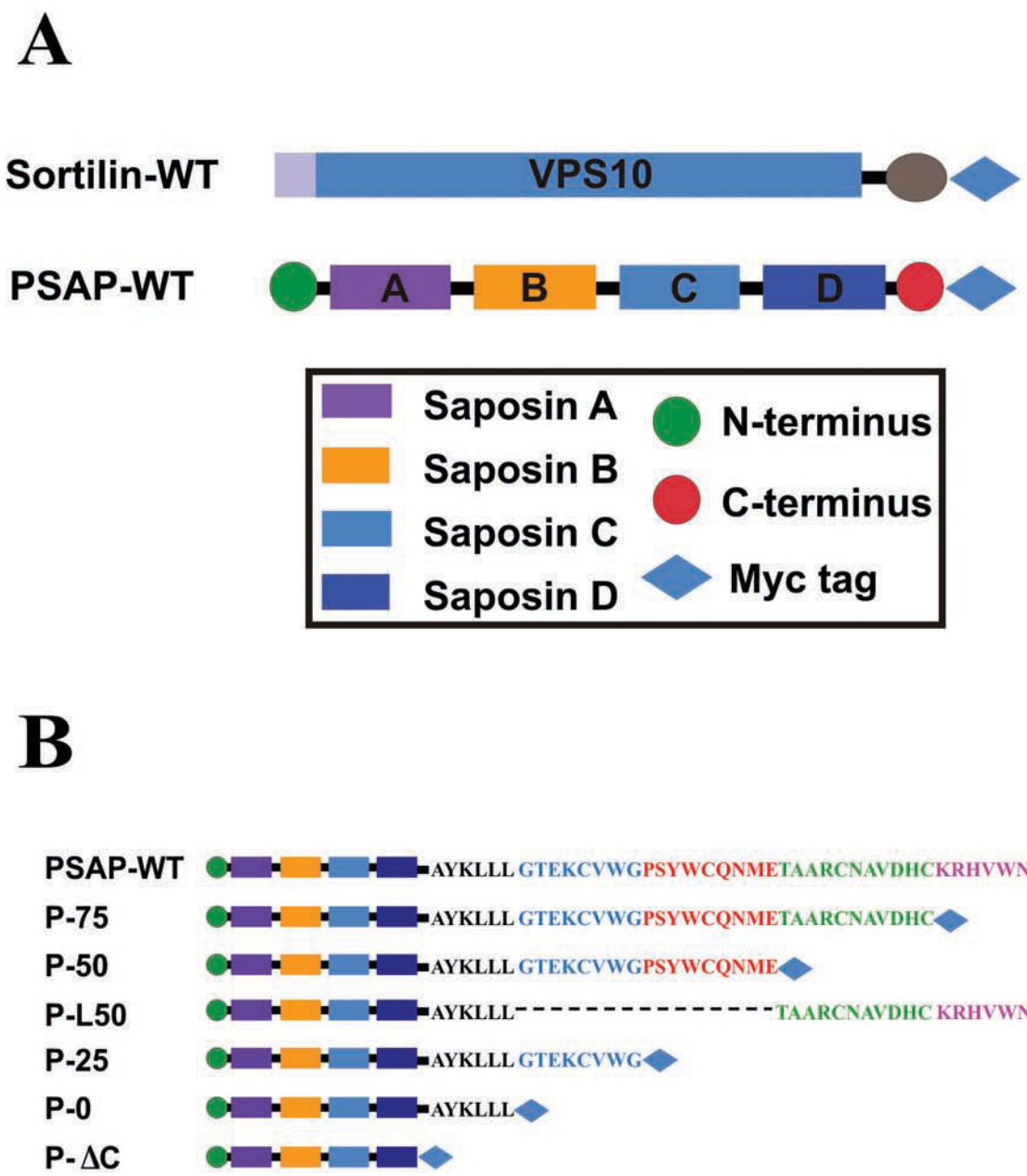

Figure II. Schematic representation of wild-type/truncated prosaposin and sortilin

Figure II. Schematic representation of wild-type/truncated prosaposin and sortilin.

A) Schematic representation of wild-type prosaposin and sortilin. Both prosaposin and sortilin constructs are linked to myc tags. B) Schematic representation of truncated prosaposin constructs. PSAP-WT is a wild-type prosaposin; P-75 lacks 25% of the A-type domain; P-50, lacks 50% of the A-type domain. P-L50 lacks the first half of the A-type domain but contains the second half. P-25 lacks 75% of the A-type domain; P-0 contains only linker region; P-ΔC lacks the whole C-terminus.

Figure III. Schematic representation of prosaposin site-directed mutations of hydrophilic residues

Figure III. Schematic representation of prosaposin site-directed mutations of hydrophilic residues

Among all of these mutations, K520F, E526F, K527F, Q537F, N538W and E540F, the hydrophilic amino acids in the first half of the A-type domain and the linker region were substituted with the hydrophobic amino acids phenylalanine or tryptophan.

Figure IV. Schematic representation of prosaposin site-directed mutations of hydrophobic residues

Figure IV. Schematic representation of prosaposin site-directed mutations of hydrophobic residues

Among these eight mutations, C528D, W530P, W530A, P532W, P532H, W535P, W535A and C536D, the hydrophobic residues in the first half of the A-type domain and the linker region were substituted with the corresponding disfavoured residues.

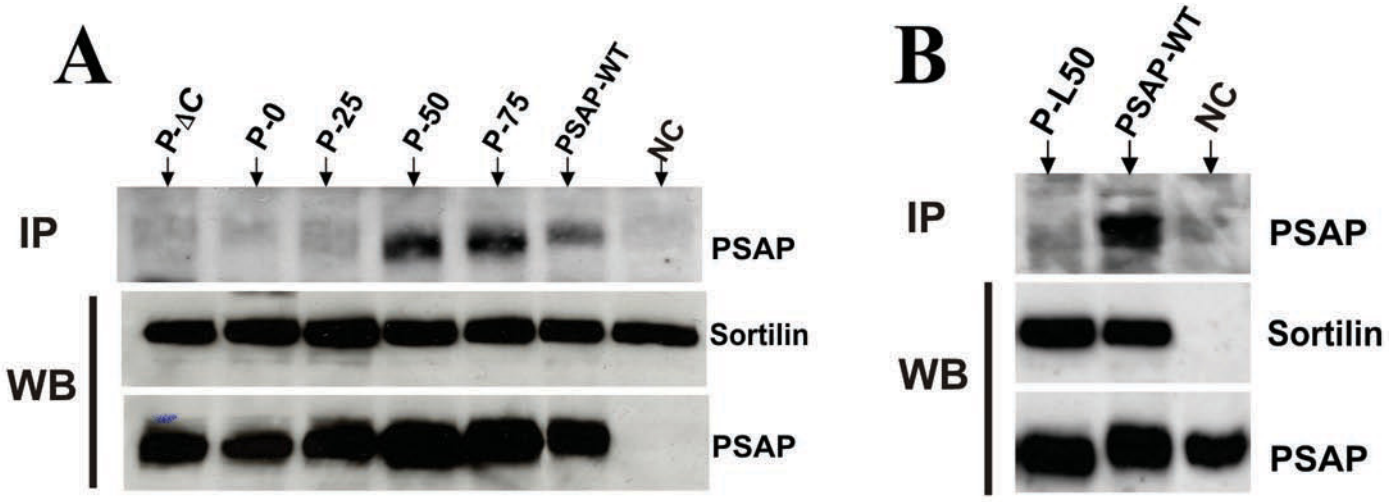

Figure 1. Co-IP: Interaction of sequential truncations of prosaposin with sortilin

Figure 1. Co-IP: Interaction of sequential truncations of prosaposin with sortilin

A) Co-immunoprecipitation with anti-sortilin antibody was conducted to identify the binding of truncated prosaposin to sortilin. While P-75 and P-50 were precipitated by sortilin, P-0 and P-25 were not. PSAP-WT was used as positive control and P-ΔC as negative control. NC was another negative control, in which the cells were only transfected with the sortilin construct. B) Contrary to PSAP-WT, P-L50 was not pulled-down by sortilin. WB stands for Western blot as 2% input of sortilin and prosaposin proteins in the crude lysate.

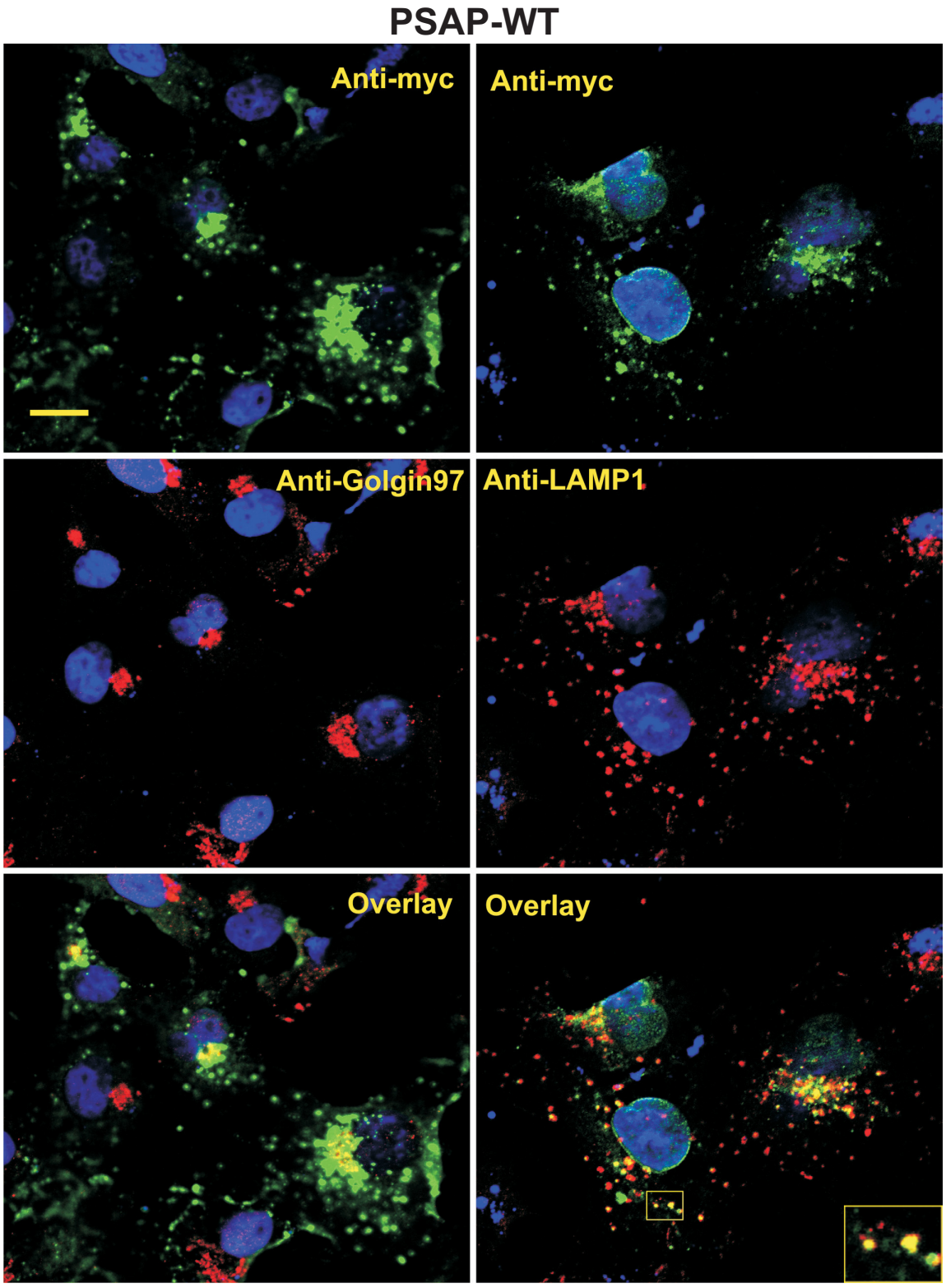

Figure 2. Confocal microscopy: Lysosomal targeting of wild-type prosaposin

Figure 2. Confocal microscopy: Lysosomal targeting of wild-type prosaposin

The COS7 cells transfected with the wild-type prosaposin construct were examined by confocal microscopy. Prosaposin was stained green with chicken anti-myc antibody, while TGN or lysosomes stained red with anti-Golgin97 or anti-LAMP-1 antibody. Nuclei appear in blue. Anti-myc staining of cells transfected with PSAP-WT construct labeled the perinuclear region and cytoplasmic vesicular structures and overlaid with anti-Golgin 97 and anti-LAMP1 staining respectively. Scale bar equals 5 μm and apply to all micrographs.

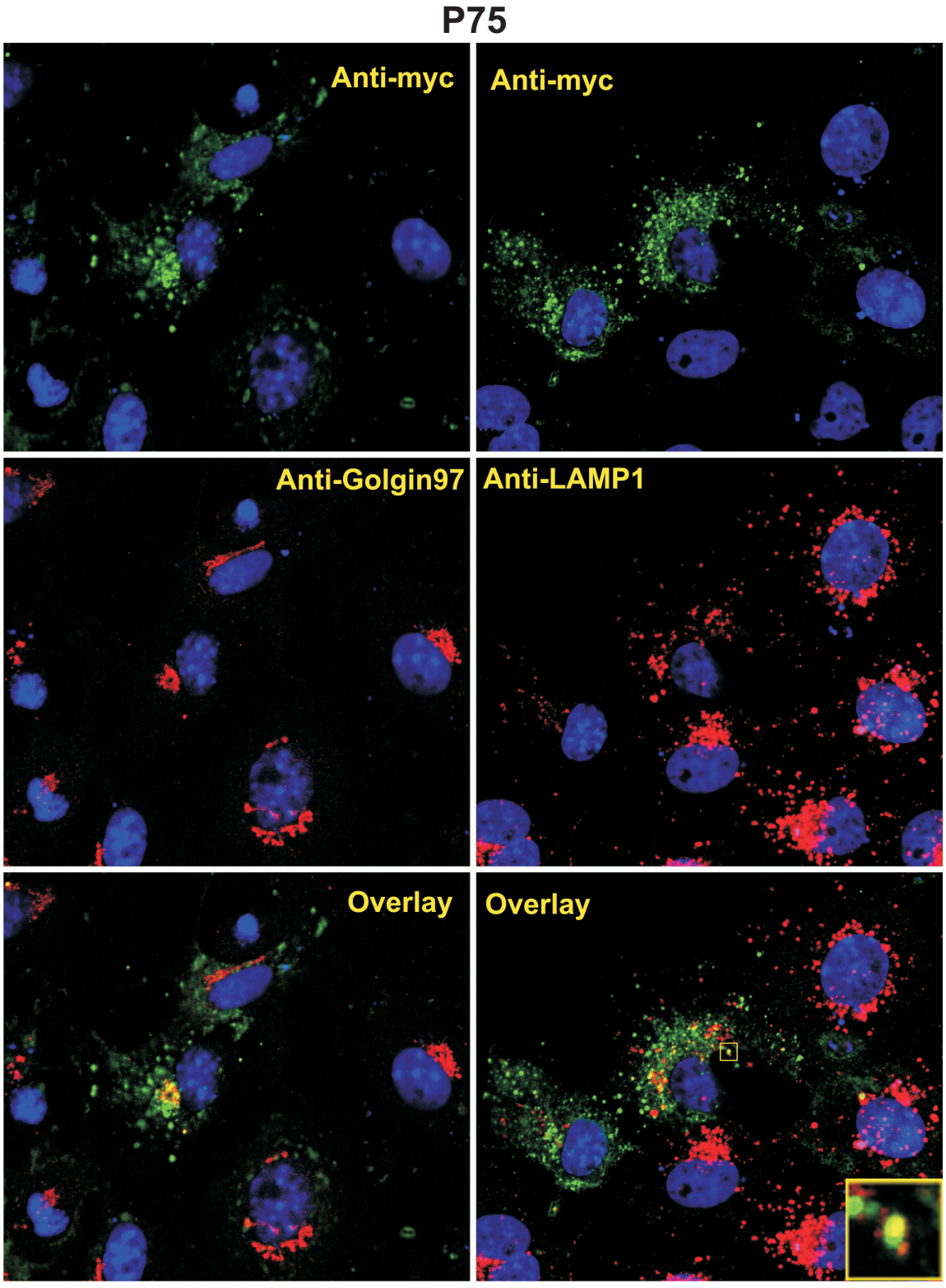

Figure 3. Confocal microscopy: Lysosomal targeting of P75

Figure 3. Confocal microscopy: Lysosomal targeting of P75

The COS7 cells transfected with the truncated prosaposin construct P75 were examined by confocal microscopy. P75 was stained green with chicken anti-myc antibody, while TGN or lysosomes stained red with anti-Golgin97 or anti-LAMP-1 antibody. Nuclei appear in blue. Anti-myc staining of cells transfected with P75 construct labeled the perinuclear region and cytoplasmic vesicular structures and overlaid with anti-Golgin 97 and anti-LAMP1 staining respectively. Scale bar equals 5 μm and apply to all micrographs.

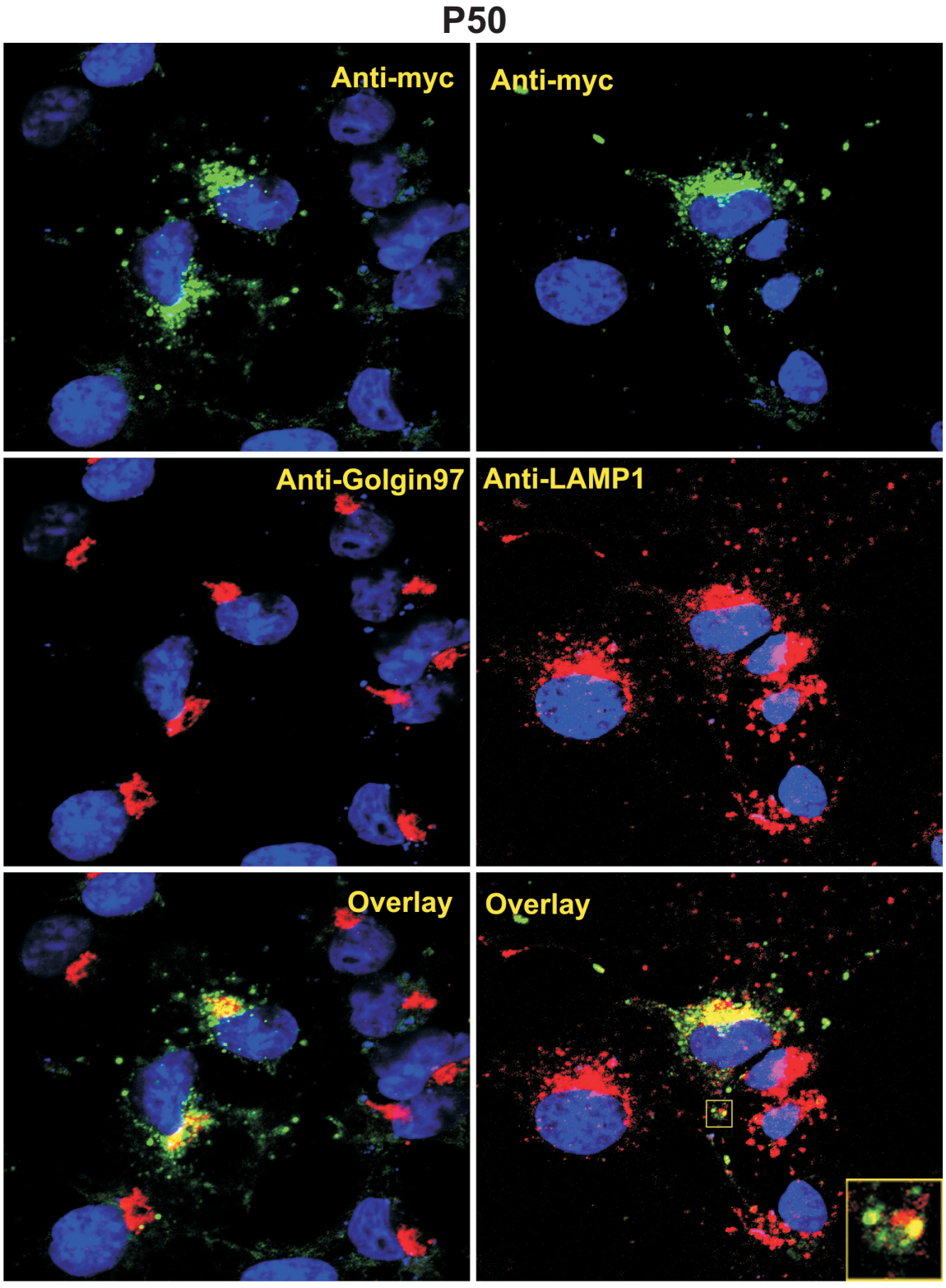

Figure 4. Confocal microscopy: Lysosomal targeting of P50

Figure 4. Confocal microscopy: Lysosomal targeting of P50

The COS7 cells transfected with the truncated prosaposin construct P50 were examined by confocal microscopy. P50 was stained green with chicken anti-myc antibody, while TGN or lysosomes stained red with anti-Golgin97 or anti-LAMP-1 antibody. Nuclei appear in blue. Anti-myc staining of cells transfected with P50 construct labeled the perinuclear region and cytoplasmic vesicular structures and overlaid with anti-Golgin 97 and anti-LAMP1 staining respectively. Scale bar equals 5 μm and apply to all micrographs.

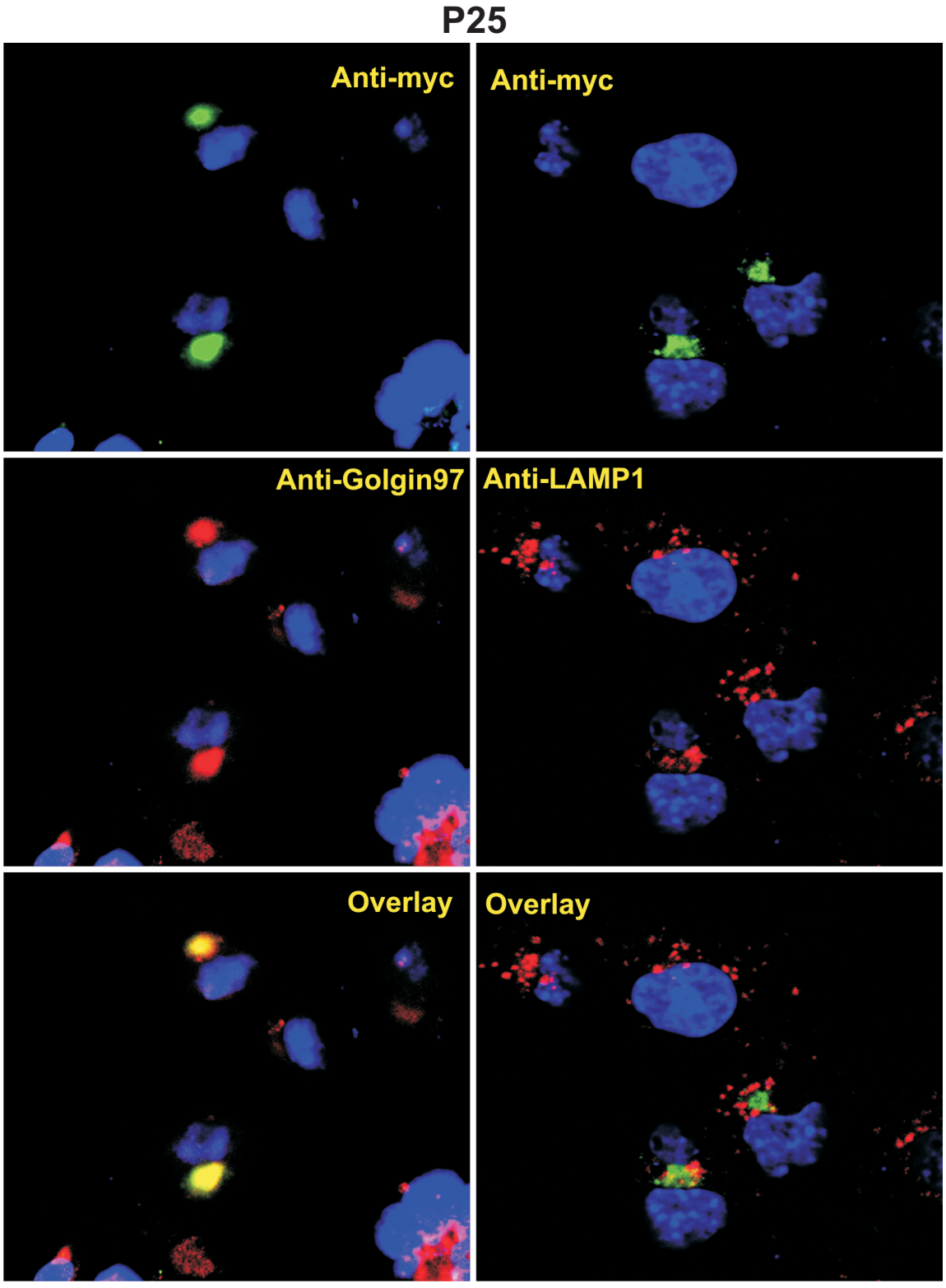

Figure 5. Confocal microscopy: Lysosomal targeting of P25

Figure 5. Confocal microscopy: Lysosomal targeting of P25

The COS7 cells transfected with the truncated construct P25 were examined by confocal microscopy. P25 was stained green with chicken anti-myc antibody, while TGN or lysosomes stained red with anti-Golgin97 or anti-LAMP-1 antibody. Nuclei appear in blue. Anti-myc staining of cells transfected with P25 overlaid only with anti-Golgin staining and labeled the perinuclear region but not the cytoplasmic vesicular structures. Scale bar equals 5 μm and apply to all micrographs.

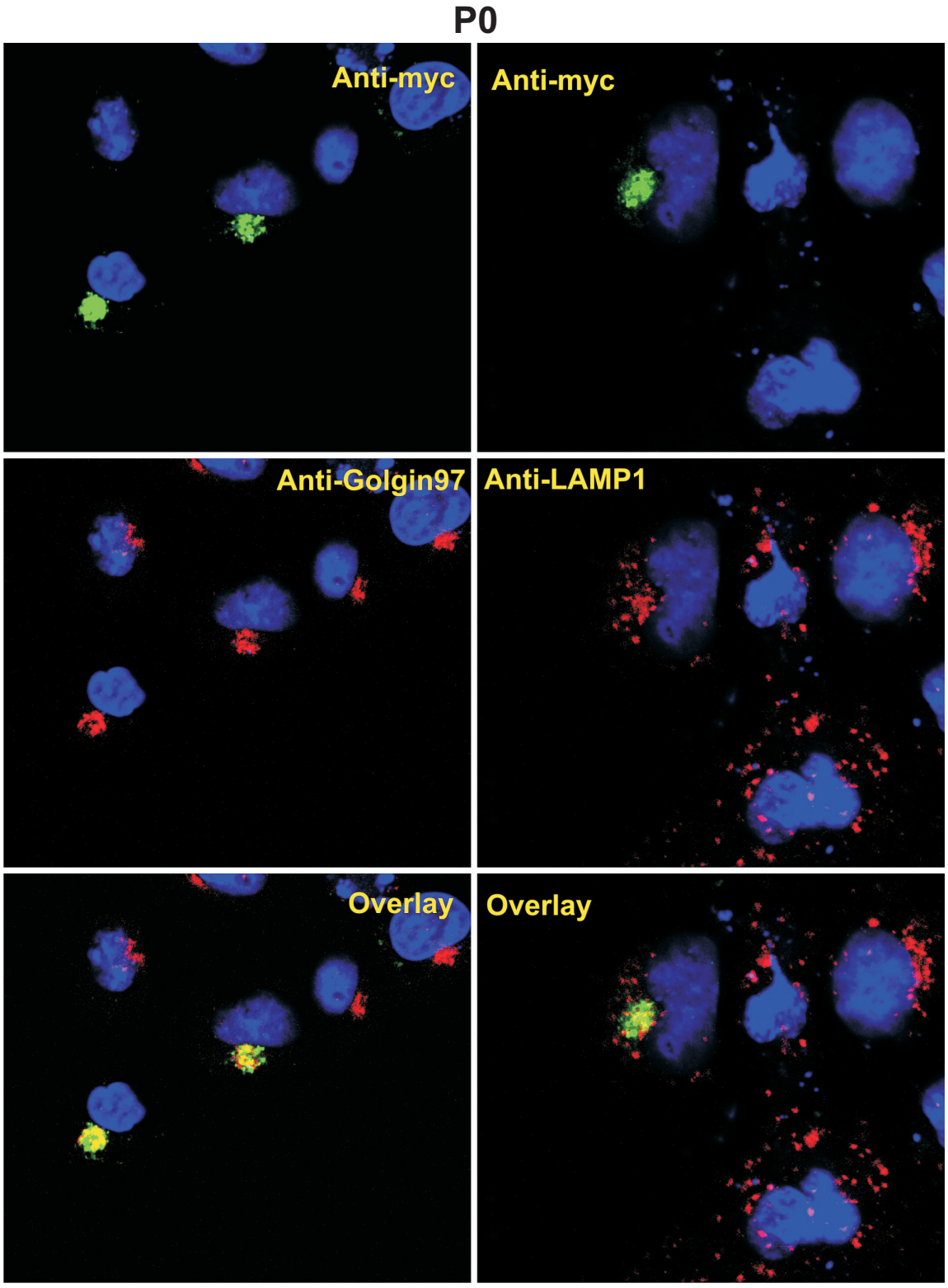

Figure 6. Confocal microscopy: Lysosomal targeting of P0

Figure 6. Confocal microscopy: Lysosomal targeting of P0

The COS7 cells transfected with the truncated construct P0 were examined by confocal microscopy. P0 was stained green with chicken anti-myc antibody, while TGN or lysosomes stained red with anti-Golgin97 or anti-LAMP-1 antibody. Nuclei appear in blue. Anti-myc staining of cells transfected with P0 overlaid only with anti-Golgin staining and labeled the perinuclear region but not the cytoplasmic vesicular structures. Scale bar equals 5 μm and apply to all micrographs.

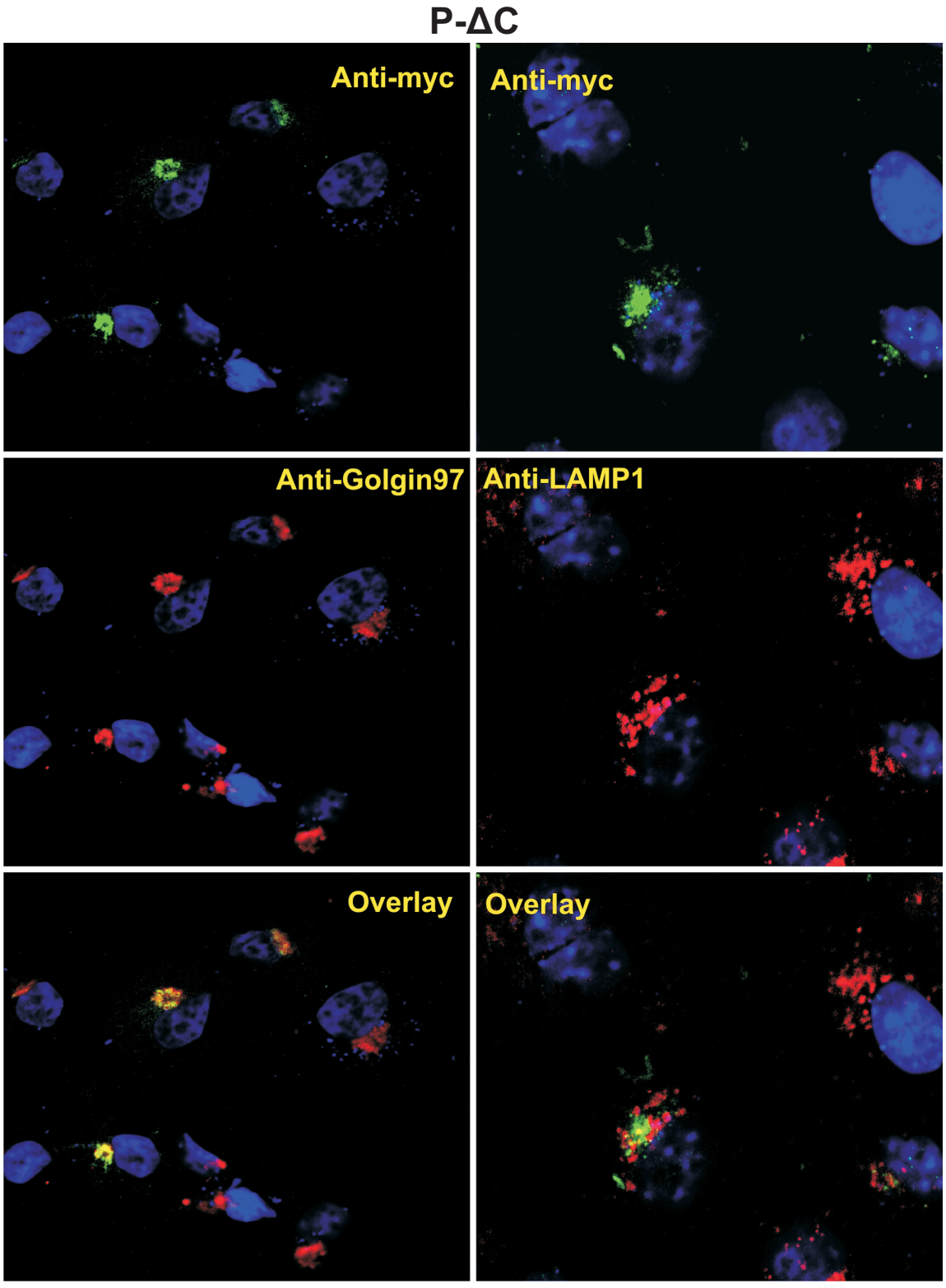

Figure 7. Confocal microscopy: Lysosomal targeting of P?C

Figure 7. Confocal microscopy: Lysosomal targeting of PΔC

The COS7 cells transfected with the truncated construct PΔC were examined by confocal microscopy. PΔC was stained green with chicken anti-myc antibody, while TGN or lysosomes stained red with anti-Golgin97 or anti-LAMP-1 antibody. Nuclei appear in blue. Anti-myc staining of cells transfected with PΔC overlaid only with anti-Golgin staining and labeled the perinuclear region but not the cytoplasmic vesicular structures. Scale bar equals 5 μm and apply to all micrographs.

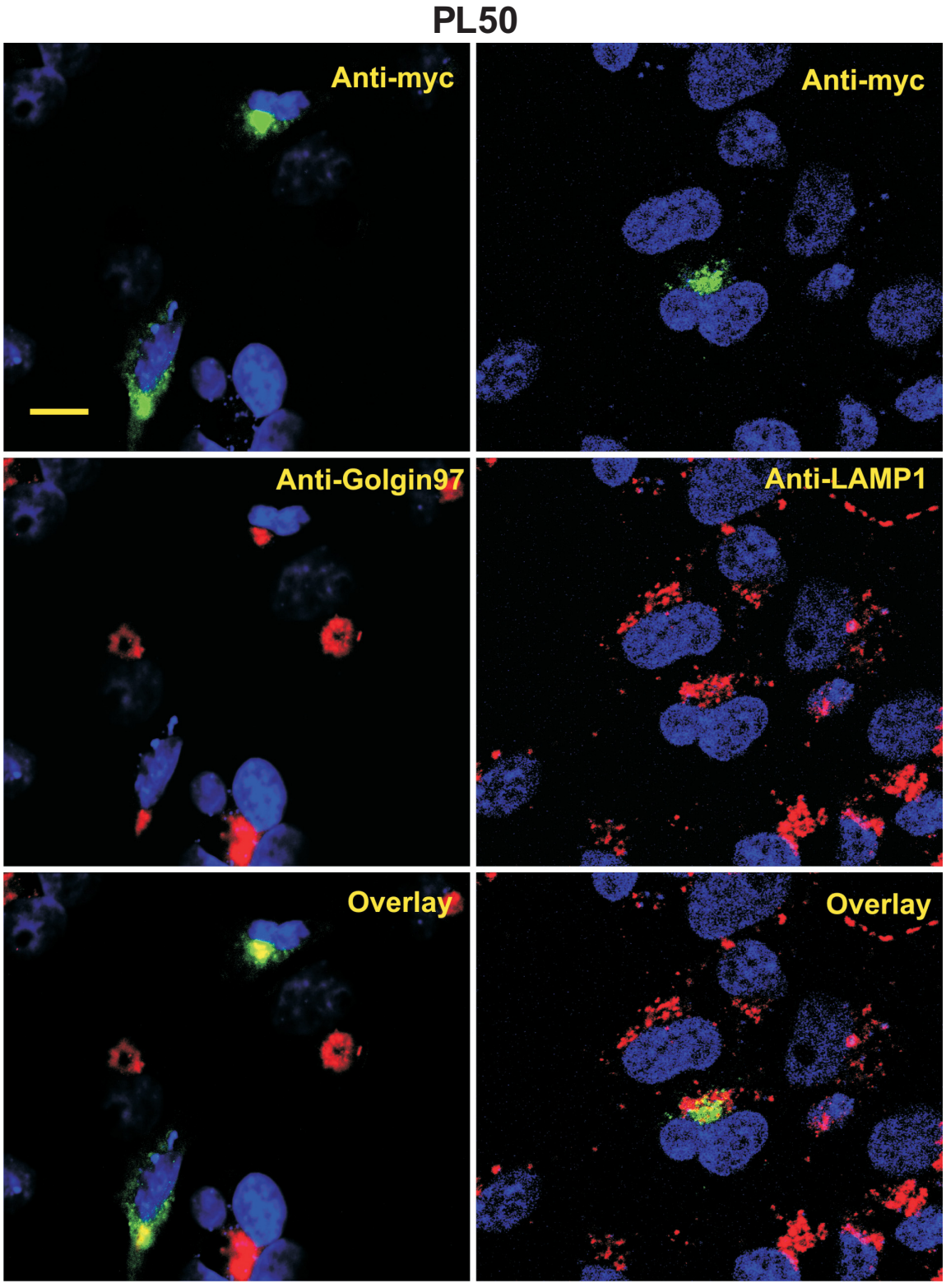

Figure 8. Confocal microscopy: Lysosomal targeting of PL50

Figure 8. Confocal microscopy: Lysosomal targeting of PL50

The COS7 cells transfected with the truncated construct PL50 were examined by confocal microscopy. PL50 was stained green with chicken anti-myc antibody, while TGN or lysosomes stained red with anti-Golgin97 or anti-LAMP-1 antibody. Nuclei appear in blue. Anti-myc staining of cells transfected with PL50 overlaid only with anti-Golgin staining and labeled the perinuclear region but not the cytoplasmic vesicular structures. Scale bar equals 5 μm and apply to all micrographs.

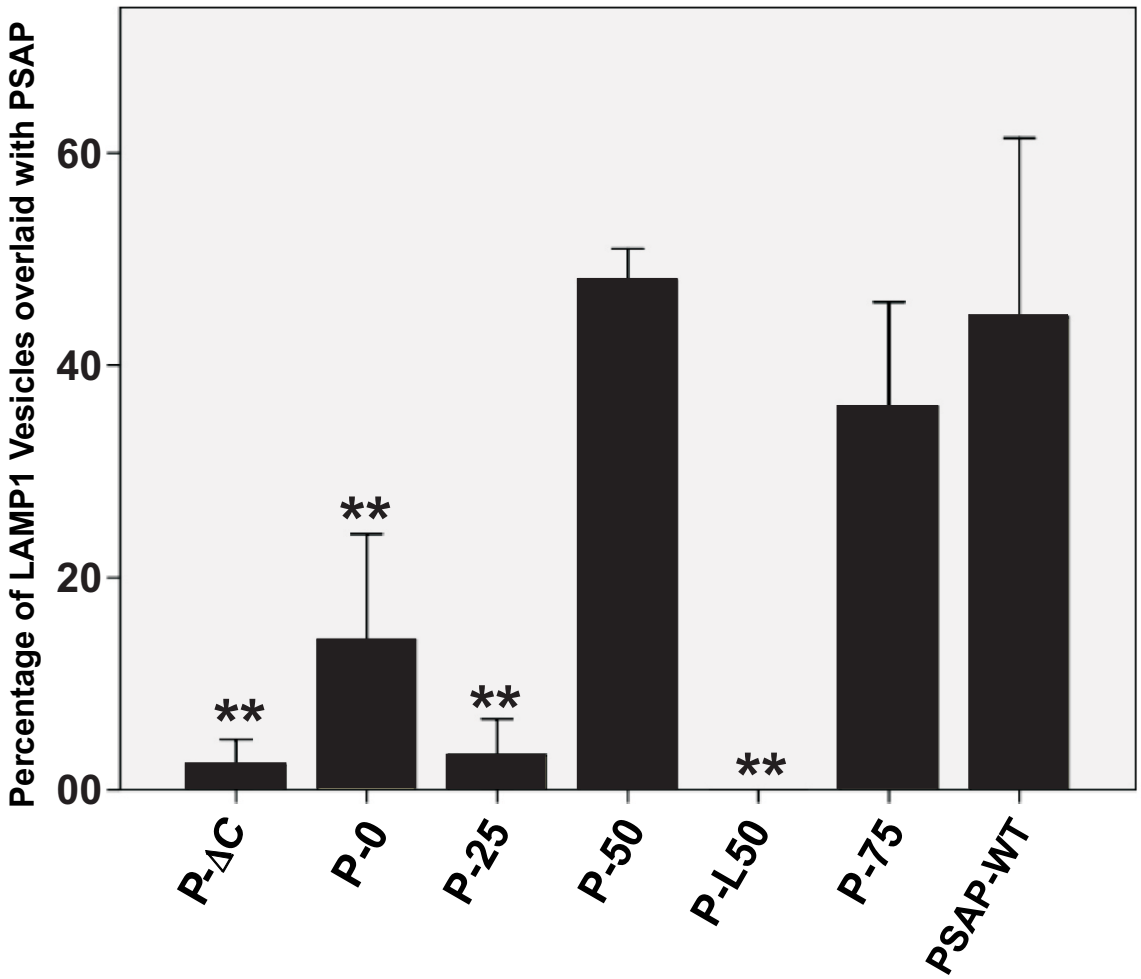

Figure 9. Statistic analysis: Lysosomal targeting of truncated prosaposins

Figure 9. Statistic analysis: Lysosomal targeting of truncated prosaposins

The percentage of LAMP-1 vesicles overlaid with each truncated prosaposin construct was calculated. P-ΔC, P-0, P-25 and P-L50 (double asterisks), showed significant decreases in lysosomal transport ($P<0.01$). The values of P-50 and P-75 were not significantly different from PSAP-WT. Error bars indicate ± S.E.

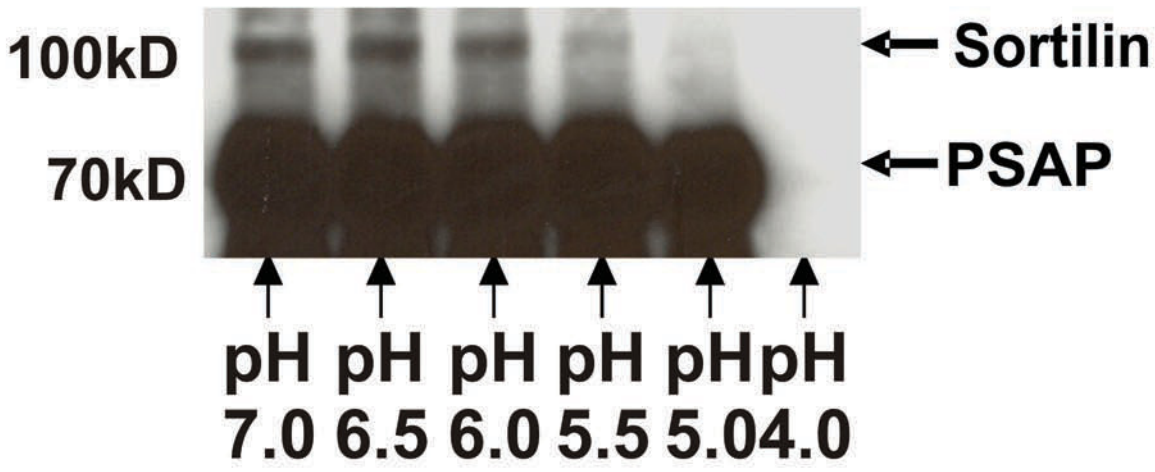

Figure 10. CO-IP: Effect of pH on the interaction of prosaposin and sortilin

Figure 10. CO-IP: Effect of pH on the interaction of prosaposin and sortilin

The co-immunoprecipitation of sortilin with anti-prosaposin antibody was conducted at different pHs. The 70kDa bands in the lower panel show that prosaposin is pulled down by anti-prosaposin antibody. The upper panel demonstrates that the 100kDa bands that represent sortilin were precipitated with prosaposin at pH 6.0, 6.5 and 7.0. At pH 5.5 the sortilin band was weak and no band was observed at pH5.0.

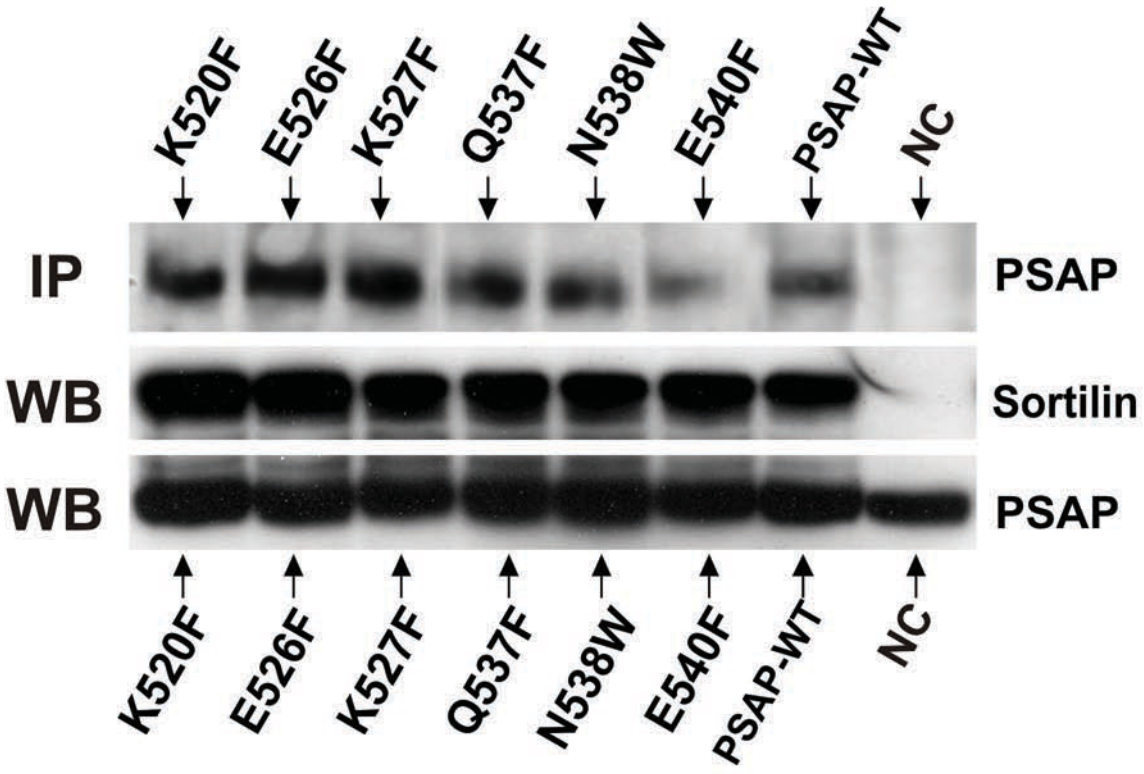

Figure 11. CO-IP: Interaction of sortilin and prosaposin with hydrophilic residue mutations

Figure 11. CO-IP: Interaction of sortilin and prosaposin with hydrophilic residue mutations

Co-immunoprecipitation was conducted with anti-sortilin antibody to identify the binding of prosaposin with hydrophilic residue mutations to sortilin. All of the mutations, K520F, E526F, K527F, Q537F, N538W and E540F, were precipitated by sortilin. PSAP-WT was used as a positive control. Negative control (NC) corresponds to cells transfected with the sortilin construct only. WB is western blot results, showing a 1.5% input of sortilin and prosaposin in the crude lysate.

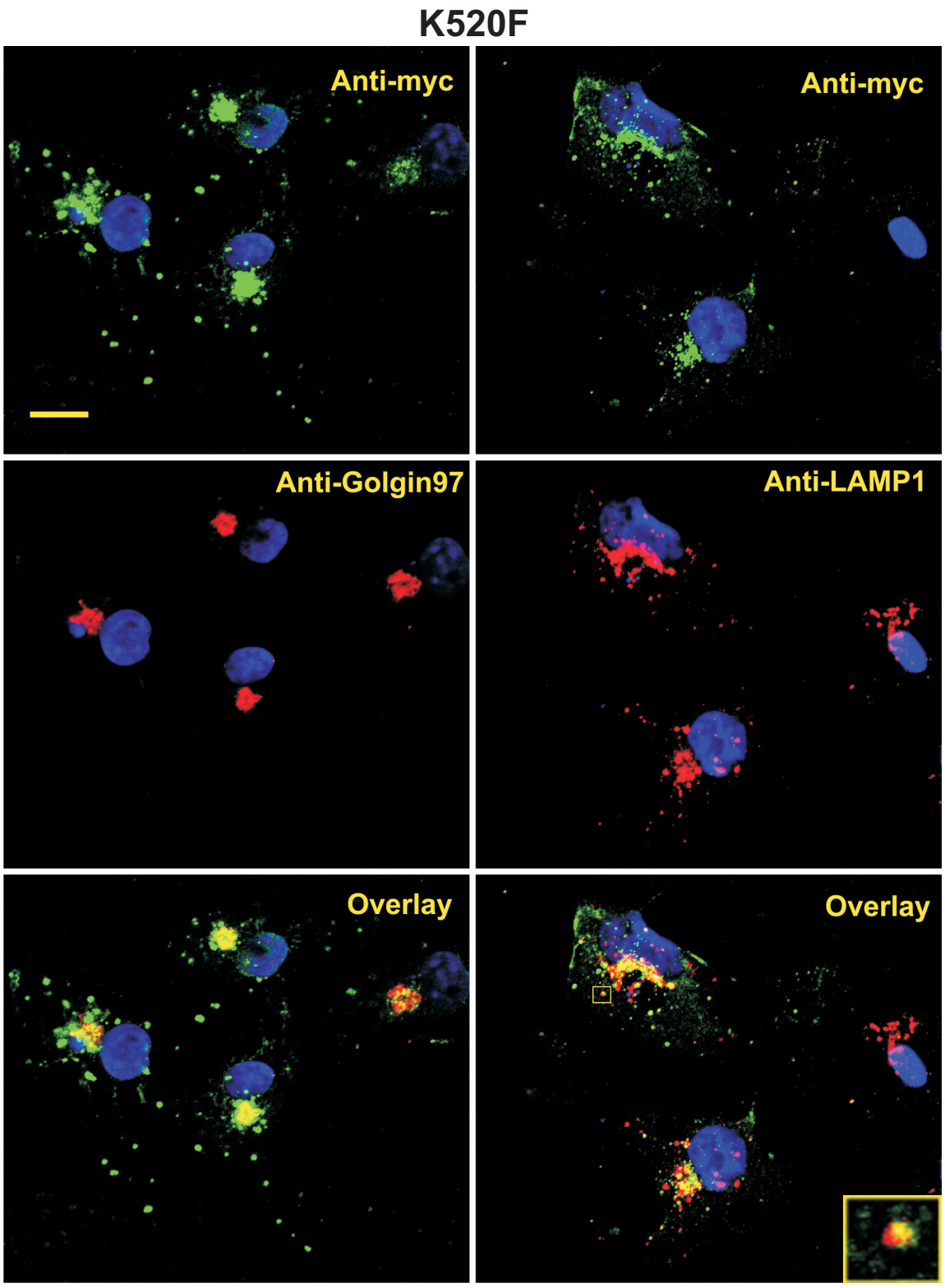

Figure 12. Confocal microscopy: Lysosomal targeting of K520F

Figure 12. Confocal microscopy: Lysosomal targeting of K520F

The COS7 cells transfected with the mutated prosaposin construct K520F were examined by confocal microscopy. K520F was stained green with chicken anti-myc antibody, while TGN or lysosomes stained red with anti-Golgin97 or anti-LAMP-1 antibody. Nuclei appear in blue. Anti-myc staining of cells transfected with K520F construct labeled the perinuclear region and cytoplasmic vesicular structures and overlaid with anti-Golgin 97 and anti-LAMP1 staining respectively. Scale bar equals 5 μm and apply to all micrographs.

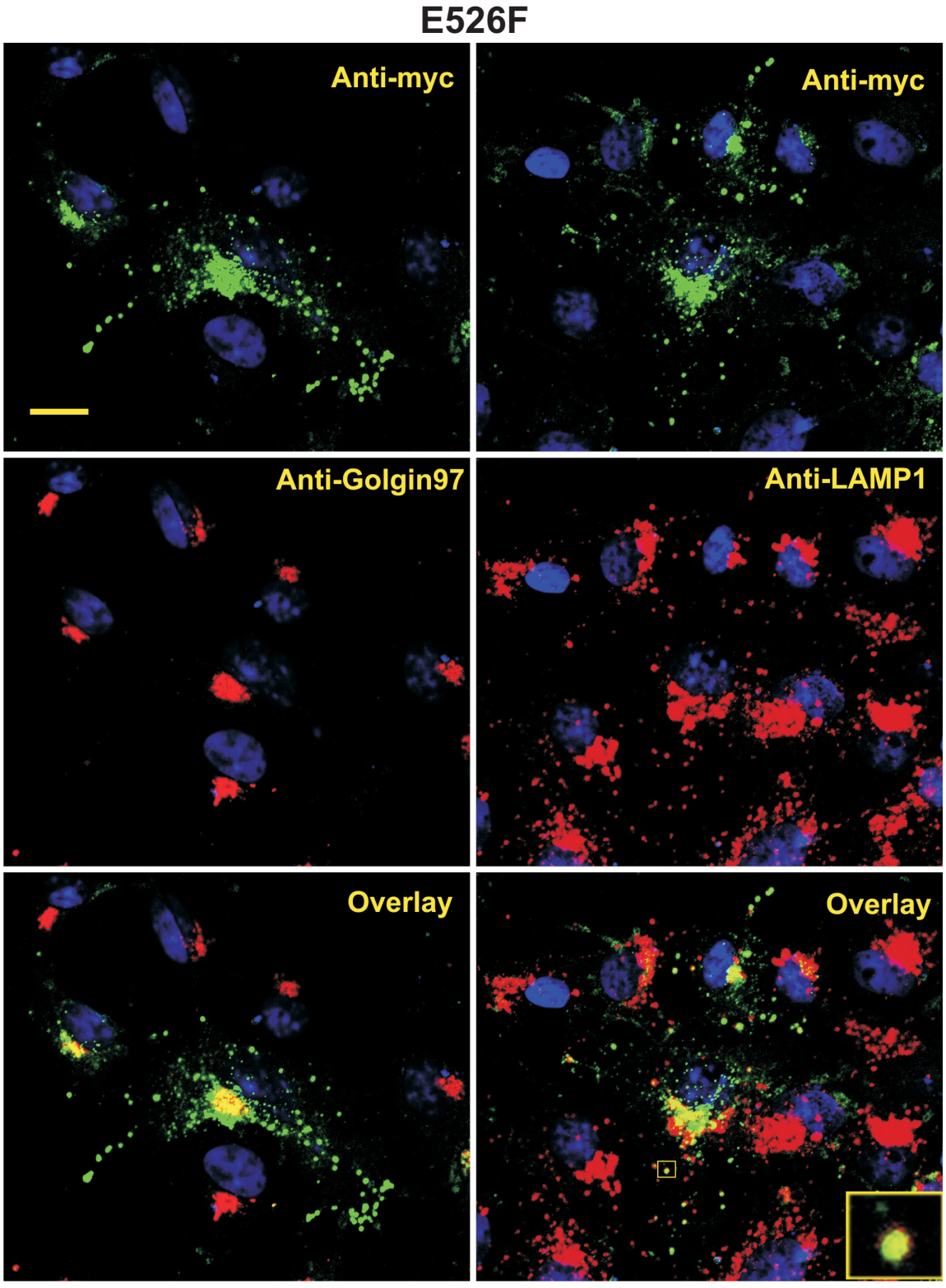

Figure 13. Confocal microscopy: Lysosomal targeting of E526F

Figure 13. Confocal microscopy: Lysosomal targeting of E526F

The COS7 cells transfected with the mutated prosaposin construct E526F were examined by confocal microscopy. E526F was stained green with chicken anti-myc antibody, while TGN or lysosomes stained red with anti-Golgin97 or anti-LAMP-1 antibody. Nuclei appear in blue. Anti-myc staining of cells transfected with E526F construct labeled the perinuclear region and cytoplasmic vesicular structures and overlaid with anti-Golgin 97 and anti-LAMP1 staining respectively. Scale bar equals 5 μm and apply to all micrographs.

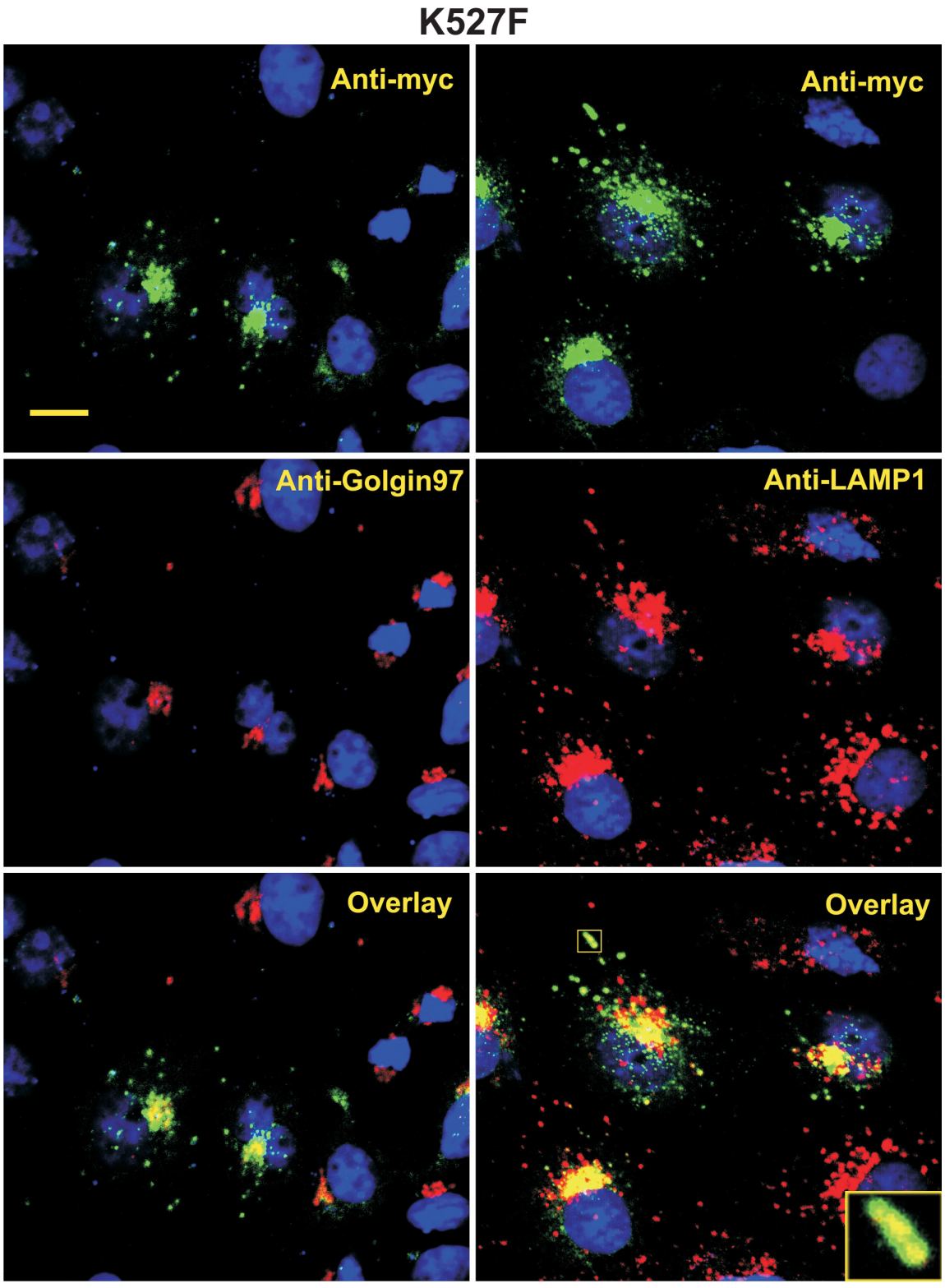

Figure 14. Confocal microscopy: Lysosomal targeting of K527F

Figure 14. Confocal microscopy: Lysosomal targeting of K527F

The COS7 cells transfected with the mutated prosaposin construct K527F were examined by confocal microscopy. K527F was stained green with chicken anti-myc antibody, while TGN or lysosomes stained red with anti-Golgin97 or anti-LAMP-1 antibody. Nuclei appear in blue. Anti-myc staining of cells transfected with K527F construct labeled the perinuclear region and cytoplasmic vesicular structures and overlaid with anti-Golgin 97 and anti-LAMP1 staining respectively. Scale bar equals 5 μm and apply to all micrographs.

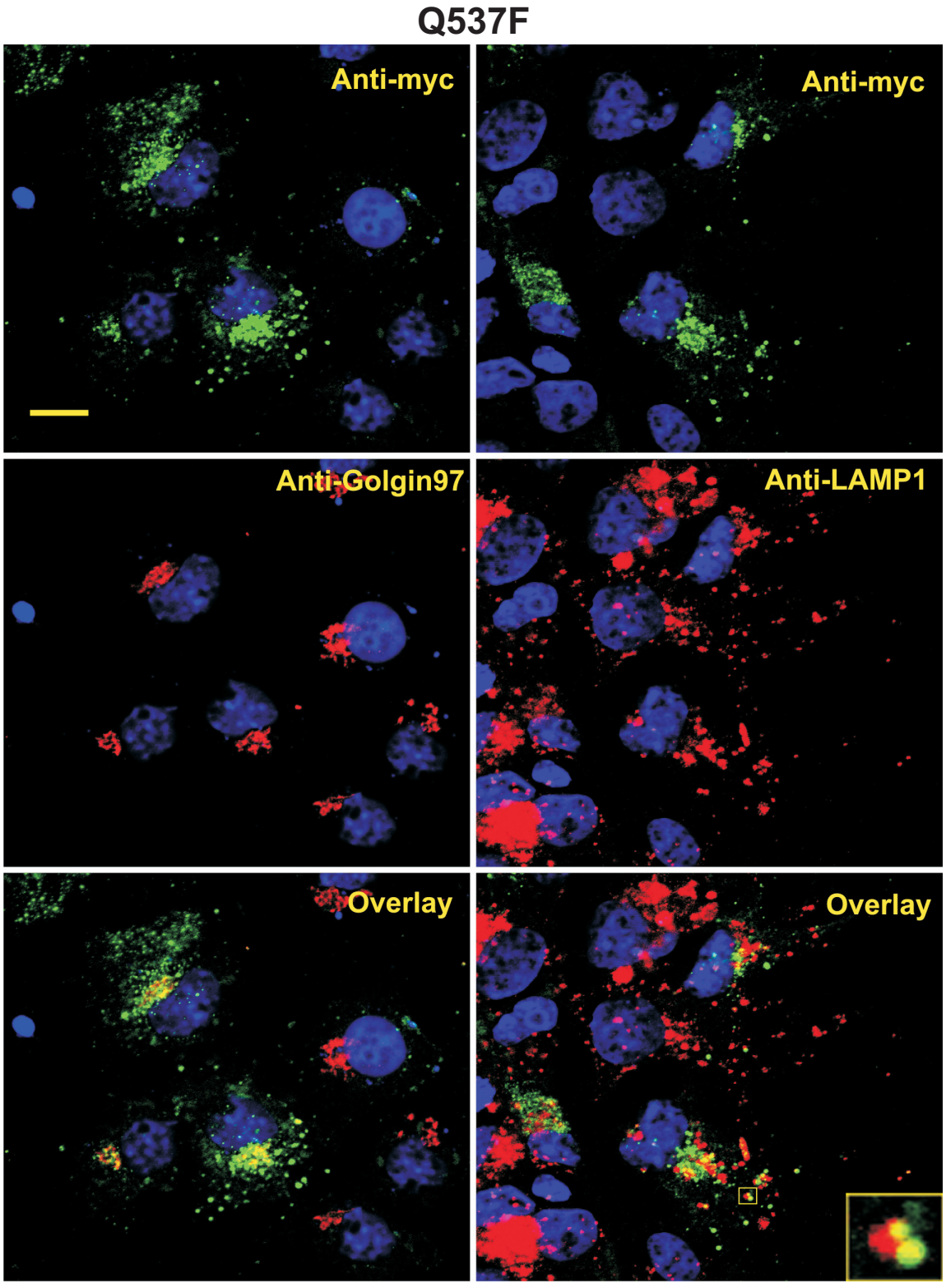

Figure 15. Confocal microscopy: Lysosomal targeting of Q537F

Figure 15. Confocal microscopy: Lysosomal targeting of Q537F

The COS7 cells transfected with the mutated prosaposin construct Q537F were examined by confocal microscopy. Q537F was stained green with chicken anti-myc antibody, while TGN or lysosomes stained red with anti-Golgin97 or anti-LAMP-1 antibody. Nuclei appear in blue. Anti-myc staining of cells transfected with Q537F construct labeled the perinuclear region and cytoplasmic vesicular structures and overlaid with anti-Golgin 97 and anti-LAMP1 staining respectively. Scale bar equals 5 μm and apply to all micrographs.

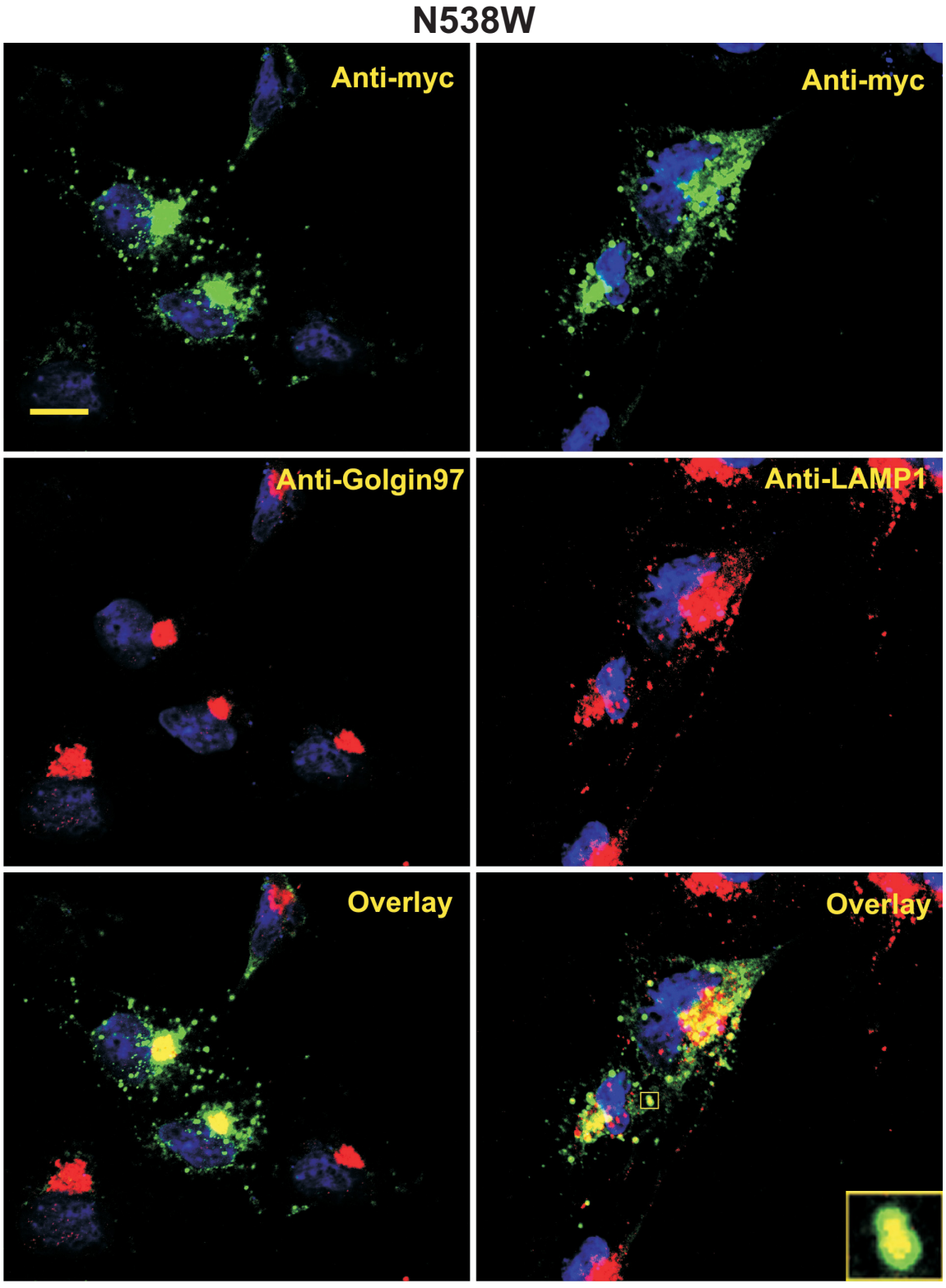

Figure 16. Confocal microscopy: Lysosomal targeting of N538W

Figure 16. Confocal microscopy: Lysosomal targeting of N538W

The COS7 cells transfected with the mutated prosaposin construct N538W were examined by confocal microscopy. N538W was stained green with chicken anti-myc antibody, while TGN or lysosomes stained red with anti-Golgin97 or anti-LAMP-1 antibody. Nuclei appear in blue. Anti-myc staining of cells transfected with N538W construct labeled the perinuclear region and cytoplasmic vesicular structures and overlaid with anti-Golgin 97 and anti-LAMP1 staining respectively. Scale bar equals 5 μm and apply to all micrographs.

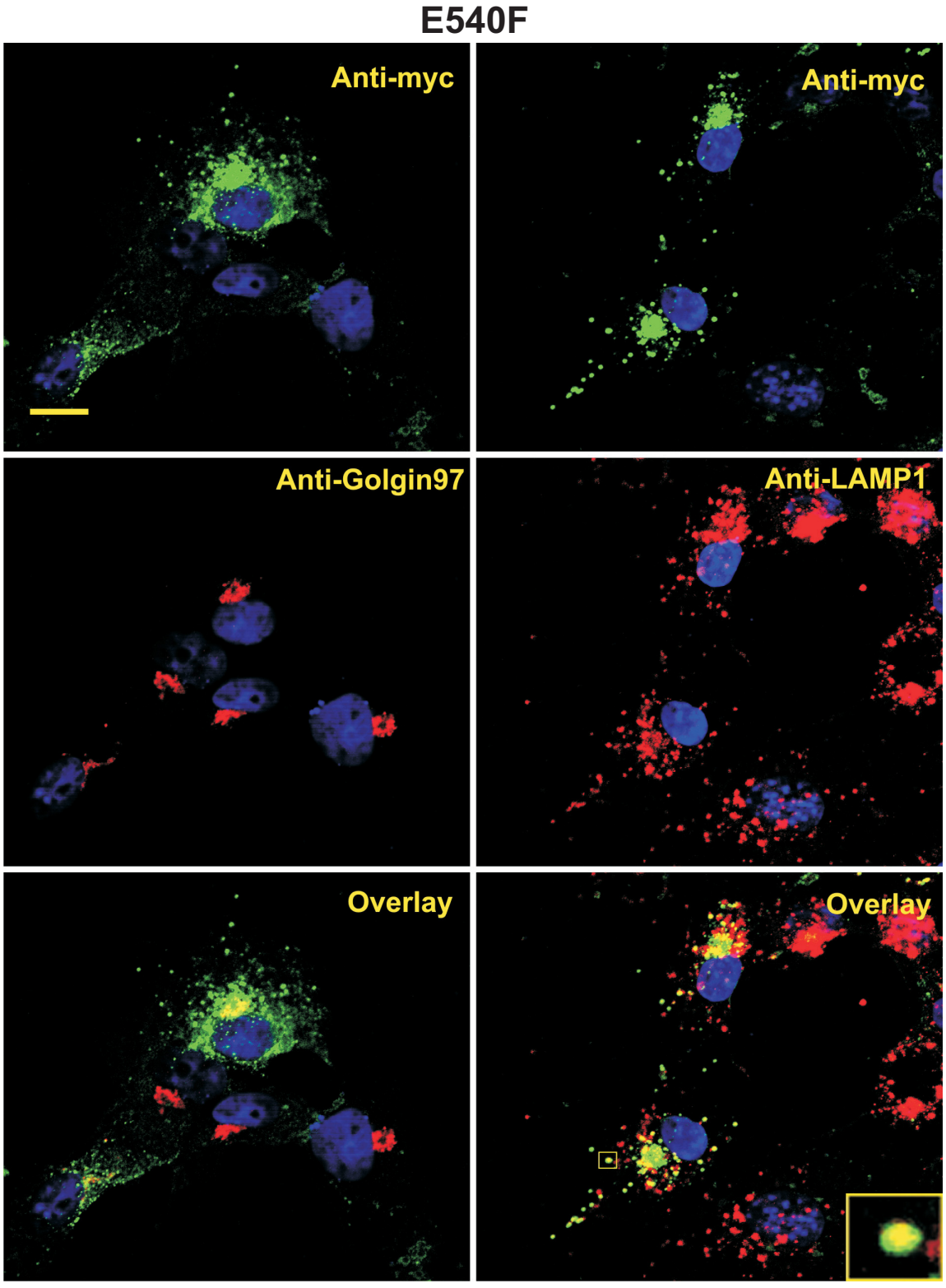

Figure 17. Confocal microscopy: Lysosomal targeting of E540F

.

Figure 17. Confocal microscopy: Lysosomal targeting of E540F

The COS7 cells transfected with the mutated prosaposin construct E540F were examined by confocal microscopy. E540F was stained green with chicken anti-myc antibody, while TGN or lysosomes stained red with anti-Golgin97 or anti-LAMP-1 antibody. Nuclei appear in blue. Anti-myc staining of cells transfected with E540F construct labeled the perinuclear region and cytoplasmic vesicular structures and overlaid with anti-Golgin 97 and anti-LAMP1 staining respectively. Scale bar equals 5 μm and apply to all micrographs.

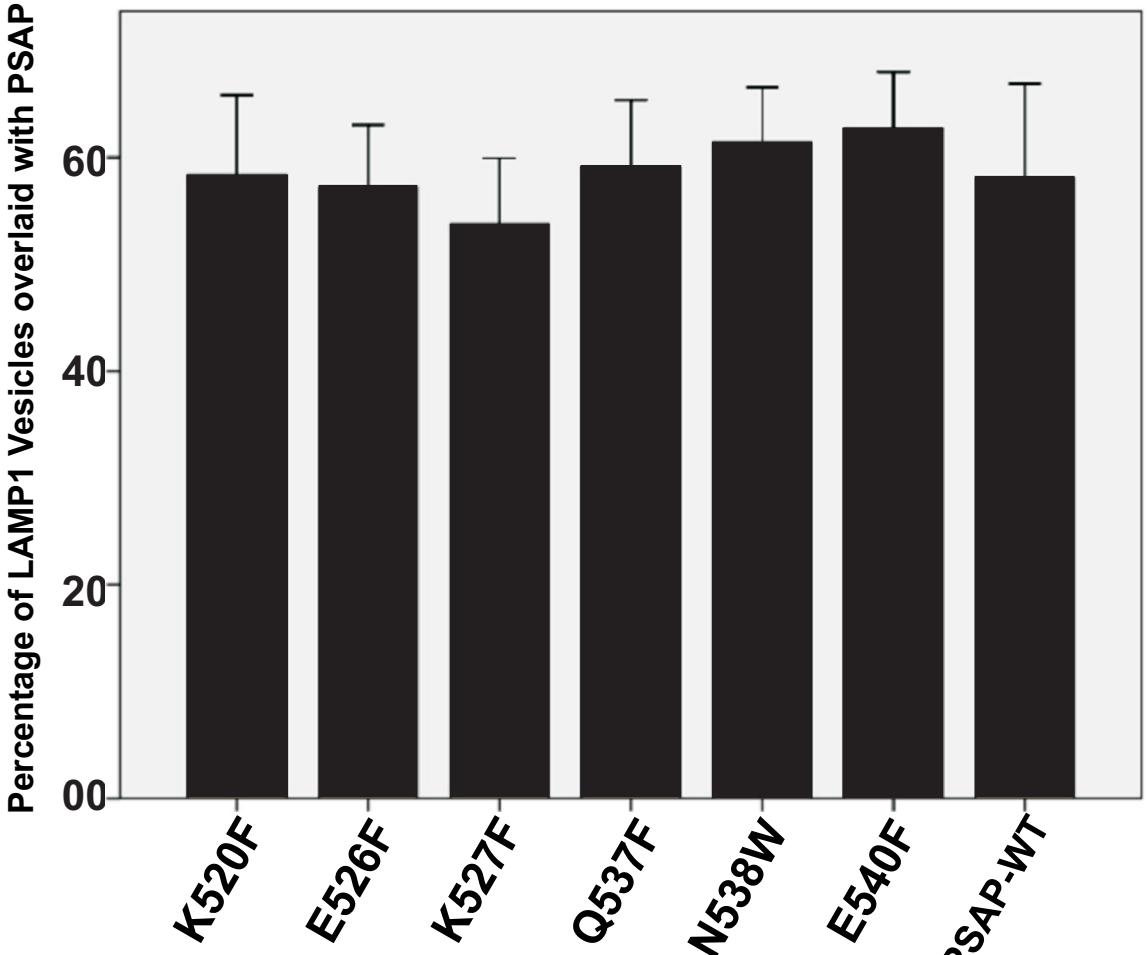

Figure 18. Statistic analysis: Lysosomal targeting of prosaposin with hydrophilic residue mutations

Figure 18. Statistic analysis: Lysosomal targeting of prosaposin with hydrophilic residue mutations

The percentage of LAMP-1 vesicles overlaid with each mutated prosaposin construct was calculated. All of the prosaposin constructs with hydrophilic residue mutations did not show significant difference from PSAP-WT. Error bars indicate ± S.E.

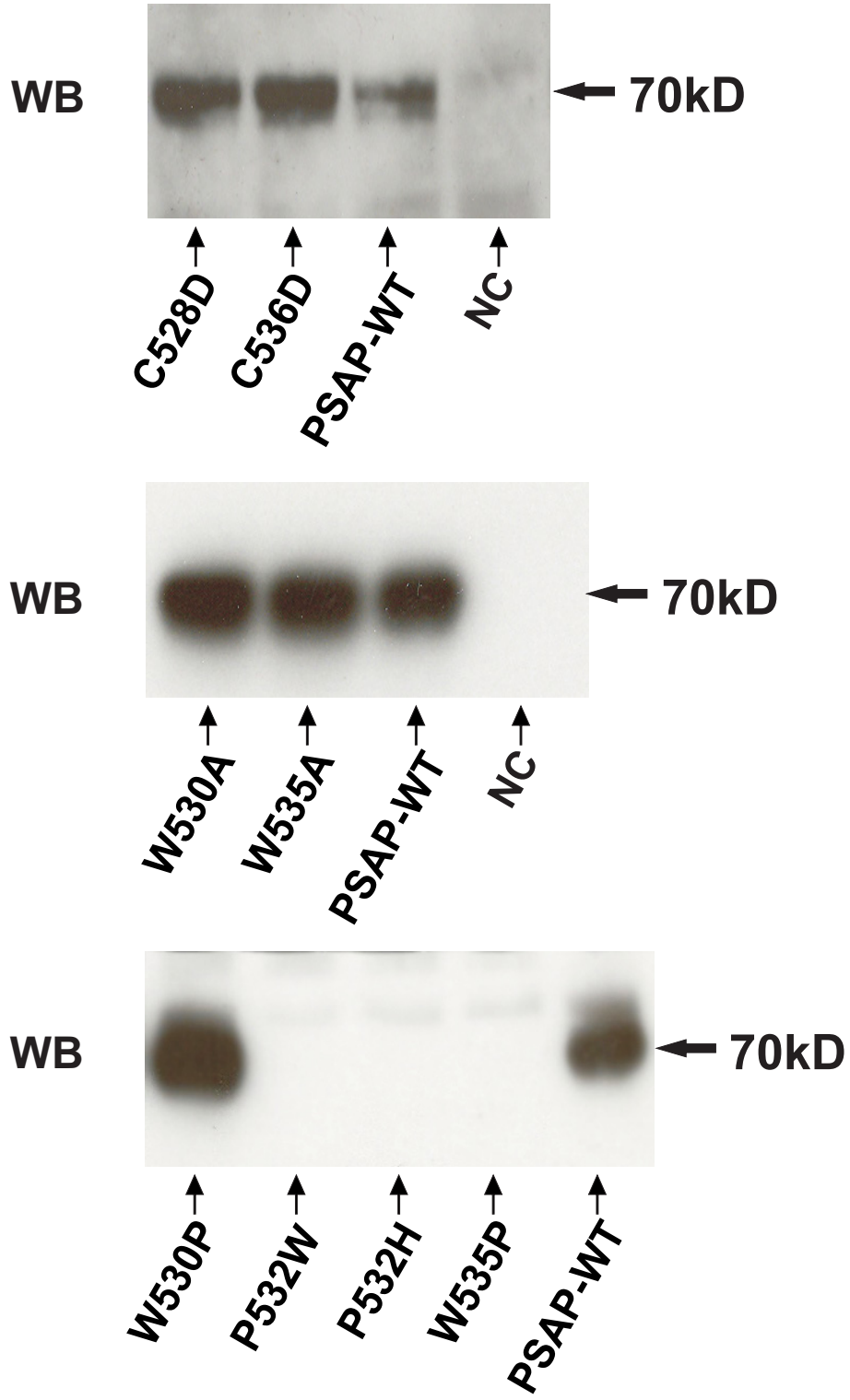

Figure 19. Western-blot: expression of hydrophobic residue mutations

Figure 19. Western-blot: expression of hydrophobic residue mutations

Western-blot was conducted to examine the expression of the mutated constructs C528D, W530A, W530P, P532W, P532H, W535P, W535A and C536D. The mutations C528D, W530A, W530P, W535A and C536D generated normal prosaposin bands. On the other hand, the Western did not detect bands for the mutations P532W, P532H and W535P. PSAP-WT was used as a positive control while the negative control (NC) corresponds to cells transfected with empty construct.

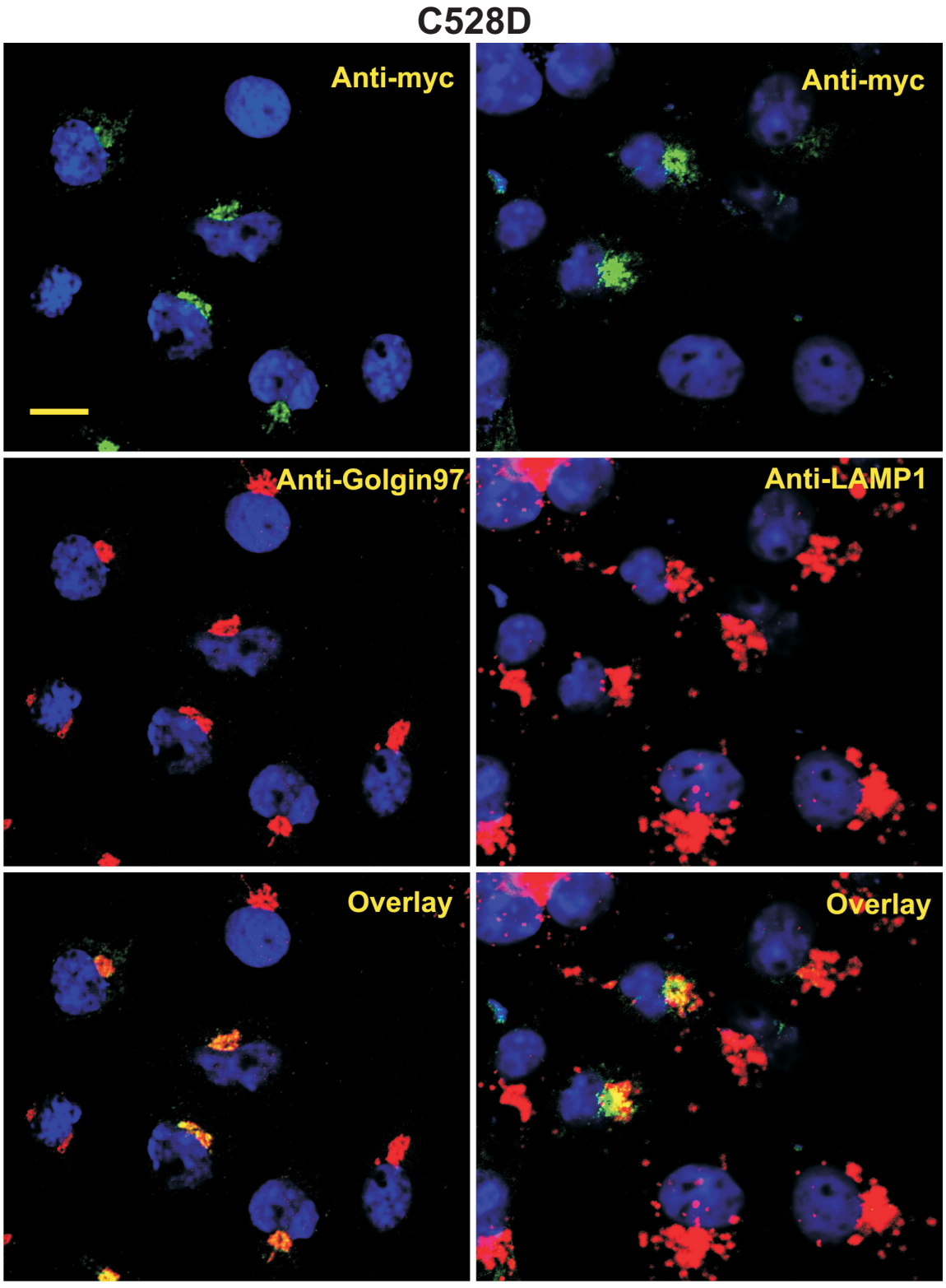

Figure 20. Confocal microscopy: Lysosomal targeting of C528D

Figure 20. Confocal microscopy: Lysosomal targeting of C528D

The COS7 cells transfected with the mutated construct C528D were examined by confocal microscopy. C528D was stained green with chicken anti-myc antibody, while TGN or lysosomes stained red with anti-Golgin97 or anti-LAMP-1 antibody. Nuclei appear in blue. Anti-myc staining of cells transfected with C528D overlaid only with anti-Golgin staining and labeled the perinuclear region but not the cytoplasmic vesicular structures. Scale bar equals 5 μm and apply to all micrographs.

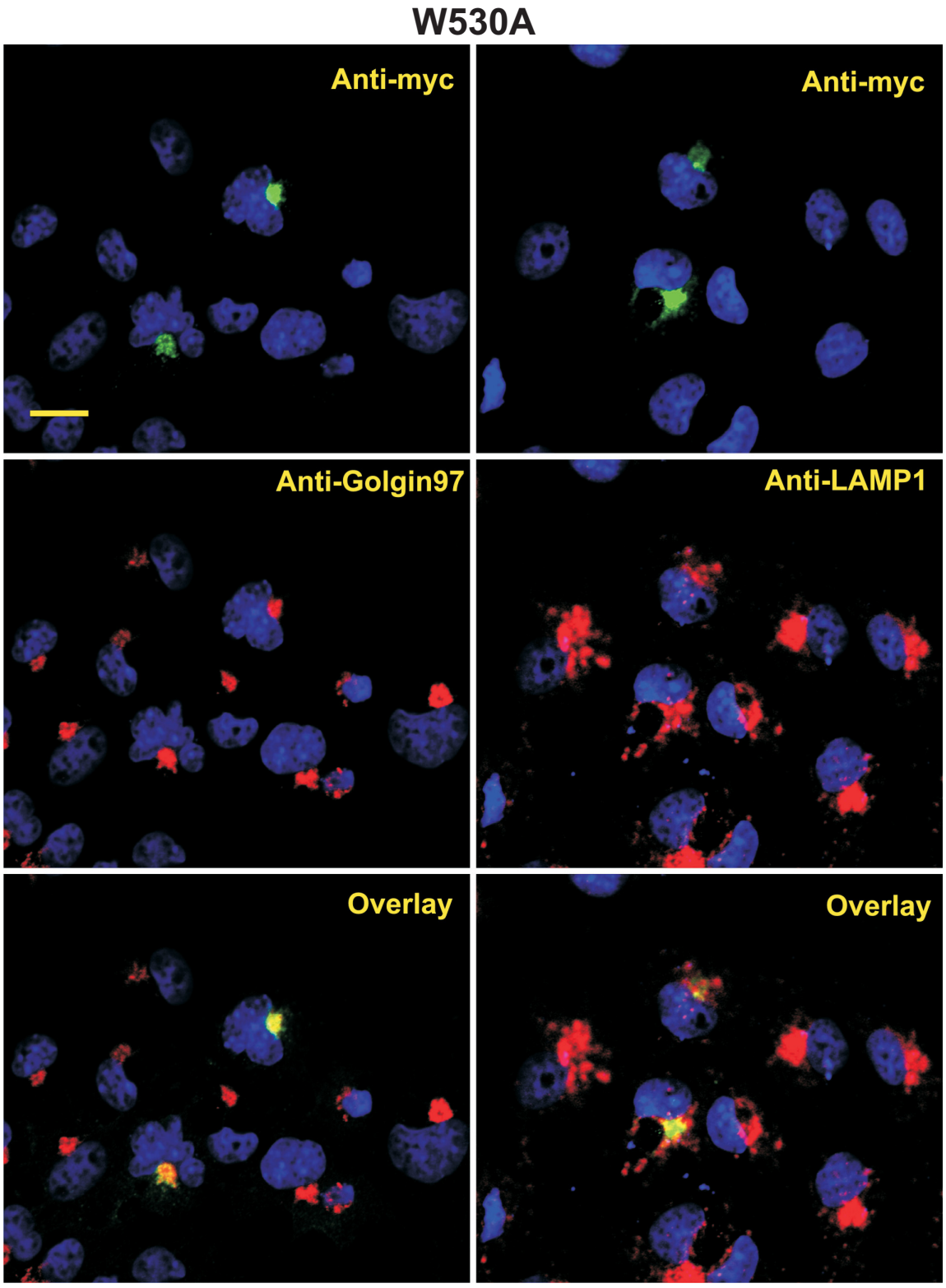

Figure 21. Confocal microscopy: Lysosomal targeting of W530A

Figure 21. Confocal microscopy: Lysosomal targeting of W530A

The COS7 cells transfected with the truncated construct W530A were examined by confocal microscopy. W530A was stained green with chicken anti-myc antibody, while TGN or lysosomes stained red with anti-Golgin97 or anti-LAMP-1 antibody. Nuclei appear in blue. Anti-myc staining of cells transfected with W530A overlaid only with anti-Golgin staining and labeled the perinuclear region but not the cytoplasmic vesicular structures. Scale bar equals 5 μm and apply to all micrographs.

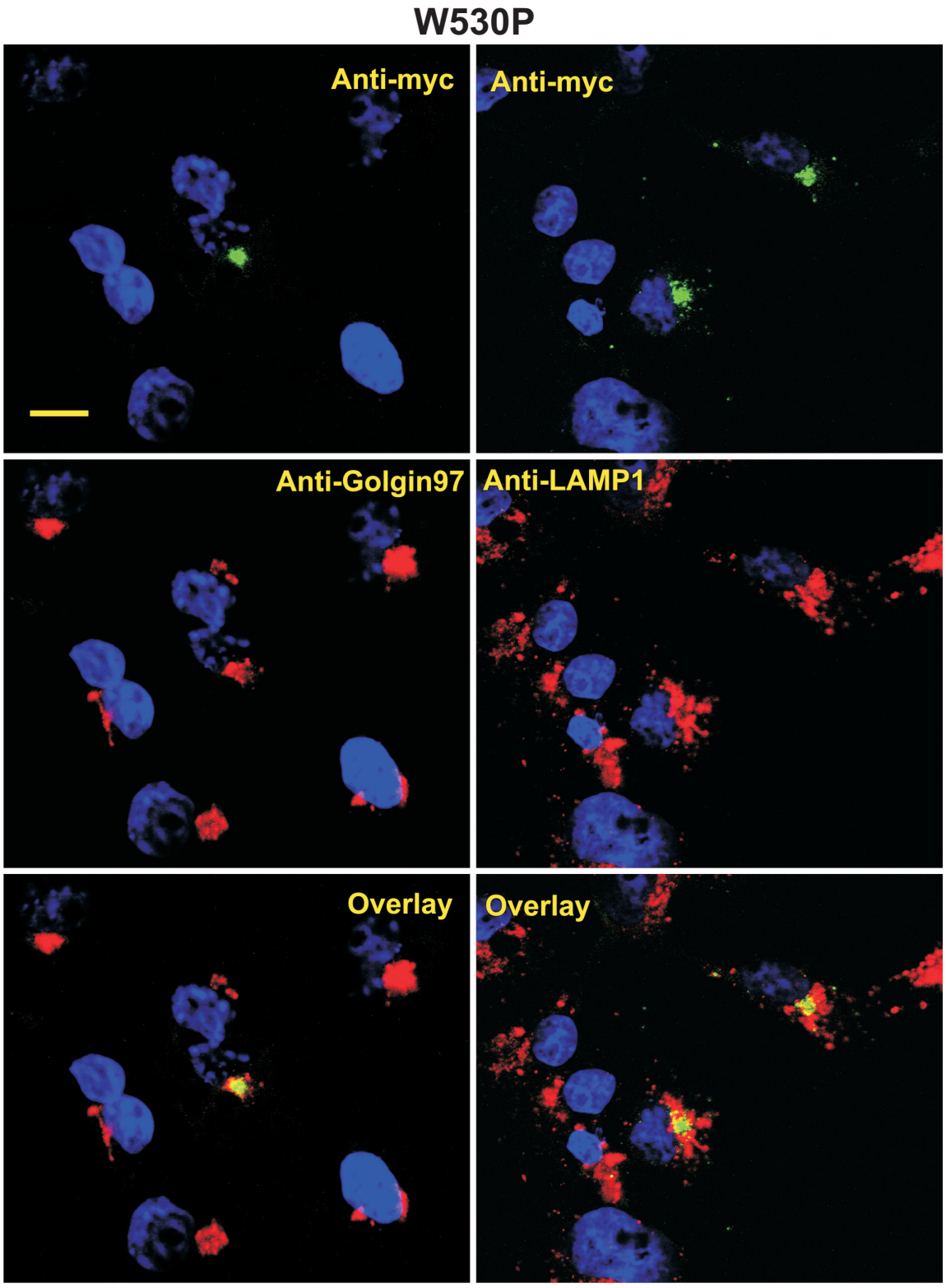

Figure 22. Confocal microscopy: Lysosomal targeting of W530P

Figure 22. Confocal microscopy: Lysosomal targeting of W530P

The COS7 cells transfected with the mutated construct W530P were examined by confocal microscopy. W530P was stained green with chicken anti-myc antibody, while TGN or lysosomes stained red with anti-Golgin97 or anti-LAMP-1 antibody. Nuclei appear in blue. Anti-myc staining of cells transfected with W530P overlaid only with anti-Golgin staining and labeled the perinuclear region but not the cytoplasmic vesicular structures. Scale bar equals 5 μm and apply to all micrographs.

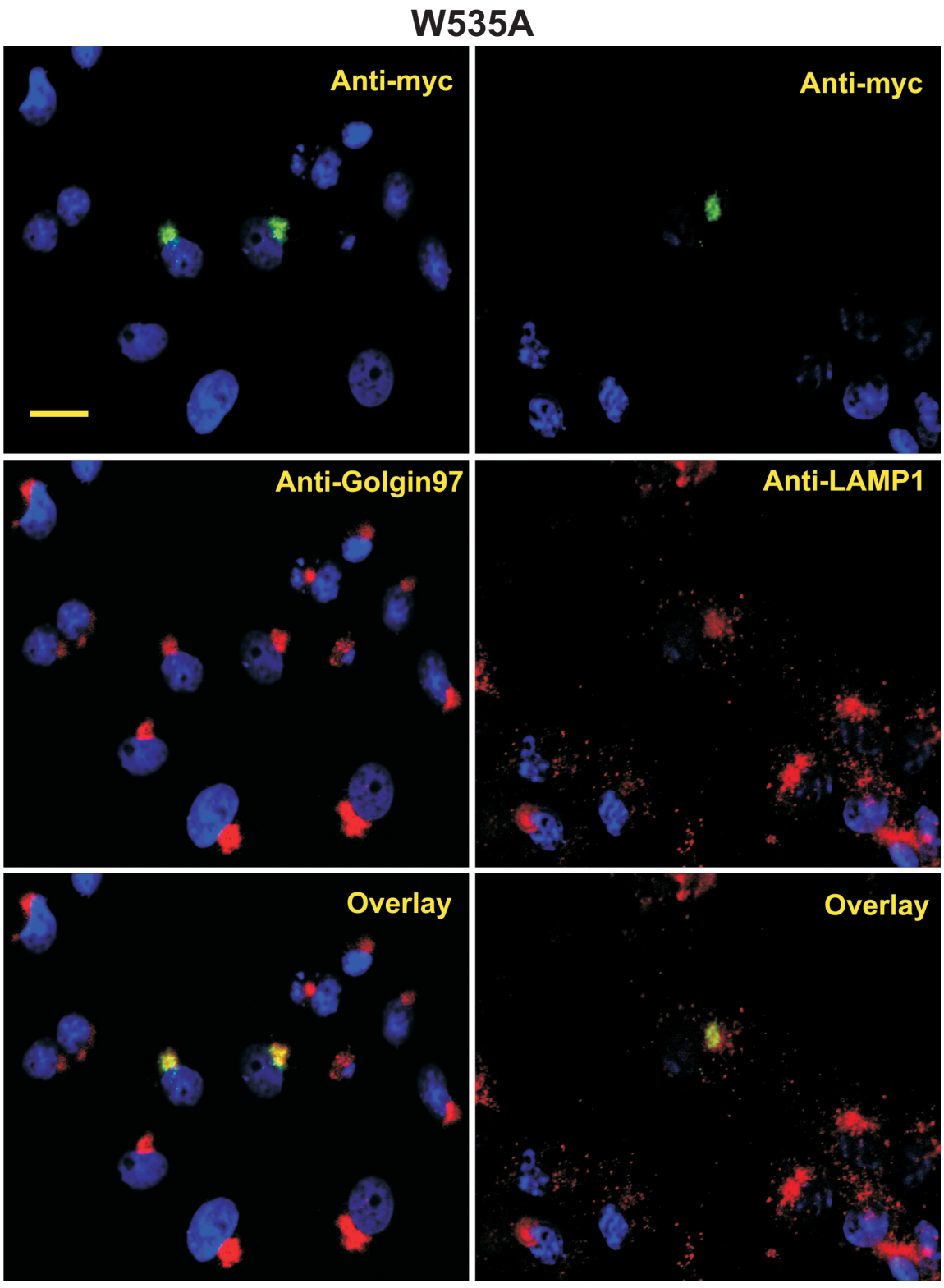

Figure 23. Confocal microscopy: Lysosomal targeting of W535A

Figure 23. Confocal microscopy: Lysosomal targeting of W535A

The COS7 cells transfected with the mutated construct W535A were examined by confocal microscopy. W535A was stained green with chicken anti-myc antibody, while TGN or lysosomes stained red with anti-Golgin97 or anti-LAMP-1 antibody. Nuclei appear in blue. Anti-myc staining of cells transfected with W535A overlaid only with anti-Golgin staining and labeled the perinuclear region but not the cytoplasmic vesicular structures. Scale bar equals 5 μm and apply to all micrographs.

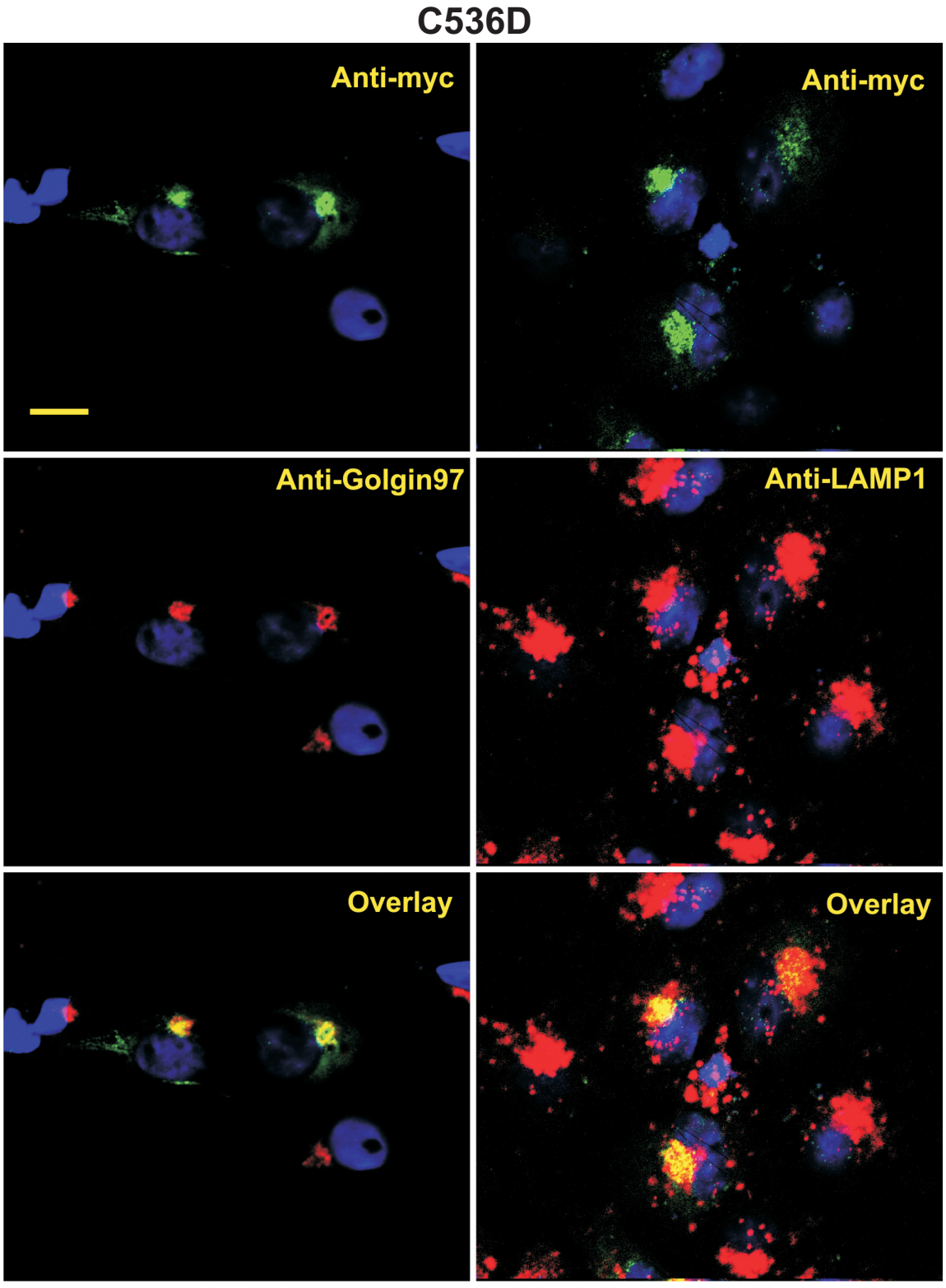

Figure 24. Confocal microscopy: Lysosomal targeting of C536D

Figure 24. Confocal microscopy: Lysosomal targeting of C536D

The COS7 cells transfected with the mutated construct C536D were examined by confocal microscopy. C536D was stained green with chicken anti-myc antibody, while TGN or lysosomes stained red with anti-Golgin97 or anti-LAMP-1 antibody. Nuclei appear in blue. Anti-myc staining of cells transfected with C536D overlaid only with anti-Golgin staining and labeled the perinuclear region but not the cytoplasmic vesicular structures. Scale bar equals 5 μm and apply to all micrographs.

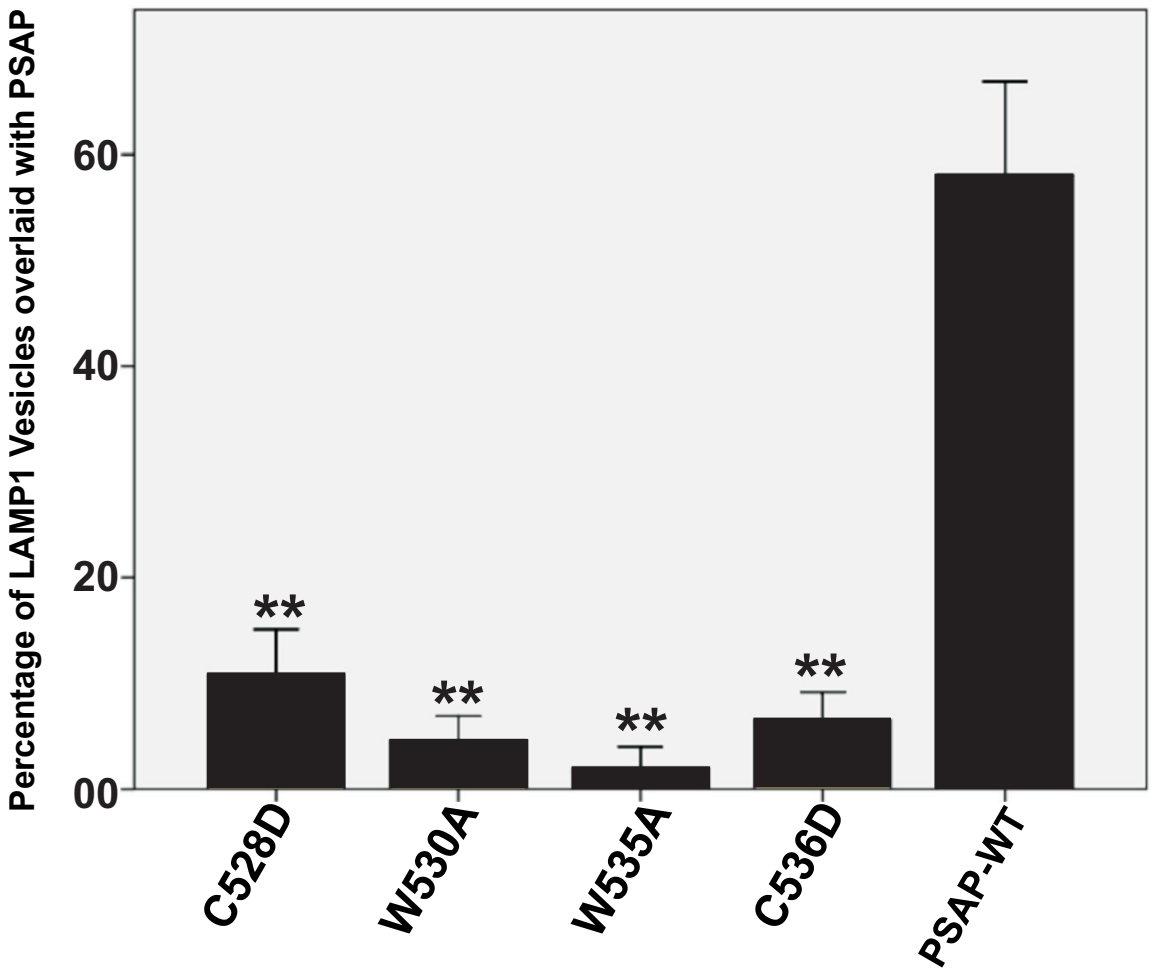

Figure 25. Statistical analysis: Lysosomal targeting hydrophobic residue mutations

Figure 25. Statistical analysis: Lysosomal targeting hydrophobic residue mutations

The percentage of LAMP-1 vesicles overlaid with each mutated prosaposin construct was calculated. All of the mutations C528D, W530A, W535A and C536D showed significant decrease in lysosomal transport (double asterisks, $P<0.01$). Error bars indicate ± S.E.

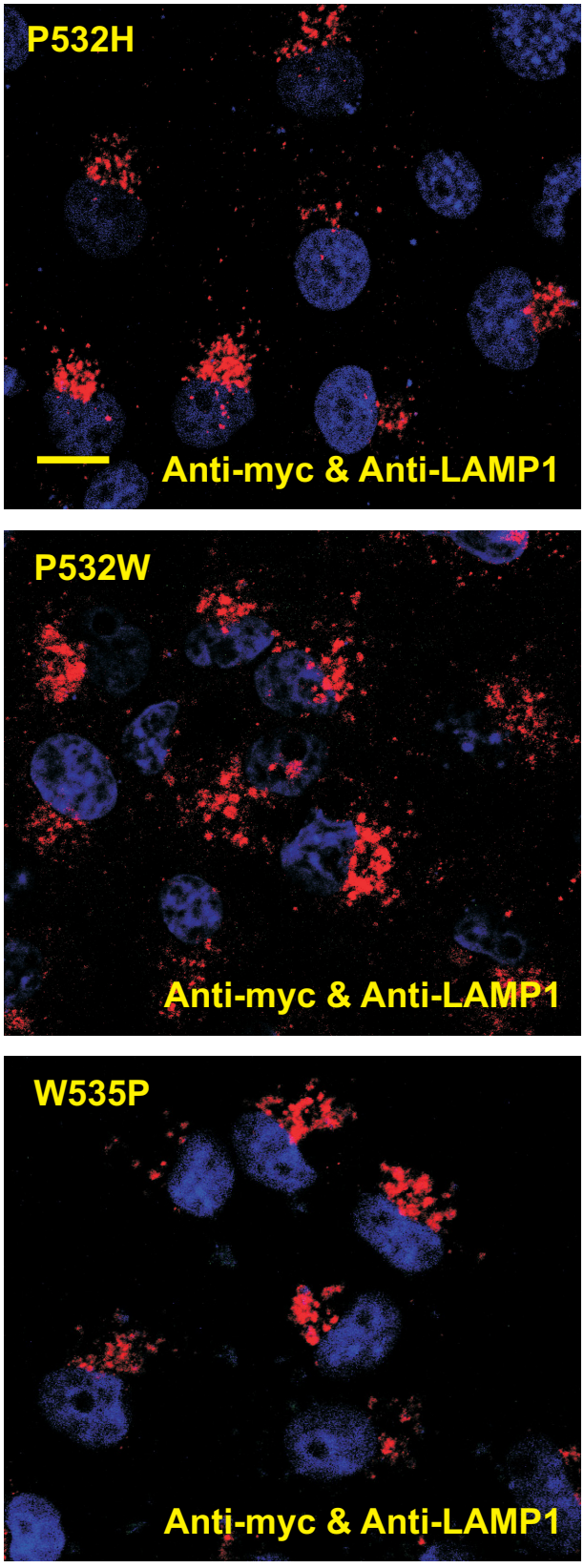

Figure 26. Confocal Microscopy: Expression of W535P, P532H, and P532W

Figure 26. Confocal Microscopy: Expression of W535P, P532H, and P532W

The COS7 cells transfected with the mutated constructs W535P, P532H, or P532W were examined by confocal microscopy. The mutated construct was stained green with chicken anti-myc antibody, while TGN or lysosomes stained red with anti-Golgin97 or anti-LAMP-1 antibody. Nuclei appear in blue. The cells transfected with P532W, P532H or W535P were not detected with anti-myc antibody. Scale bar equals 5 μm and apply to all micrographs.

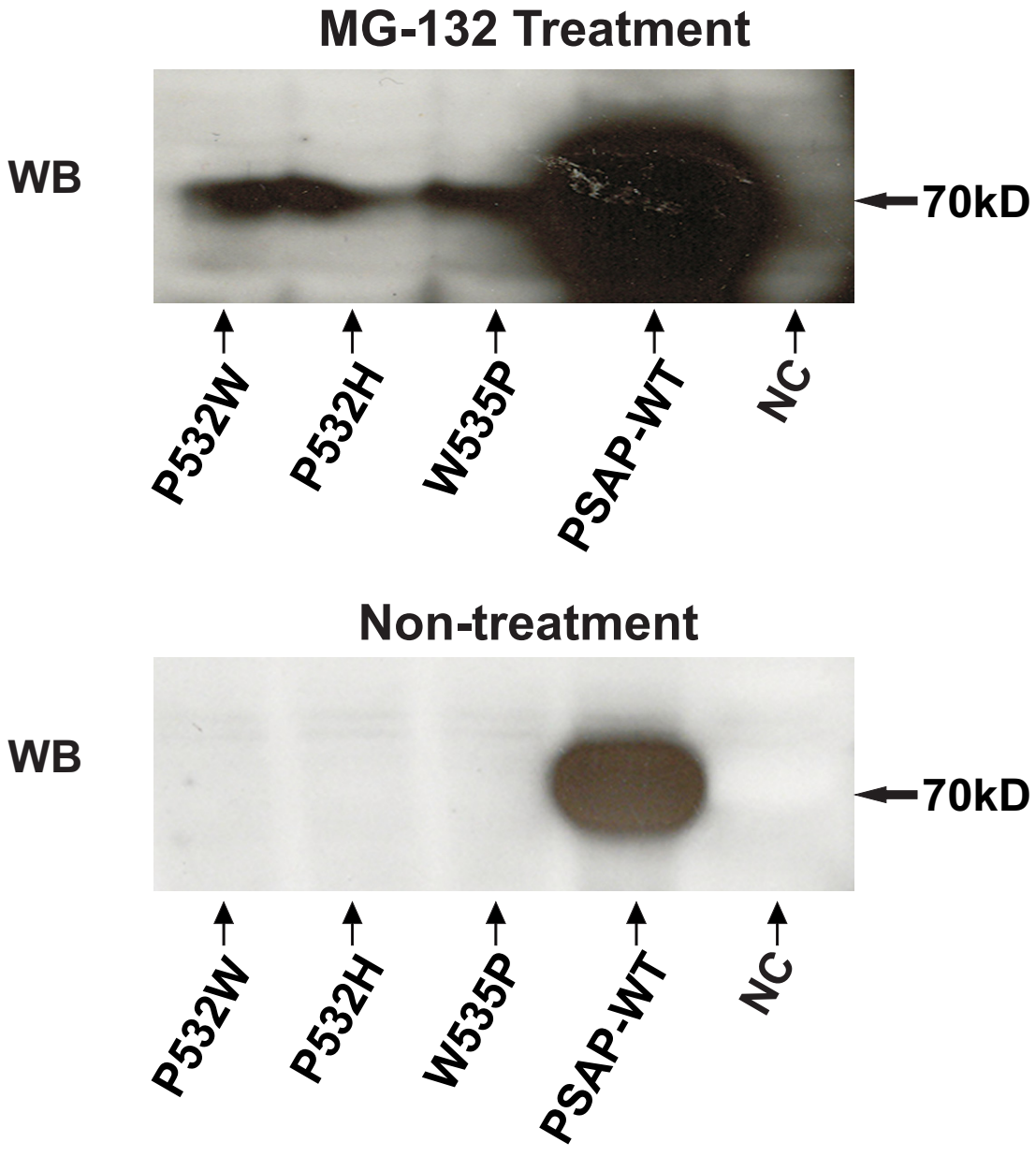

Figure 27. Western-Blot: MG132-Inhibition Assay of P532W, P532H and W535P

Figure 27. Western-Blot: MG132-Inhibition Assay of P532W, P532H and W535P

The cells transfected with P532W, P532H or W535P were treated with or without proteasome inhibitor MG-132. The mutated constructs were detected as 70 kDa bands in the lysates of cells treated with MG-132 (upper panel) but not in the lysates of the non treated cells (lower panel). PSAP-WT was used as a positive control while the negative control (NC) was the cells transfected with empty construct.

Table 1 Statistical significance testing of the overlaid LAMP-1/prosaposin percentage in sequentially truncated PSAP constructs

Weltch t-test

	P-ΔC	P-0	P-25	P-50	P-L50	P-75
Significance (P=)	0.000	0.003	0.000	0.133	0.000	0.057

Table 2 Statistical significance testing of the overlaid LAMP-1/prosaposin percentage in Site-directed PSAP mutations of hydrophilic residues

One-way ANOVA

	K520F	K526F	K527F	Q537F	N538W	E540F
Significance (P=)	0.479	0.131	0.474	0.237	0.312	0.067

Table 3 Statistical significance testing of the overlaid LAMP-1/prosaposin percentage in Site-directed PSAP mutations of hydrophobic residues

Weltch t-test

	C528D	W530A	W535A	C536D
Significance (P=)	0.000	0.000	0.000	0.000